(1)

DEPARTMENT OF THE AIR FORCE

AIR UNIVERSITY

AIR FORCE INSTITUTE OF TECHNOLOGY

Wright-Patterson Air Force Base, Ohio

(1)

AFIT/GSO/ENP/88D-8

GEOSYNCHRONOUS HIGH ENERGY ELECTRON (1.2 - 16 MeV) - SOLAR WIND CORRELATION ANALYSIS

THESIS

Gary P. Grover
Captain, USAF

AFIT/GSO/ENP/88D-8

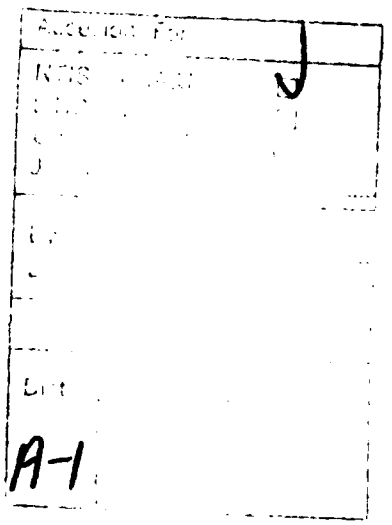

Approved for public release; distribution unlimited

AFIT/GSO/ENP/88D-8

GEOSYNCHRONOUS HIGH ENERGY ELECTRON (1.2 - 16 MeV) - SOLAR WIND CORRELATION ANALYSIS

THESIS

Presented to the Faculty of the School of Engineering
of the Air Force Institute of Technology
Air University
In Partial Fulfillment of the
Requirements for the Degree of
Master of Science in Space Operations

Gary P. Grover, B.S.
Captain, USAF

December, 1988

Preface

The purpose of this study was to continue with the work of three previous theses done here at AFIT. Theses done by Captain Warren Smith (GSO-83D), Captain Douglas McCormick (GSO-84D), and Major Michael Halpin (GSO-86D) investigated the relationship between solar wind velocity, interplanetary magnetic field (IMF), and high energy electron count rates at earth geosynchronous altitude. This thesis effort first attacked the problem of data gaps that caused computational problems for the previous three theses. Where possible, these data gaps were filled in. In investigating the relationship between the solar wind and high energy electrons three separate approaches were undertaken to determine if better correlation results could be obtained.

When I accepted this thesis topic I hoped to accomplish two things. First, because of my prior interest in solar phenomena, I wanted to expand my limited knowledge of how solar dynamics effect the near earth space environment. Second, I hoped to show that through the use of innovative data manipulation techniques, I could better quantitate the solar wind's effect on high energy electrons at earth geosynchronous altitude.

In my quest to finish this thesis I have received assistance from several people to whom I am greatly

indebted. First and formost is my advisor Major James Lange. Major Lange's understanding of the near earth space environment, his encouragement, and his ability to keep my thesis efforts focused have been instrumental in the progression and completion of this project. Lt. Col. James Robinson and Professor Daniel Reynolds provided me with timely and insightful statistical guidance. Finally, and definately the most important person in my life, I must thank my wife, [redacted] On several occasions she gave up her free time while our [redacted] boys were napping to either read or type-in some of the tens of thousands of numbers that had to be manually entered into the computer. If it were not for my wife's support and assistance, this thesis effort would have died a sad death several months ago. [redacted] I love you "bunches and bunches" and thank you very much for all your help.

Gary P. Grover

Table of Contents

	Page
Preface	ii
List of Figures	vi
List of Tables	vii
Abstract	viii
I. Introduction	1
Background	1
Objective of the Research	4
Overview	6
II. Literature Review	7
Organization	7
Discussion of the Literature	7
III. Data Collection, Analysis, and Preparation	17
Data Collection	17
Data Analysis	20
Data Preparation	20
1979 Data	21
1983 Data	23
IV. Methodology	25
Approach 1	27
Approach 2	29
Approach 3	31
V. Results of the Analysis	34
Daily Average Plots	34
1979-1981 Data	34
1983-1985 Data	37
Distribution Identification	40
Min, Mean, Max, Standard Deviation	40
1979-1981 Data	40
1983-1985 Data	41
Frequency and Probability Plots	42
1979-1981 Data	42
1983-1985 Data	45

Page

1979 Data Set 48
Approach 1 48
Approach 2 51
Approach 3 54
1983 Data Set 56
Approach 1 56
Approach 2 59
Approach 3 61

VI. Conclusions and Recommendations 64
Conclusions 64
Recommendations 67

Appendix A: Plots of Original Data 69
1979-1981 Data 70
1983-1985 Data 82

Appendix B: Frequency Plots 94
1979-1981 Data 95
1983-1985 Data 101

Appendix C: Normal Probability Plots of Ln(Data) . . . 107
1979-1981 Data 108
1983-1985 Data 114

Appendix D: Scatter Plots of 2-Day Solar Wind Lags vs Electron Count Data for R-Squared Values Greater than 0.10 120
1979-1981 Data 121
Original Data 121
Percentiled Data 123
1983-1985 Data 125
Original Data 125
Percentiled Data 130

Appendix E: Plots of R-Squared vs Solar Wind Lags . . 135
1979-1981 Data 136
1983-1985 Data 141

Bibliography 146

Vita 148

List of Figures

Figure			Page
1.	Cross Section of the Earth's Magnetosphere		1
2.	Observed Sunspot Numbers for Solar Cycle 21 . . .		5
3.	Plot of Daily Average Count Rate for Variable X .		32
4.	1979-1981 Data	Plot of Original SEESSD Data . .	34
5.	1983-1985 Data	Plot of Original SEE1 Data . . .	38
6.	1979-1981 Data	Frequency Plot of Solar Wind Data	42
7.	1979-1981 Data	Normal Probability Plot of Ln(Solar Wind) Data	43
8.	1983-1985 Data	Frequency Plot of SEE4 Data . . .	45
9.	1983-1985 Data	Normal Probability Plot of Ln(SEE4) Data	46
10.	1979-1981 Data	Scatter Plot of 2-Day Solar Wind Lag vs SEESSD Data	50
11.	1979-1981 Data	R-Squared vs Solar Wind Lags for SEE1 Channel	52
12.	1979-1981 Data	Scatter Plot of Percentiled 2-Day Solar Wind Lag vs PSSD	53
13.	1983-1985 Data	Scatter Plot of 2-Day Solar Wind Lag vs SEESSD	57
14.	1983-1985 Data	R-Squared vs Solar Wind Lags for SEE1 Channel	60

List of Tables

Table			Page
I.	1979-1981 Data	Minumum Mean Maximum Standard Deviation	40
II.	1983-1985 Data	Minimum Mean Maximum Standard Deviation	41
III.	1979-1981 Data	R-Squared Values of Solar Wind Lags vs Original Electron Data	48
IV.	1979-1981 Data	R-Squared Values of Percentiled Solar Wind Lags vs Percentiled Electron Data	51
V.	1979-1981 Data	Five-channel Event Identification Results	55
VI.	1983-1985 Data	R-Squared Values of Solar Wind Lags vs Original Electron Data	56
VII.	1983-1985 Data	R-Squared Values of Percentiled Solar Wind Lags vs Percentiled Electron Data	59
VIII.	1983-1985 Data	Five-channel Event Identification Results	62

AFIT/GSO/ENP/88D-8

Abstract

This thesis investigated the relationship between high energy electron (1.2-16 MeV) count rates and solar wind velocity. The analysis used daily averages for all variables. Two data sets were examined: the first, from 13 June 1979 to 18 May 1981 occurred slightly after solar maximum; the second, from 8 May 1983 to 12 April 1985 occurred slightly before solar minimum. The electron count rate data came from DOD satellite 1979-053 in geosynchronous orbit while the solar wind data was collected by other satellites directly in the unobstructed solar wind. Methods used to analyze the data were daily average plots, frequency plots, probability plots, descriptive statistics, linear correlation analysis of both original and percentiled data, and event analysis.

The results of this study showed that solar wind velocity correlates differently with high energy electron count rates depending on where in the solar cycle the solar wind events occur. It was shown through event analysis that two to three days prior to a significant rise in high energy (1.2-16 MeV) electron count rates, a significant rise in solar wind velocity also occurred. However, due to the low linear correlation results achieved (all R-Squared values

were less than 0.50), it is likely that solar wind velocity is only one of several variables determining the occurrences of high energy electron events at earth geosynchronous altitude.

GEOSYNCHRONOUS HIGH ENERGY ELECTRON

- SOLAR WIND

CORRELATION ANALYSIS

I. Introduction

Background

The interaction of the sun's outward streaming solar wind and the earth's magnetic field produces a cavity in interplanetary space more commonly referred to as the earth's magnetosphere. (See Figure 1)

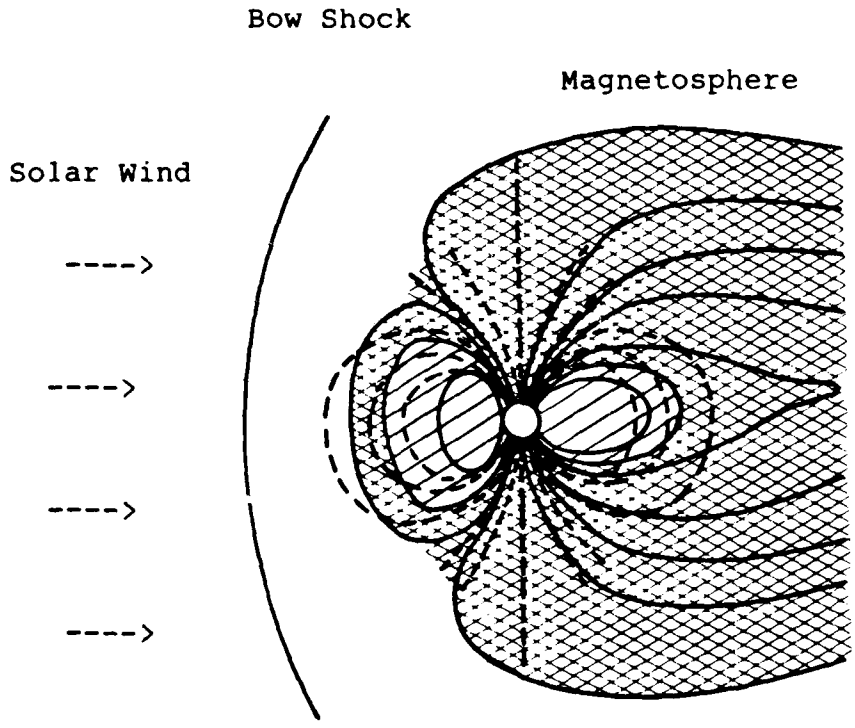

Contained in the radiation belts of the magnetosphere are numerous electrons, protons, and various other ions with energies ranging from a few KeV to hundreds of MeVs. Over the past thirty years many experiments have been conducted in order to gain knowledge of magnetospheric particle populations as well as processes that produce these energetic particles. Much data and theory has been generated on this subject. To date there have been numerous analyses done attempting to relate solar phenomena and lower energy electrons (below two MeV). Su and Konradi in 1979 showed that a correlation does exist between lower energy electrons (below two MeV) and solar wind velocity (19:25). Given that this initial clue did not address high energy electrons (greater than two MeV), the source of high energy electrons that are produced by or trapped in the earth's magnetosphere needs to be investigated.

The US Air Force has shown interest in determining the source of high energy electrons. These ultrahigh energy electrons can cause irreparable damage to sophisticated yet delicate space systems. Systems such as the Space Shuttle, communication satellites, and early warning sensors are particularily sensitive to high energy electrons. These energetic particles can and do interrupt high frequency (HF) radio communications between ground control stations and satellites (6:1).

Energetic particles can also cause problems with satellite circuitry. Radiation induced errors in critical control systems or decision making circuitry can be particularly damaging to a satellite. Even though non-essential components can continue to function with "false" information, critical systems such as attitude control could reorient the satellite into an undesired position from which the satellite may not recover. Repeated circuit switching caused by the continual bombardment of high energy electrons onto delicate circuitry can cause electrical systems to burnout or worse when propulsion or weapon systems are involved (12:5-49).

High energy electron induced errors in satellite circuitry is a serious problem for the Strategic Air Command (SAC). SAC uses HF satellite communications for positive control of its bomber and reconnaissance aircraft. Any interruption of critical satellite communications for SAC or any other key DOD organization could have grave implications for our national security (6:1).

DOD needs reliable and survivable communications, reconnaissance, and early warning systems. These systems must give unambiguous observations and warnings to our national leaders. The occurrences of high energy electrons in the near-earth space environment can degrade, damage, and even destroy satellite systems working in this adverse environment (6:1).

Adverse environmental events routinely cause commanders and satellite owner-operators to take specific actions to protect their satellites. The need for satellite protection is expressed in an Air Force Statement of Operational Need (SON). This SON, MAC 01-83, identifies the basis of the Air Force's needs and calls for further research into the linkage between solar phenomena and high energy electron events. The goal of Air Force research is to gain a deeper understanding of the mechanism causing high energy electrons at earth geosynchronous altitude. As part of this greater understanding, the Air Weather Service would like to develop a predictor of high energy electron events so that satellite owner-operators and commanders can take the necessary actions to protect their satellites (6:1-6).

Objective of the Research

The objective of this research will be to analyze spacecraft acquired data of energy specific electron count rates which were measured from a satellite at geosynchronous altitude and solar wind velocity data gathered from two different satellites both positioned outside of the earth's magnetosphere directly in the unobstructed solar wind stream. The ultimate goal of this research is to determine the extent of the correlation between the number of high energy electrons occurring at geosynchronous altitude and solar wind velocity. This study will also determine if

solar wind velocity holds any promise as a predictor of high energy electron events.

The scope of this study will be limited to electron energy levels ranging from 1.2 to 16 MeV. The time frame investigated by this research will encompass two 706-day time periods. The first period, June 13, 1979 to May 18, 1981, occurs slightly after the maximum of solar cycle 21. The second period, May 8, 1983 to April 12, 1985, also occurs during the declining phase of solar cycle 21 near solar minimum. (See Figure 2)

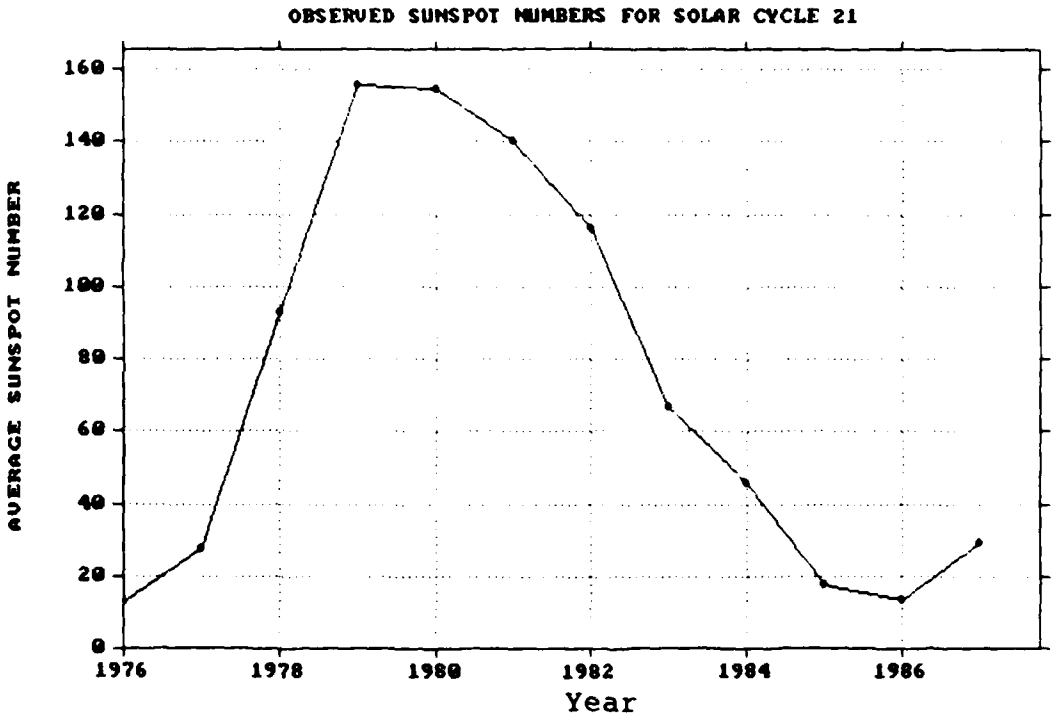

Figure 2: Observed Sunspot Numbers for Solar Cycle 21
NOTE: Points plotted are representative numbers for 1 July of year indicated.
(Values from 11:15)

Overview

The remainder of this report includes a literature review of articles on solar phenomema-magnetospheric interactions (Chapter II), data collection, analysis, and preparation (Chapter III), methodology used to attack the problem (Chapter IV), results of the analysis (Chapter V), and finally, appropiate conclusions and recommendations (Chapter VI).

II. Literature Review

Organization

This literature review examines fourteen reports in a chronological fashion. The citations presented are meant to be representative of the types of research done in the field of solar phenomena-megnetospheric interactions. They are by no means meant to be exhaustive.

Discussion of the Literature

Ever since the first scientific satellite was launched into the Earth's magnetosphere almost thirty years ago, scientists have studied magnetospheric processes. The goal of these scientific studies has been to explore and describe the Earth's magnetospheric environment. One of the most prominent scientists in this field is Syun-Ichi Akasofu from the Geophysical Institute, University of Alaska, Fairbanks.

Akasofu envisioned the magnetosphere to be either a driven system or an unloading system. He described a driven system to be a resistor directly connected to a dynamo (a dynamo is a machine capable of converting electrical energy into mechanical energy or vice versa). The electrical current input into the system through the dynamo and the heat output of the resistor will show similar variations, i.e., the output is "driven" by the input. In describing an unloading system, Akasofu envisioned a device, most likely a

capacitor, placed between the dynamo and the resistor. The capacitor will store electrical energy until the capicator's critical storage value is reached. Once the critical value is passed, the capacitor will suddenly release all its stored electrical energy to the resistor. There will be no correlation between the input current to the dynamo and the heat output from the resistor. The input current is stored in the capacitor, then "unloaded" to the output device, the resistor. Many scientists believe that the magnetosphere is an "unloading" system. Although this may not be the case, many scientists will hold to this thought until it can be shown that there is a good correlation between inputs (solar phenomena) and outputs (high energy electrons) (1:127).

From Akasofu's simplistic "unloading system" explanation have evolved the complex equations and models that attempt to explain the plasma processes that dominate the Earth's magnetosphere. Because of the ever growing number of satellites operating within the magnetosphere, it is no surprise that solar-magnetospheric interaction has been an area of much interest and study.

The study of highly energetic electrons within the magnetosphere has been responsible for much theoretical research. This research has been driven by the need to protect sensitive satellite systems from the damaging effects of highly energetic electrons. Electrons of the mega-electron volt (MeV) energies are likely to do damage to

orbiting satellites. Energetic electrons were initially postulated to occur with magnetospheric disturbances. Arnoldy and Chan identified electron intensity fluctuations at geosynchronous altitude in 1969. They showed that electrons of greater than 50 KeV were produced during magnetospheric storms (2:5019). Subsequently, Su and Konradi showed that at geosynchronous altitude electron energy fluxes can vary up to a factor of 750. These dramatic fluctuations were directly linked to quiet versus disturbed magnetospheric conditions (19:25).

In the 1960's, Akasofu proposed that disturbed magnetospheric conditions may be caused by a neutral ion component of the solar wind. He suggested that neutral ions, most likely hydrogen atoms propagating outward from the sun at the speed of the solar wind, freely penetrate the outer boundaries of the magnetosphere. (Here Akasofu is talking about high energy thermal neutrals because lower energy neutrals would be ionized by the extremely high temperatures of the sun's corona). Once inside the magnetosphere, the neutral hydrogen atom is stripped of its electron. The remaining positively charged hydrogen atom and the negatively charged electron are subsequently accelerated in different directions by the earth's magnetic field. The resulting effects of charge separation and magnetospheric conditions can give rise to a sudden magnetospheric storm. Akasofu went on to suggest that the

variety of development and level of intensity of magnetospheric storms may be due to the degree of ionization of the solar wind. He showed how several magnetospheric storms could be explained in terms of the variability of ionization of the solar wind plasma. The main point of Akasofu's paper was not to overemphasize the importance of solar wind ionization, "but to indicate that one must find an 'unknown' quantity in the solar wind to explain the variety of the development of magnetospheric storms" (1:123-125).

In 1976, L.J. Lanzerotti of Bell Laboratories continued the search for the "unknown" in the solar wind. He did research on the degree of ionization of the solar wind. Lanzerotti found that particle intensities measured at geosynchronous altitude which can be linked to solar disturbances are extremely unpredictable. The amount of particles emitted from the sun appears to be related to the solar sunspot cycle. However, Lanzerotti stated that in order to obtain a reasonable measure of solar particle fluxes, we must conduct "extensive monitoring of the interplanetary particle population covering several solar cycles" (14:400-401).

Lanzerotti's study did reveal a very interesting point. He showed that from 1964-1972, ninety-five percent of all occurrences of solar electron events (electrons greater than 45 KeV) originated from flares located between

zero and ninety degrees west solar longitude. He noted that the optimal location for flare occurrence such that the maximum number of solar particles reaches the earth is approximately sixty degrees west solar longitude and fifteen degrees north solar latitude. Lanzerotti did not consider these solar electrons to be the source of high energy electrons at earth geosynchronous altitude primarily because the solar particles are of such low energy. He believed that some other mechanism had to be at work (14:395-397).

Other scientists have also been searching for this unknown mechanism. Higbie indicated that the unknown quantity in the solar wind may be determined by solar flare activity. He stated that electrons are first imparted energy through solar phemonenon such as flares. These solar electrons travel outward from the sun at the speed of the solar wind and eventually penetrate the Earth's magnetosphere. A second process for electron acceleration may occur in the magnetosphere itself by means of processes that are not yet fully understood. Higbie goes on to say that either or both of these processes could be acting to generate high energy electrons (10:433).

Hundhausen in a short report on plasma flow from the sun tried to shed more light on the "unknown" electron acceleration mechanism. He believed that neither the solar wind nor solar flare activity causes geomagnetic storms. Hundhausen stated that the association of solar wind

structure with solar flare activity is not good at all. The detailed association of transient solar wind shock waves, which are believed to produce geomagnetic storms, with solar flares is far from one to one. He goes on to state that monthly solar wind properties do vary in phase with monthly sunspot numbers, but that sunspots are probably not the cause of the variation in geomagnetic activity at the earth (11:37-38).

John A. Eddy from the High Altitude Observatory at the National Center for Atmospheric Research echoes Hundhausen's remarks. Eddy stated that sunspots themselves are not necessarily fundamental in solar activity. They are not indicative of solar output, nor are they a specific cause of any known geomagnetic effect. Eddy did state that "sunspots are convenient as an index of almost all other activity on the sun, including flares, prominences, and to some extent, changes in the coronal form and in the solar wind" (8:51).

In 1973 scientists took advantage of Skylab's unobstructed view of the sun by having astronauts extensively monitor solar activity. Astronauts and sensors aboard Skylab regularly took pictures of the sun in the soft x-ray with a specially made telescope. During this time (Jun-Nov,1973), geomagnetic storms on earth were recurring every twenty-seven days. From the Skylab pictures, scientists made an interesting discovery. Whenever dark

areas (low emission) in the soft x-ray crossed the sun's central meridian near the sub-earth point, geomagnetic storms would occur on earth a few days later. This series of events persisted throughout the Skylab missions. These dark areas in the soft x-ray were named coronal holes (12:1-20).

Shortly after their discovery, coronal holes were found to be the source of high-speed solar wind streams. Everytime that a high-speed solar wind stream associated with a coronal hole reached the earth's magnetosphere, a geomagnetic disturbance occurred. It was evident from this discovery that coronal holes can and do determine the structure of the solar wind (12:3-17). The existance of coronal holes helped to explain one more piece of the complex solar puzzle. With this new understanding of the solar wind structure, researchers rushed to show the significance of high-speed solar wind streams.

In one such report, Paulikas and Blake studied the effects of the solar wind on magnetospheric dynamics. They used satellite data from 1974 to 1977 to support their claims. Paulikas and Blake showed that the "flux of energetic electrons at synchronous altitude is strongly correlated with the presence of high-speed streams in the solar wind" (16:15). Their results also showed that about one day is needed to generate 140 to 600 KeV electrons, while two days are necessary to generate 3.9 MeV or higher

electrons. Their report also states that "the velocity of the solar wind is the most important parameter in determining the flux levels of energetic electrons in the outer magnetosphere" (16:16). Paulikas and Blake did state some strong conclusions, however their reported work did not present a solid statistical analysis.

In a more heavily documented statistical study, Baker and others summarized energetic electron measurements made by the Los Alamos National Laboratory. The measurements specifically address electrons at geosynchronous altitude. "Daily averages of electron flux for both 200 to 300 KeV and 1.4 to 2.0 MeV electrons are clearly correlated to solar wind velocities" (3:87). Also noted was the much higher relative change in electron flux for the 1.4 to 2.0 MeV electrons than for the 200 to 300 KeV electrons. These flux changes also showed the characteristic one- and two-day time delays following maximum solar wind velocities that Paulikas and Blake had earlier demonstrated (3:87).

Smith, in a thesis based on Baker's findings, statistically analyzed the relationship between energetic electrons (1.2 to 16 MeV) at geosynchronous altitude and interplanetary parameters (solar wind and interplanetary magnetic field). His work revealed a weak correlation between two-day-old solar wind values and electron fluxes in the 1.2 to 6.6 MeV energy range. No correlation was found

between the 6.6 to 16 MeV energy range and solar wind data. Smith's analysis also revealed no correlation between the z-component of the interplanetary magnetic field and electrons in the 1.2 to 16 MeV range (18:50-54).

In a follow up to Smith's thesis, McCormick used different statistical techniques to analyze Smith's data. McCormick's results were similar to Smith's. Both stated that there seem to be two separate processes at work. Their statistical analyses show that 1.2 to 6.6 MeV electrons appear to have a different energy source than do the 6.6 to 16 MeV electrons. McCormick suggested that galactic cosmic rays may be the energy source of ultrahigh energy (6.6 to 16 MeV) electrons (15:63).

In conclusion it is apparent that the source of high energy electrons at geosynchronous altitude continues to elude scientists even though much research has been conducted on the workings of the magnetosphere. Akasofu asked the question over twenty years ago, "Is the magnetosphere a driven system or an unloading system?" The definitive answer is still unknown. Scientists continue to formulate new ideas on the source of magnetospheric high energy electrons. Many believe that the answer is somehow linked to the solar wind. Much statistical analysis of satellite data has been done to unlock the secret of high energy electron generation, but the truth has proven to be elusive. Scientists have shown that the solar wind appears

to play an undetermined role in the generation of lower energy (less than 6.6 MeV) electrons. Also remaining to be uncovered is if and/or how the solar wind works with an "unknown" source to generate ultrahigh energy electrons (greater than 6.6 MeV).

III. Data Collection, Analysis, and Preparation

Data Collection

The data used in this study was obtained from special instrumentation onboard three different satellites. The high energy electron data was collected by spacecraft 1979-053 and made available through the Los Alamos National Laboratory (LANL). The detailed orientation of satellite 1979-053 and a description of its high energy electron instrumentation can be found in Bakers and others' report, (3:82-90). Solar wind data was collected by the International Magnetospheric Probe, more commonly referred to as IMP-8 and the International Sun-Earth Explorer satellite also known as ISEE-3. For a detailed explanation of IMP-8 and ISEE-3 orientation, orbit location, and instrumentation, the reader is referred to two sources, Rosenvinge, (17:1-9) and King, (13:10-20). The data from IMP-8 and ISEE-3 was made available through the National Space Science Data Center (NSSDC).

The high energy electron data obtained from the Los Alamos National Laboratory was sent on a magnetic tape. The original Los Alamos tape contained daily averages for ten variables. Among these ten variables were the daily averages for five energetic electron channels. These five channels measured electron flux levels (electron flux levels can be directly transformed to electron count rates) for

energy ranges of 1.2 - 1.8 MeV, 3.4 - 4.9 MeV, 4.9 - 6.6 MeV, 6.6 - 9.7 MeV, and 9.7 - 16 MeV. The lowest energy channel, 1.2 - 1.8 MeV, was recorded by the high energy electron (HiE) detector from the Charged Particle Analyzer instrumentation onboard satellite 1979-053. This detector is commonly referred to as the solid state detector (SSD). The remaining four channels were collected by the satellite's other onboard detector, the spectrometer for extended electron measurements (SEE) (3:83). In shorthand form, the five high energy electron channels from lowest to highest energy will be subsequently referred to as: SEESSD, SEE1, SEE2, SEE3, AND SEE4. The electron data for the five energy channels was provided by the Los Alamos National Laboratory in daily average form.

Solar wind velocity data was obtained from the National Space Science Data Center (NSSDC) and originally came on magnetic tape. IMP-8 and ISEE-3 were the collecting satellites for the solar wind data. Thanks to the previous thesis work done by Captain Smith and Major Halpin, this author was able to use the compiled solar wind data listings from their theses as the solar wind data sets for this study. The daily averages previously computed by Smith and Halpin were checked by this author. No discrepancies were found.

At the time of Smith's thesis work, Fall 1983, the NSSDC had complied only a partial listing of satellite data

for solar wind velocity. Consequently, there were gaps in the solar wind data provided by the NSSDC. This author attempted to fill-in, where possible, the gapped solar wind data sets used by Smith, McCormick, and Halpin. The April 1986 edition of the NSSDC Interplanetary Medium Data Book - Suplement 3A, 1977 - 1985 provided the necessary information to fill-in the data gaps for the June 13, 1979 to May 18, 1981 data set. This data set will subsequently be referred to as the 1979 data set. ISEE-3 data as reported by the Massachusetts Institute of Technology (MIT) filled all of the data gaps for this first 706-day time period.

The same was not true for Halpin's data set, May 8, 1983 to April 12, 1985 (9:109-125). This second data set will subsequently be referred to as the 1983 data set. The gaps in this data set are genuine data gaps. In early 1983, ISEE-3 malfunctioned and stopped recording solar wind properties. Consequently, for this period only IMP-8 data is available.

Because of the nature of its orbit, IMP-8 is in the unobstructed solar wind stream for seven to eight days of each orbit then in the earth's magnetosphere for four to five days (13:11). While it is in the earth's magnetosphere, IMP-8 is not able to record free stream solar wind velocity. This inability of IMP-8 to record solar wind velocity for four to five days of each orbit gives rise to

the periodic data gaps in the May 8, 1983 to April 12, 1985 data set.

Data Analysis (Computer Hardware and Software)

For this thesis effort, the author choose to use the computer facilities located at AFIT. The system of choice was the Classroom Support Computer (CSC). The CSC is a VAX 11/785 computer running VMS version 4.6. During heavy usage times on the CSC, the author transferred files to the Information Support Computer (ISC). (Both the CSC and the ISC had identical copies of the statistical packages used in this thesis.) The ISC is a VAX 8650 computer also running VMS version 4.6. Approximately ninety percent of the statistical work for this study was accomplished on the CSC. The software package used to analyze the data was SAS. SAS was developed and is maintained by the SAS Institute of Cary, North Carolina. SAS was chosen primarily because of its superb statistical analysis procedures and also because of its extensive use at AFIT. The author had used SAS in three classes before this thesis effort and was familar with SAS' power and command structure. Another important reason for choosing SAS was its ability to read data prepared in a variety of different ways.

Data Preparation

The importance of data preparation to this study can not be overstated. Approximately 16,000 values needed to be

assimulated and verified. Data entry and verification were an important part of the data preparation process.

The major task of perparing the data was to obtain the proper time synchronized data sets necessary to carry out the statistical analysis portion of this thesis. Due to the different data retrieval methods necessary for the 1979 data versus the 1983 data, the preparations for each data set are presented separately.

1979 Data

The electron data for the 1979 data set provided and interesting and difficult challenge. The original high energy electron data for this time period came to AFIT on magnetic tape. Both Smith and McCormick used this original tape for their high energy electron data. However, in the four years since McCormick's thesis, the magnetic tape containing this data was destroyed. The only records available were thirteen typed pages containing all the high energy electron count rates. The author was faced with an interesting dilemma. How to get this large volume of data into the computer in a timely manner? Manually typing in the thirteen pages was possible, but this would take considerable time. What was needed was some type of optical reader which would automatically read the typed pages and transform them into an ASCII text file.

After several days of office searching, one such device was found. AFWAL owns and maintains a PC SCAN 1000 which can read 8.5 by 11 inch sheets of typed information and store the data as an ASCII text file on a floppy disk. The PC SCAN 1000 worked surprisingly well. All thirteen pages were read and stored on a floppy disk. The author then verified and merged all files through the use of PC EDT, a word processing software package. When complete, the entire ASCII file was uploaded to the CSC. Now that the high energy electron data was successfully entered and verified, the next step was to attack the solar wind data.

A portion (approximately 75%) of the solar wind data for the 1979 data set came from Smith's previous thesis work. Each daily average for the solar wind was manually entered and verified. Five hundred thirty daily averages came directly from Smith's thesis. The remaining 176 daily averages were computed by a spreadsheet program from the hourly averages obtained from the NSSDC Interplanetary Medium Data Book for 1977-1985. These 176 solar wind daily averages completely filled all of the solar wind data gaps in the 1979 data set. With the solar wind data correctly entered and verified, the next step was to merge the two files.

The merging of the two files was accomplished via the SAS software on the CSC. One-, two-, three-, and four-day solar wind lag files were created by adding one,

two, three, or four rows of zeros to the front of the original solar wind data file and rerunning the SAS merge program. Once the five files were created, each was checked for days where either solar wind or electron count rates were missing. Any day encountered that had missing data was deleted. In all, twenty-seven days were deleted from the 1979 data set due to missing high energy electron satellite data.

With the merged solar wind - five electron channel file and the four solar wind lag files correctly time synchronized and all missing data days deleted, the 1979 data set was now ready for analysis.

1983 Data

As was explained earlier, the electron data for this time period was provided by the LANL on magnetic tape. Thanks to the help of the AFIT computer consultant, Janet Maywhither, the daily average count rates for the five different energy channels contained on the LANL tape were successfully transferred to the author's personnel disk file on the CSC. With the file successfully transferred, the author manually verified all electron data entries with the tape listing provided by the LANL. The next step in the data preparation process was to enter the solar wind daily averages.

The solar wind data for the 1983 data set came from Halpin's thesis work (9:109-125). Just as for the 1979 data set, each solar wind value was manually entered into the CSC. The entered data was verified with Appendix C of Halpin's thesis. As was explained earlier, the data gaps in the solar wind values for the 1983 data set are genuine satellite data gaps and can not be filled-in. The next step was to merge the two files.

The solar wind and high energy electron files were merged with the exact same SAS program as the 1979 data set. One-, two-, three-, and four-day solar wind lag files were created. Each file was checked for missing solar wind or high energy electron data. For the 1983 data set, 276 days were deleted due to missing satellite data. This accounts for the approximately forty percent data dropout rate of this time period. With all files correctly time synchronized, verified, and days with missing data deleted, the 1983 data set was properly prepared for analysis.

IV. Methodology

The first step toward objective achievement was data collection. As was explained in the Data Preparation section of Chapter III, the data for this thesis needed to be compiled from several sources and transferred to the computer. Any data not in daily average form, was first converted into the proper average. Once the data had been correctly entered, verified, and time ordered, all data was plotted. These plots of time sequential daily averages showed the make-up and variability of each component. (NOTE: For this thesis there were two data sets, 1979 and 1983. Consequently, this entire methodology was done twice, once on each set.) In order to gain a better understanding of the relative distribution of data in each of the five high energy electron channels and the solar wind, distribution identification was undertaken.

Distribution identification began by calculating the maximum, minimum, mean, and standard deviation for all data categories. The data was then sorted. From the sorted data, frequency plots were generated to graphically present the distribution history of each variable. Based on the distribution type (if any) depicted in the frequency plot, a probability plot was constructed to confirm or deny the likely distribution.

For example, a likely distribution may be the lognormal distribution. In this case the probability plot would be constructed as follows: First, the natural logarithm of all data points (Ln[data]) would be calculated. Next, the n sample observations would be ordered from smallest to largest. Then the ith smallest observation in the list is taken to be the [(i - .5)/n]th sample percentile. In turn, the Z-percentile for each data point is expressed as the number of standard deviations away from the mean (assuming a standard normal distribution) corresponding to the calculated sample percentile (7:166-169). For an indepth explanation of Z-percentiles associated with probability plot construction, the reader is referred to Devore (7:165-174).

Once all Z-percentiles have been computed, a plot of sorted logarithmic data versus associated Z-values is constructed. This plot is commonly referred to as a normal probability plot. A linear trend in the probability plot would indicate that the underlying logarithmic data is of the distribution type postulated (normal). The existance of a linear trend for the logarithmic data would in turn mean that the original data is lognormally distributed.

Since the data used in this analysis was generated by natural processes (as opposed to computer simulated or manually derived from a particular distribution type), rigorous statistical testing such as K-S or Chi-Squared

goodness of fit testing was not attempted. The intented approach was to theorize a distribution type from the frequency plot and confirm or deny the postulation via a probability plot.

Distribution identification was not the main objective of this thesis effort. The main objective was to determine the extent of the correlation between high energy electron count rate and solar wind velocity. In order to fully investigate the degree of correlation between electron count rates and solar wind velocity, three approaches were undertaken.

Approach 1

This approach dealt with the original data. Via SAS a linear correlation analysis was done between solar wind velocity and data for all five electron channels. Solar wind velocity was the independent variable with electron count rate the dependent variable. The results of a linear correlation were manifested in two statistical measures: R, the coefficient of correlation, and R-Squared, the coefficient of determination.

R is a parameter which measures the strength of the linear relationship between two sample variables (7:484). R-values can range from negative one to positive one. Negative one indicates a perfect linear fit with one variable decreasing while the other increases. Positive one

also indicates a perfect linear fit with both variables rising or falling in tandom. R-values between negative one and one show lesser degrees of linear correlations with zero indicating virtually no linear relationship.

Providing somewhat different statistical information is the second linear correlation measurement, R-Squared. R-Squared is a measure of the "proportion of observed y variation that can be explained by the simple linear regression model attributed to an approximate linear relationship between y and x." (7:465). R-Squared values range between zero and one. Values close to one indicate a strong linear association between the independent and dependent variables, while R-Squared values near zero indicate virtually no association.

The analysis encompassed zero-, one-, two-, three-, and four-day solar wind lags correlated with all five electron channels. The resulting R-Squared values were graphically presented to show the overall trend for zero- to four-day solar wind lags. Representative scatter plots of solar wind velocity versus electron count rates were generated for all five electron channels for the highest R-Squared solar wind lag day provided that the R-Squared value was greater than .10.

Approach 2

This second approach was identical to Approach 1 with the following exception: each variable's daily average was transformed via its cumulative distribution to a percentile value. The percentile value was computed as follows: The n sample observations were ordered from smallest to largest just as for the construction of probability plots. Then the ith smallest observation was transformed to be the [(i - .5)/n]th sample percentile. Once all percentiles had been calculated, the integrity of the daily average series was restored by resorting the sample in date order.

The rationale for this approach came from the author's analysis of daily average plots. The visual analysis of daily average plots revealed what appeared to be the correlation of extreme events, i.e., the occurrence of electron events substantially above each variable's baseline value appeared to correlate with the occurrence of solar wind events not necessarily of the same relative magnitude. Even though this trend appeared to be present, the amplitudes of each variable's events could differ substantially. For example, the top three SEESSD events for the 1979 data set had count rates of 1588, 1438 and 1223 counts/sec. Each one of these three events matched up with solar wind events of 638, 808, and 561 km/sec, respectively. A simple linear correlation between these three point data

sets produced a small R-Squared value of 0.1604, even though the overall visual analysis indicated that there was a much stronger correlation.

Transforming these extremely high electron count rates and solar wind velocities to their respective sample percentiles produced a much higher determination coefficient. SEESSD count rates of 1588, 1438, and 1223 counts/sec transformed to SEESSD percentile values of 0.999, 0.998, and 0.995 respectively. While the solar wind velocities of 638, 808, and 561 km/sec equated to solar wind percentiles of 0.993, 0.999, and 0.967 respectively. The simple linear correlation of these percentile values yielded an R-Squared value of 0.8338. This high R-Squared value indicated that the sample percentile values are much more correlated than were the actual electron count rates and solar wind velocities.

Based on these findings and similar findings in other electron channels, the author felt that this approach may yield significantly stronger correlation results for high energy electron count rates and solar wind velocities than were reported in earlier studies.

As a result of the transformation of all electron count rates and solar wind velocities to their respective sample percentile values, all data for Approach 2 ranged from zero to one. The numerical transformation used in this approach was designed to remove the relative variability of

each component yet retain the overall information of the data sets. This approach was determined to be a reasonable method of assessing if upper and lower percentile events do in fact correlate.

Approach 3

Approach 3 was designed to analyze the "event" nature of high energy electron count rates and solar wind velocities. An "event" for this analysis was defined as a systematic rise and fall in daily average of one variable over a specified number of days. The number of days in any "event" can vary substantially. For example, an "event" may last for three days (low, high, low) or it may last for ten days, slowly rising and falling over the time period. Figure 3 which depicts the possible behavior of variable X will be used to demonstrate this methodology.

From Figure 3 two events are visible. The first event is an example of a low-high-low event. This event would be designated by the value of its peak amplitude and the occurrence date of peak amplitude. Event one would be identified as Day 4, 6.10 counts/sec. The second event is an example of an extended rise and fall event. Event two would also be classified by peak amplitude and occurrence date in a manner similar to all other events. Hence, event two would be identified as Day 16, 9.2 counts/sec.

Based on peak amplitude, the top twenty-five "events" were independently identified for each electron channel and the solar wind. These top twenty-five "events" for each variable were highlighted on the computer printout of the original time ordered data.

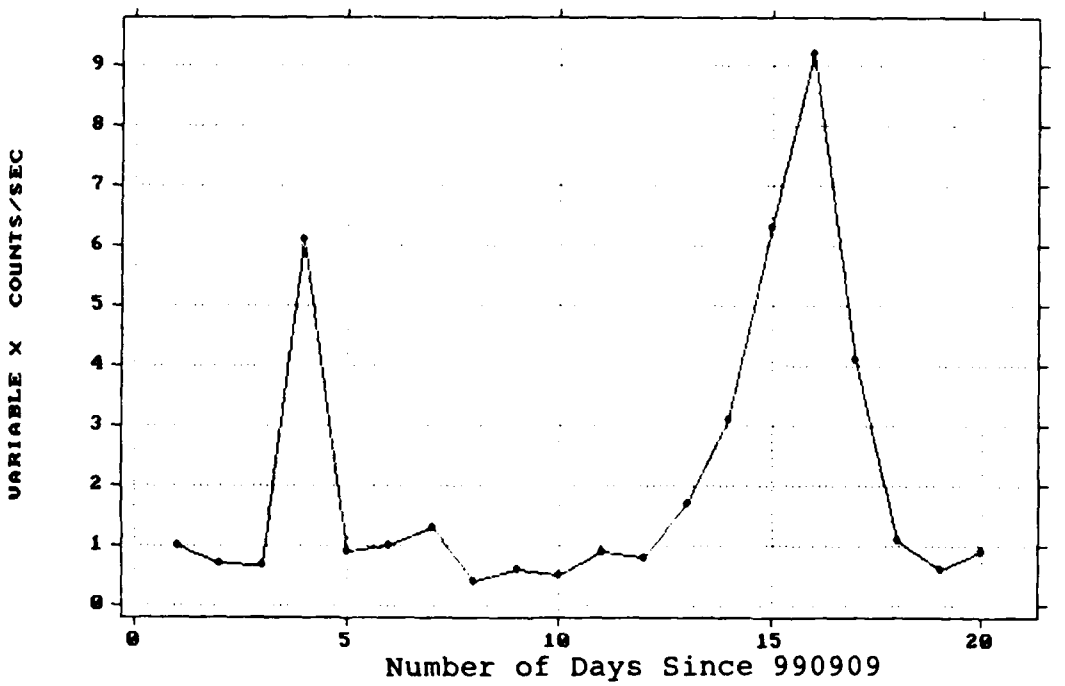

Figure 3: Plot of Daily Average Count Rate for Variable X

Once the top twenty-five "events" for each of the six variables had been designated, the number of occurrences of "five-channel events" were determined. A "five-channel event" was defined as an "event" occurring in all five high energy electron channels. A "five-channel event" must also have had all separate channel "events" occurring within a two day time period.

With all "five-channel events" identified, the data was next examined for the occurrence of a solar wind trigger. A solar wind trigger was defined as any solar wind "event" (not necessarily a top twenty-five "event") occurring four days prior or closer to the "five-channel event". The "five-channel event" date, trigger velocity, net velocity rise from "event" minimum to "event" maximum, and trigger occurrence (date) were recorded. The results of Approach 3 were presented in tabular form.

V. Results of the Analysis

Daily Average Plots

1979-1981 Data

The analysis of the plots of consecutive daily averages reveals some interesting points. The SEESSD channel shows the greatest amount of variability among the five high energy electron channels. Figure 4 depicts the daily average plot for the first 358 days of the SEESSD channel.

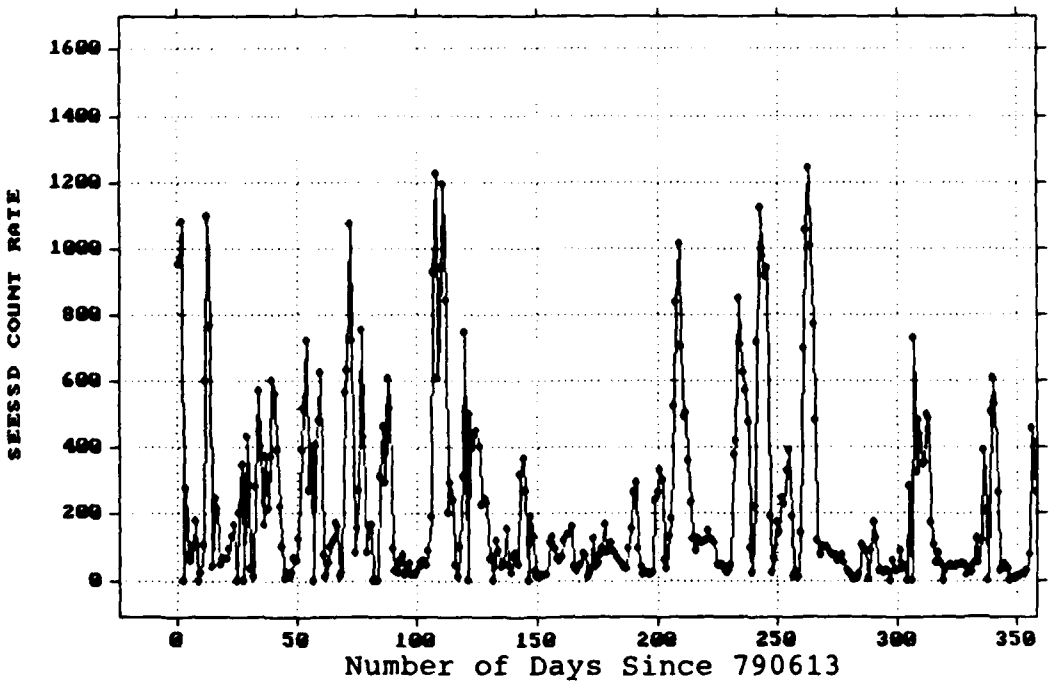

Figure 4: Plot of Original SEESSD Daily Averages for 1979-1981 Data Set

All other daily average plots for the 1979 data set were done in the exact same format and can be found in Appendix A. The initial inspection of these plots gives the

following results: In the SEESSD channel, the variability is by far the most pronounced. Numerous events occur within the SEESSD channel and can be easily identified. There appears to be no predictable behavior present in the SEESSD events. However, the last 150 days (days 550-700) of the SEESSD daily average plot is of interest. Visual analysis of the graph reveals the systematic occurrence of five events each occurring approximately twenty-seven days apart. This 27-day periodicity tends to indicate that some long-term solar phenomenon (the sun rotates on its axis once every twenty-seven days) is causing these repetitive SEESSD events.

Other researchers have also reported the occurrence of 27-day periodicity in high energy electron activity. Paulikas and Blake in a study conducted on similar data over ten years ago noticed this same phenomenon. They noted that event occurrences in the high electron channels were associated with the 27-day solar rotation period (16:22). Baker and others in a separate report done at the Los Alamos National Laboratory in 1985 also reported that "highly relativistic electron events occur with a relatively regular 27-day periodicity" (4:1).

Moving up in energy to the SEE1 channel, it is obvious that event occurrences drop-off substantially. The events in the SEE1 channel are of much smaller magnitude and there are fewer than for the SEESSD channel. Twenty events

are readily discernable from the SEE1 channel while more than thirty are evident in the SEESSD data. Continuing to move upward in energy, the SEE2 plot of daily averages looks remarkably similar to the SEE1 plot. Seventeen events are identifiable. All SEE2 events appear to match up with SEE1 events.

The top two energy chanels, SEE3 and SEE4, exhibit trends substantially different from the lower three energy channels, but similar among themselves. Either channel shows only a few discernable events with the relative variability in the daily averages appearing to mask any event occurrence. One important quality of the SEE3 and SEE4 plots is that both plots show a downward trend is present in the daily count rates for these two upper energy channels. Neither the SEESSD, SEE1, nor the SEE2 channel exhibits this downward bias.

Also exhibiting a trend is the solar wind plot. For the first 500 days, the solar wind remains within a narrow range of 300-600 km/sec and shows no systematic trends. The last 200 days of the solar wind data indicates a change from the behavior of the previous 500 days. The baseline solar wind velocity increases from the mid-300 km/sec range to the mid-400 km/sec range. This upward trend in the baseline solar wind velocity is in direct contrast to the downward trend evident in both the SEE3 and SEE4 channels. With the exception of this baseline increase, the magnitude of the

solar wind modulation appears to remain constant throughout the 1979-1981 time period.

1983-1985 Data

The daily average plots for the 1983-1985 data exhibit some decidedly different characteristics from their 1979-1981 counterparts. All five electron channels and the solar wind show much more modulation. An excellent example of this occurs in the plots of days 350-706 for the SEE1 channel. The SEE1 plot of days 350-706 for the 1979-1981 data shows virtually no modulation with only a handful of events discernable. In contrast, the 1983 data shows much greater variation: more than twenty events are easily identifiable. This substantial increase in modulation for the 1983-1985 data is depicted in Figure 5. All daily average plots for the 1983 data set were similarly done and can be found in Appendix A.

The comparison of Figure 5 versus its 1979 counterpart shows that the modulation of the SEE1 channel is substantially greater for the 1983-1985 data. Maximum amplitude for the SEE1 channel is 32.984 counts/sec versus a maximum amplitude of 9.189 counts/sec for the 1979-1981 data set.

As was seen in the 1979 data set, the SEESSD channel shows the greatest variability. SEESSD events in the 1983 data set appear to occur at random with no apparent

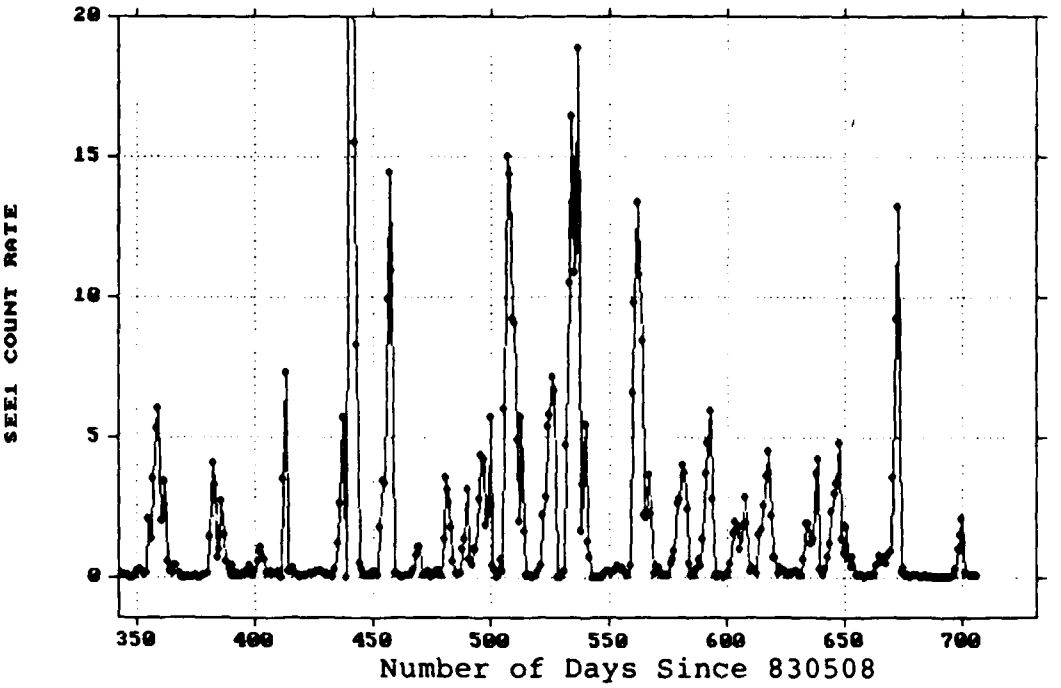

Figure 5: Plot of Original SEE1 Daily Averages for 1983-1985 Data Set

long-term trend. A visual analysis of the SEESSD, SEE1, and SEE2 channels reveals some obvious similarities among these lower three energy channels. Thirty events are easily identifiable in any of these lower three channels. Every event in both the SEE1 and SEE2 channels can be mapped to a corresponding event in the SEESSD channel. This was not the case with the 1979-1981 data.

Another striking difference between the 1979 data set and the 1983 data set occurs in the behavior of the two upper energy channels, SEE3 and SEE4. Both of these channels show an upward trend in count rate with the SEE4 channel showing a much stronger upward movement than the SEE3 channel. This upward trend is opposite to the obvious

downward trend in these upper two energy channels for the 1979 data set. The second visible difference concerns the modulation of both the SEE3 and SEE4 channels. SEE3 and SEE4 modulation has substantially increased. The average count rate for these two channels no longer remains relatively constant with only a few events, but now exhibits a multitude of events. Approximately twenty-five events are discernable from either daily average plot with virtually all SEE4 events occurring with an SEE3 event of a similar relative magnitude.

The plot of solar wind daily average velocity for the 1983-1985 time period was the hardest to analyze. Systematic data drop-outs caused by IMP-8's orbit in and out of the unobstructed solar wind, made for daily average plots which contain many missing values. Despite this substantial data drop-out (approximately 40%) some interesting points can be made about the solar wind for this time period. The modulation of the solar wind appears to increase as we approach the minimum of Solar Cycle 21. Also, the mean solar wind velocity appears to be nearly 80 km/sec higher (481 vs 402 km/sec) than for the 1979-1981 data set . Based on these pronounced changes in solar wind characteristics, it is likely that the increases in solar wind modulation and velocity were factors in determining the greater modulation of all five high energy electron channels for the 1983-1985 time period.

Distribution Identification

The investigation into and identification of distribution types can be a very challenging and laborious task. That statement was definately true for both the 1979 and 1983 data sets.

Min, Mean, Max, and Standard Deviation

1979-1981 Data

The results of the min, mean, max, and standard deviation analysis of the 1979-1981 time period are presented in Table I. Similar values for the 1983-1985 data are presented in Table II.

TABLE I

1979-1981 DATA CHARACTERISTICS

VARIABLE	UNITS	MIN	MEAN	MAX	STD DEV
SEESSD	counts/sec	3.68	214.07	1587.67	255.55
SEE1	counts/sec	0.05	0.38	9.19	0.75
SEE2	counts/sec	0.04	0.07	0.73	0.05
SEE3	counts/sec	0.08	0.12	0.25	0.02
SEE4	counts/sec	0.15	0.23	0.30	0.03
SOLAR WIND	km/sec	261.78	402.49	808.33	76.34

From the analysis of these four statistical measures, it is apparent that all five electron channels and the solar wind are right-skewed distributions. SEE2 and SEE3 appear to be the most peaked of the skewed distributions as the mean for both of these channels is very

near distribution minimums and their respective standard deviations are extremely small.

TABLE II

1983-1985 DATA CHARACTERISTICS

VARIABLE	UNITS	MIN	MEAN	MAX	STD DEV
SEESSD	counts/sec	3.41	254.25	2710.30	380.71
SEE1	counts/sec	0.04	1.23	32.98	3.12
SEE2	counts/sec	0.04	0.13	2.62	0.24
SEE3	counts/sec	0.08	0.11	0.29	0.03
SEE4	counts/sec	0.18	0.25	0.40	0.03
SOLAR WIND	km/sec	308.80	480.84	760.60	99.37

SEESSD and SEE1 both exhibit an interesting trait in that each have standard deviations which are greater than their respective means. Only SEE4 and solar wind velocity possess min, mean, max, and standard deviation characteristics which may indicate a normal distribution.

1983-1985 Data

The examination of the 1983 data set shows some enlightening results. All five high energy electron channels and the solar wind show across-the-board increases in mean, max, and standard deviation from their 1979-1981 results. The only exceptions were the mean for SEE3 which decreased to 0.11 counts/sec from 0.12 counts/sec and the maximum for the solar wind velocity which decreased to 760 km/sec from 808 km/sec. Also of interest is the fact that

the minima decreased for the SEESSD, SEE1, SEE2, and SEE3 channels. Only slight rises in minimum values were recorded for the SEE4 channel and the solar wind. Overall, these descriptive results indicate that the 1983-1985 data exhibits much more modulation than does the corresponding 1979-1981 data.

Frequency and Probability Plots

1979-1981 Data

The visual analysis of the frequency plots reveals what was uncovered in the Min, Mean, Max, and Standard Deviation section. Figure 6 depicts solar wind relative frequency counts versus solar wind velocity.

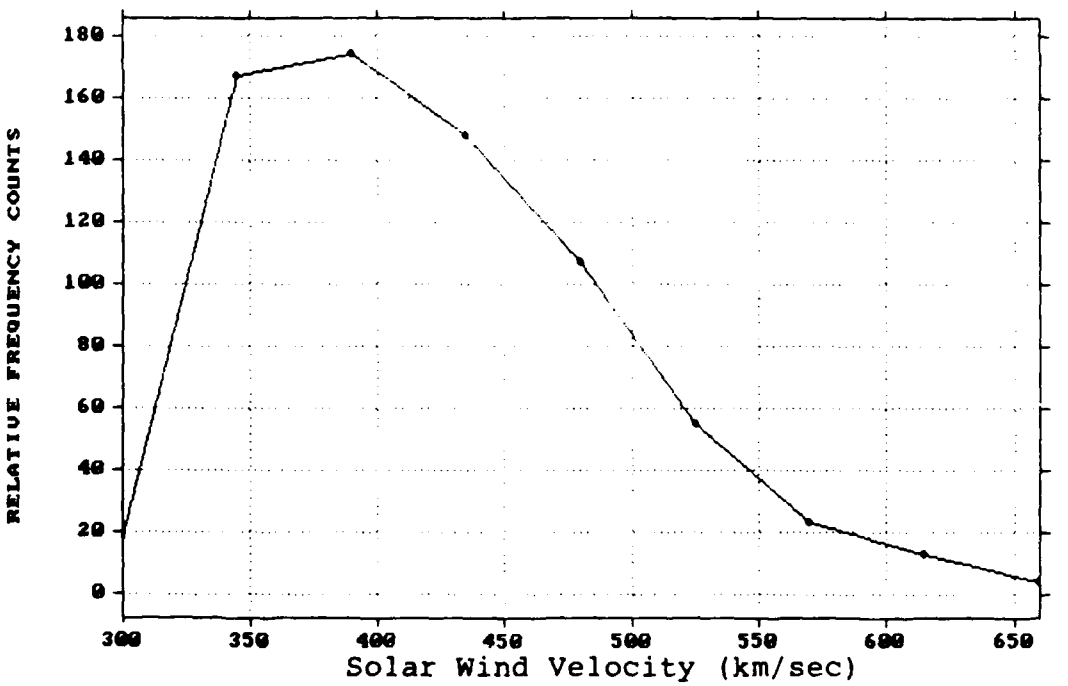

Figure 6: Frequency Plot of Solar Wind Data for 1979-1981 Data Set

All high energy electron and solar wind distributions are skewed right and have substantial tail populations. The solar wind frequency plot indicates that the solar wind may belong to the lognormal family of distributions.

For this frequency plot, each velocity bin is 45 km/sec wide. The first bin starts at 300 km/sec and bins progress at 45 km/sec intervals ending at 660 km/sec. All other similarly constructed frequency plots for the 1979 data set can be found in Appendix B.

The accompanying probability plot for the solar wind assuming a lognormal distribution is presented in Figure 7.

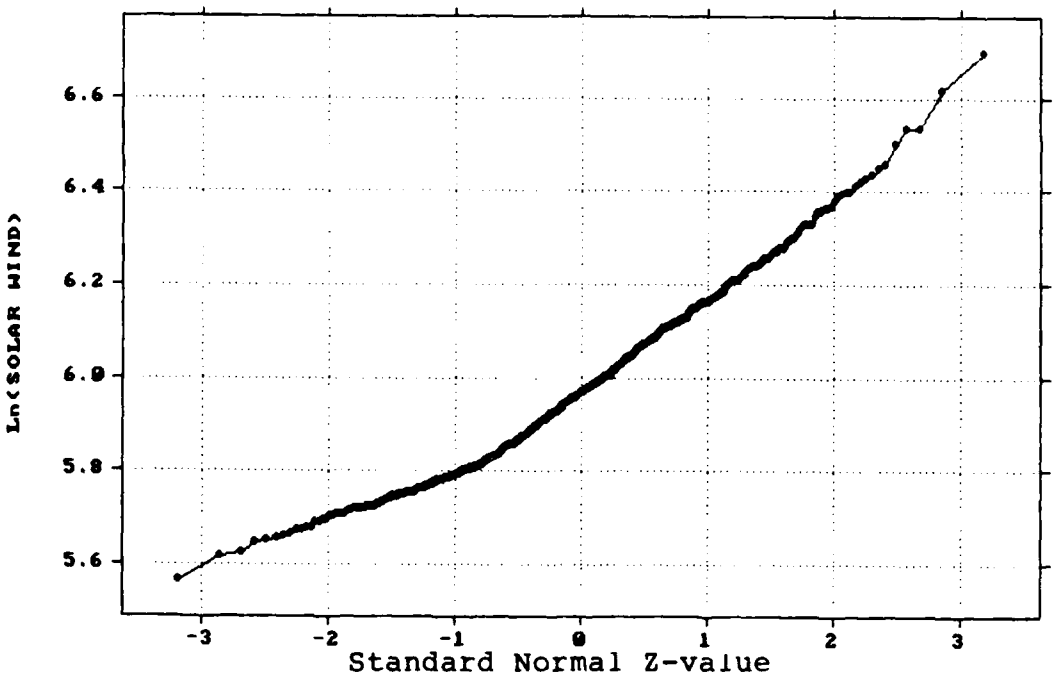

Figure 7: Probability Plot of Solar Wind Velocity Data for 1979-1981 Data Set

The relatively linear graph of the natural logarithm of solar wind velocity, Ln(Solar Wind), versus standard normal Z-values indicates that the underlying data (solar wind) is very likely lognormally distributed. All probability plots for the 1979-1981 data can be found in Appendix C.

The frequency plots for SEESSD, SEE1, and SEE2 show similar characteristics. All three are heavily populated near their minima and all have substantial right-sided tails. Exponential and normal probability plots for these three channels had no linear sections whatsoever. Lognormal probability plots showed the greatest linearity. SEESSD is very likely lognormally distributed, while SEE1 and SEE2 behavior may be classified by two separate lognormal distributions as evidenced by the sharp changes in slope on their respective probability plots. Each plot has two linear sections with an abrupt transition section between the two.

The investigation of high energy electron frequency plots shows a possible split from the three lower energy distribution types. Both, SEE3 and SEE4 exhibit bimodal characteristics. The SEE3 and SEE4 frequency plots are double humped with the first peak larger than the second. As with SEE1 and SEE2, the SEE3 and SEE4 probability plots of Ln(SEE3) and Ln(SEE4) versus Z-values show decidedly linear sections with abrupt transition zones. It is possible that SEE3 and SEE4 can each be characterized by two

separate lognormal distributions as evidenced by the sharp change in slope on their respective probability plots..

1983-1985 Data

As with the 1979 data set, a case can be made to show that all six variables possess qualities of a lognormal distribution. SEE4 and the solar wind have frequency plots most strongly resembling lognormal distributions. Figure 8 shows the relative frequency history for the SEE4 channel. All remaining 1983 data set frequency plots can be found in Appendix B. The 1983 SEE4 frequency distribution shows a substantial change from the bimodal characteristic of the 1979 plot.

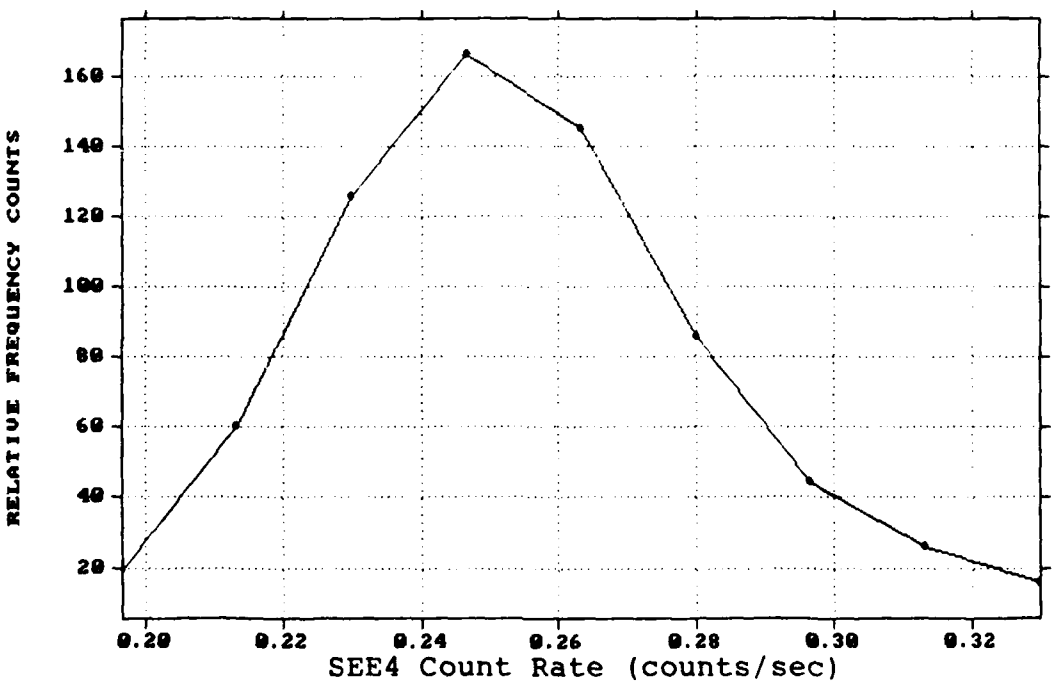

Figure 8: Frequency Plot of SEE4 Data for 1983-1985 Data Set

However, just as for the 1979-1981 data, the probability plots for both the solar wind and SEE4 indicate that the underlying data is most likely lognormally distributed. Figure 9 depicts the SEE4 normal probability plot for the natural logarithm of SEE4 count rate. The SEE4 probability plot is similar to the solar wind plot. Both show linearity with the SEE4 plot being slightly more linear. The remainder of the 1983-1985 probability plots are located in Appendix C.

The graph of relative frequency counts for SEESSD, SEE1, SEE2, and SEE3 show similar traits. All have substantial right-sided tails with SEE2 showing the most

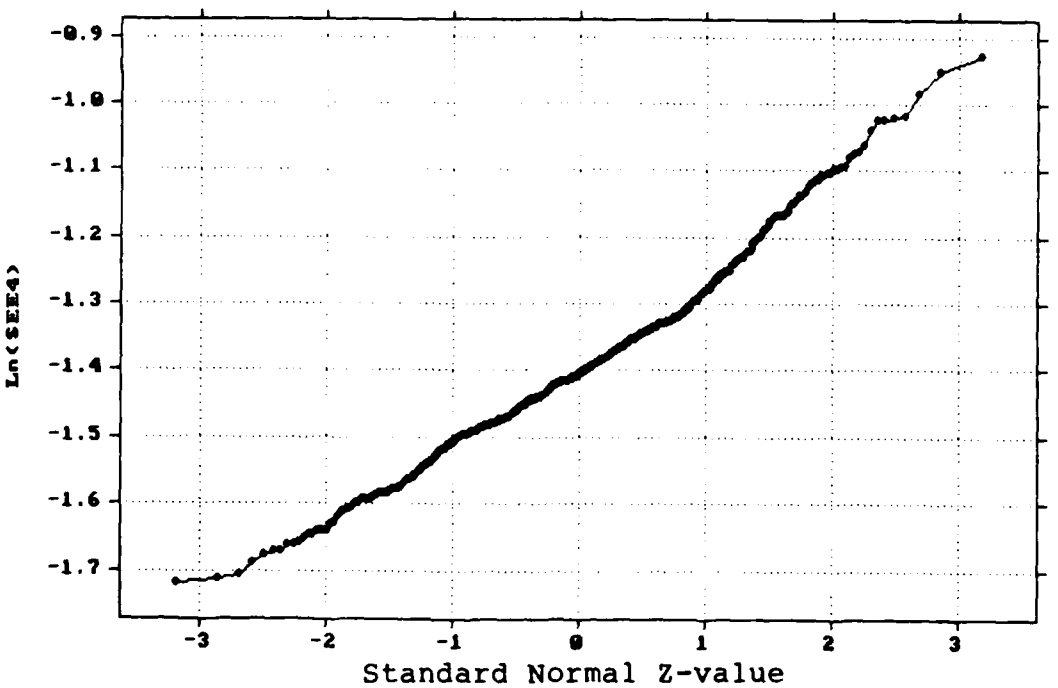

Figure 9: Probability Plot of SEE4 Data for 1983-1985 Data Set

peakedness. Of the three probability plots (normal, exponential, and lognormal) constructed for each channel, the lognormal probability plots showed the largest linear sections. Just as for the 1979-1981 data, SEE1 and SEE2 each have two distinct linear regions indicating the possibility of two lognormal distributions working together to characterize SEE1 and SEE2 events. SEESSD can most likely be represented by a single lognormal function, while SEE3 is apparently neither an exponential nor a normal distribution with lognormal being the most probable of the three.

In summary, the results of the frequency and probability plot section for both the 1979-1981 and 1983-1985 data sets indicate that all five high energy electron channels and the solar wind may best be characterized as having some type of lognormal distribution.

Now that the distributions of all six variables have been investigated and classified, the analysis turns to the actual correlation of solar wind velocity to high energy electron count rate. The format of result presentation for Approaches 1, 2, and 3 will be as follows: The results of all three Approaches (1, 2, and 3) for the 1979-1981 data will be presented first followed by the results for the 1983-1985 data.

1979 Data Set

Approach 1 (Original Data)

The linear correlation analysis done on all five high energy electron channels with current and lagged solar wind values generated R-Squared values less than 0.25. The significance level for all correlations as determined by SAS' computations of two-sided P-values were all less than 0.01. These very low P-values indicate that all correlations were statistically significant.

The calculated R-Squared values for all five electron channels versus solar wind lags are presented in Table III. The correlation results presented in Table III

TABLE III

1979-1981 DATA
R-SQUARED VALUES OF SOLAR WIND LAGS vs HIGH ENERGY ELECTRONS
(NOTE: Results are for Original Data)

SOLAR WIND	SEESSD	SEE1	SEE2	SEE3	SEE4
0-DAY LAG	0.03933	0.02166	0.00563	0.05172	0.09211
1-DAY LAG	0.17218	0.08420	0.02759	0.02066	0.05455
2-DAY LAG	0.24947	0.13070	0.04184	0.01383	0.04062
3-DAY LAG	0.19052	0.12966	0.04403	0.01795	0.04193
4-DAY LAG	0.11139	0.10772	0.04110	0.02019	0.04147

are very similar to the results reported by Smith in 1983 and McCormick in 1984 in their respective theses. These low R-Squared values, less than 0.25, imply that only weak

correlations exist between solar wind velocity and high energy electron count rates.

The SEESSD channel showed the highest correlation with solar wind velocity (R-Squared = 0.249). Stated in a different way, an R-Squared value of 0.249 implies that 24.9% of the variation in SEESSD count rate can be explained by the variation in solar wind velocity. This SEESSD R-Squared value of 0.249 occurred with two-day old solar wind data.

SEE1 and SEE2 also showed their highest correlation with two-day old solar wind velocity. R-Squared values were 0.131 and 0.042 respectively. Despite these very low determination coefficients, it is apparent that the three lowest electron channels are influenced, though very slightly, by the two-day old solar wind.

An excellent means of showing the relationship between two variables is to construct a scatter plot. Figure 10 is a scatter plot of SEESSD count rate versus two-day solar wind lag velocity. The data presented in Figure 10 has an R-Squared value of 0.249.

If a strong relationship were to exist between SEESSD count rate and solar wind velocity, the scatter plot would show some type of curvilinear trend (i.e., linear, exponential, etc) between the two variables. Due to the trendless nature of Figure 10, it is apparent that solar wind velocity has minimal direct impact on SEESSD count

rate. Scatter plots of original data for both the 1979 and 1983 data sets with R-Squared values greater than 0.10 can be found in Appendix D.

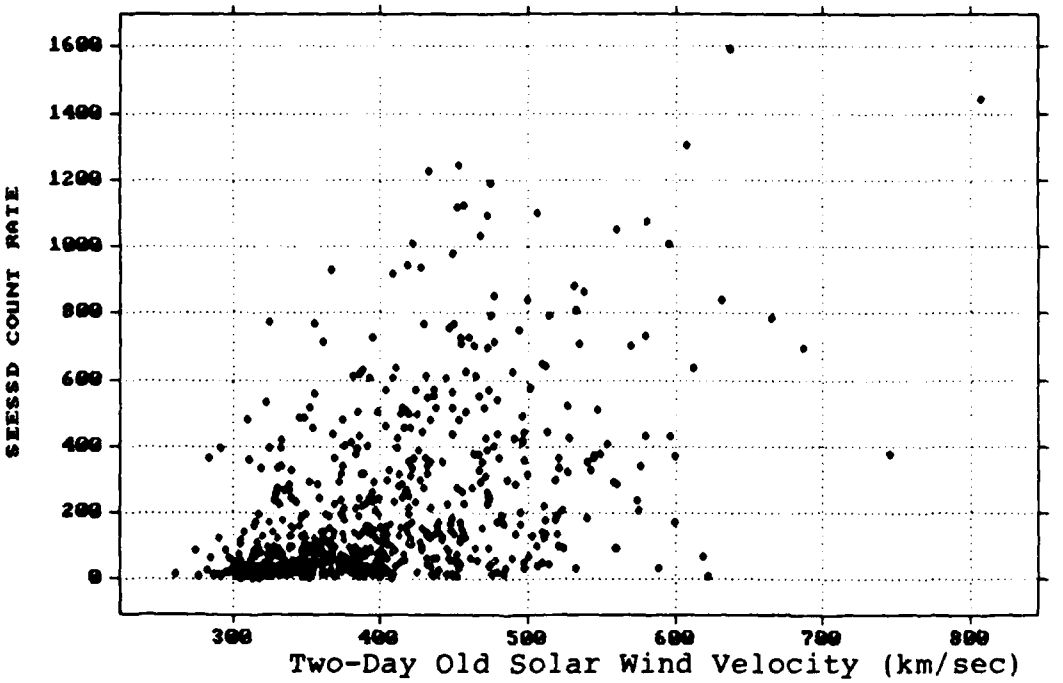

Figure 10: Scatter Plot of 2-Day Old Solar Wind Velocity vs SEESSD Count Rate for 1979-1981 Data Set

SEE3 and SEE4 exhibited different correlation characteristics than did the three lowest energy channels. The correlation coefficient, R, for both SEE3 and SEE4 with solar wind was negative (the R values for SEESSD, SEE1, and SEE2 were all positive). A negative R value indicates an inverse relationship between solar wind velocity and electron count rate. This negative correlation was expected. It was discovered during the analysis of daily average plots that both SEE3 and SEE4 exhibit downward

trends while the solar wind baseline was relatively constant or trended upward. This difference would induce a negative correlation coefficient between SEE3 or SEE4 count rate and solar wind velocity. As a result of these opposing trends, both SEE3 and SEE4 correlated best with current solar wind values. R-Squared values were 0.052 and 0.092 respectively.

Approach 2 (Percentiled Data)

The percentiling of data did have an effect on R-Squared values. Table IV presents the correlation results for the percentiled data.

TABLE IV

1979-1981 DATA
R-SQUARED VALUES OF SOLAR WIND LAGS vs HIGH ENERGY ELECTRONS
(NOTE: Results are for Percentiled Data)

SOLAR WIND	SEESSD	SEE1	SEE2	SEE3	SEE4
0-DAY LAG	0.03553	0.01811	0.01501	0.08146	0.09773
1-DAY LAG	0.16708	0.11234	0.00036	0.04017	0.05780
2-DAY LAG	0.26690	0.21237	0.00951	0.02577	0.04204
3-DAY LAG	0.22825	0.19700	0.00681	0.02762	0.04369
4-DAY LAG	0.15345	0.13991	0.00210	0.02900	0.04522

The largest increase in R-Squared value over the results for the original data was measured in the SEE1 channel. The SEE1 R-Squared value for two-day old solar wind velocity was increased from 0.131 to 0.212. Figure 11 plots the R-Squared values of the SEE1 channel for the original and

percentiled data versus solar wind lag days. Similar increases in R-Squared were recorded across all electron channels with the exception of SEE2.

The SEE2 channel showed some interesting correlation results. The original data showed the characteristic rise in R-Squared value reaching a maximum with two-day solar wind lag. However, the percentiled data showed a substantially different trend.

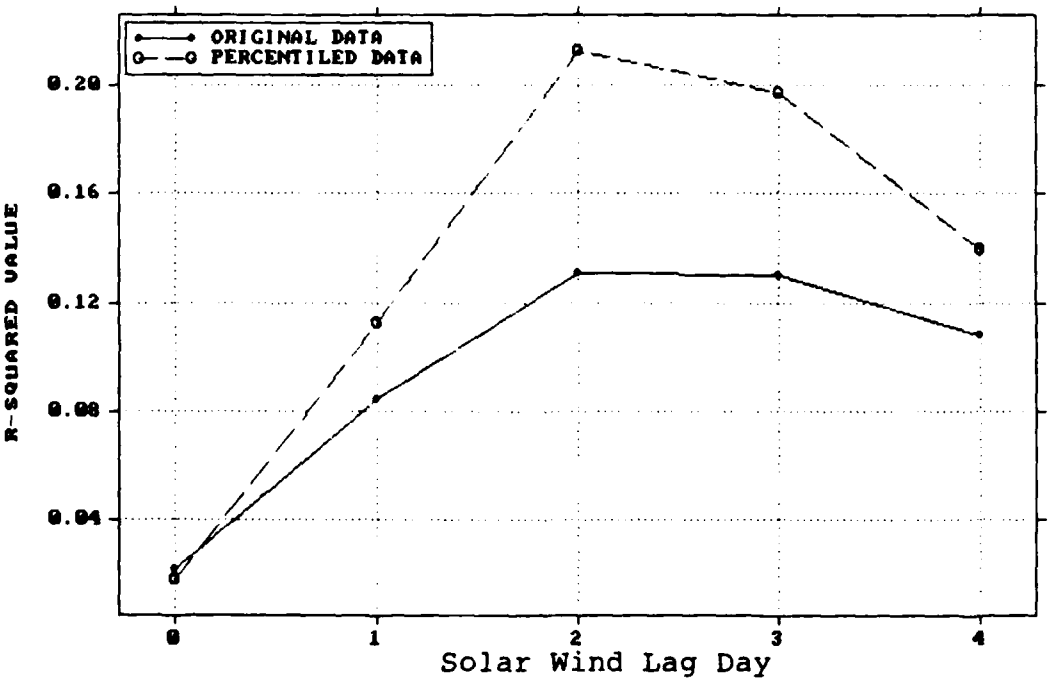

Figure 11: Plot of R-Squared Values for Both Original and Percentiled SEE1 Data vs Solar Wind Lags for 1979-1981 Data Set

The SEE2 percentiled data showed almost the exact same behavior as the SEE3 and SEE4 channels. All three achieved maximum R-Squared values with current solar wind velocity. All three showed decreasing R-Squared values for

increasing solar wind lag days. This split in R-Squared trends for SEE2 original versus percentiled data suggests that the SEE2 series of daily average count rates has characteristics of both the two upper energy channels and the two lower channels. The remaining plots of R-Squared values vs solar wind lag days for the 1979 data set can be found in Appendix E.

The lowest energy channel's (SEESSD) scatter plot of two-day old solar wind percentiles versus SEESSD percentiles shows no striking trend. Figure 12 depicts percentiled two-day old solar wind velocities and plots them against

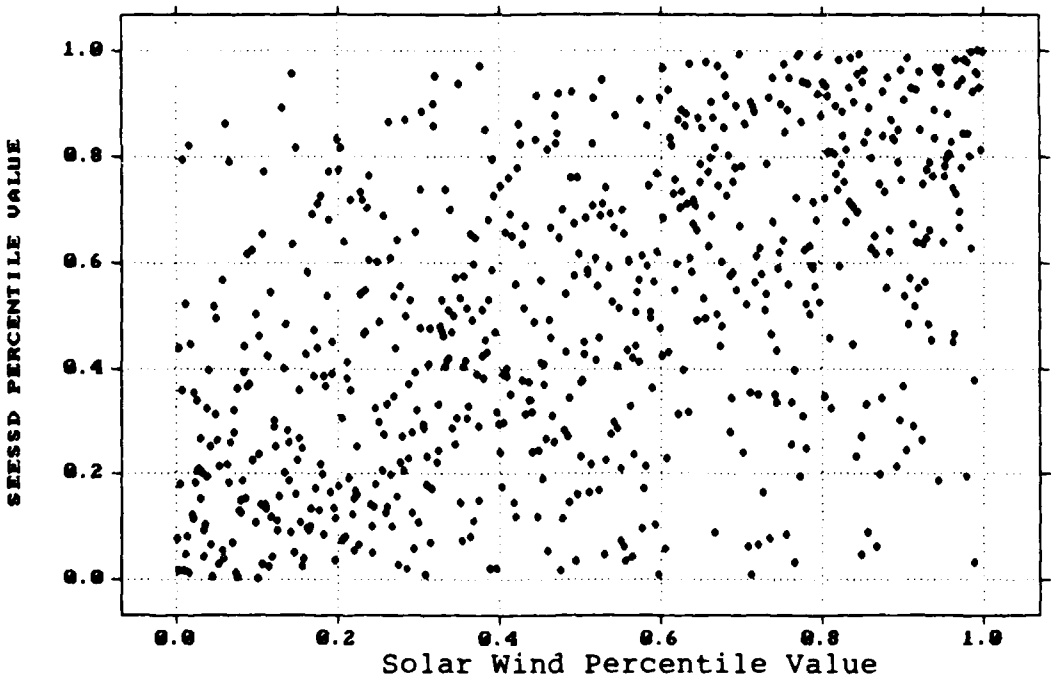

Figure 12: Scatter Plot 2-Day Old Solar Wind Percentile Values vs SEESSD Percentile Values for 1979-1981 Data

percentiled SEESSD count rates. The R-Squared value for this graph is 0.267. Appendix D contains scatter plots of percentiled data for both the 1979 and 1983 data sets with R-Squared values greater than 0.10.

The important picture to remember from Figure 12 is the lack of points in the upper left and lower right corners of the plot. This lack of points in opposite extremes indicates that low solar wind percentile readings do not coincide with high percentile SEESSD readings or vice versa. The high density of points in the lower left and upper right tell a different story. This bunching of points in similar corners shows that low percentile SEESSD events seem to occur with low solar wind events and high SEESSD events seem to occur with high solar wind events. This trend indicates that the solar wind does have some ability, though apparently small, to modulate SEESSD count rates.

Approach 3 (Event Analysis)

Approach 3 investigates the "event" nature of both high energy electron count rates and solar wind velocities. Approach 3's independent identification of the top twenty-five events in each of the five electron channels yielded some noteworthy results. Of the events identified for each channel there were seven occurrences of five-channel events. This translates into a 28% likelihood that an event in one channel is part of a five-channel

event. Solar wind triggers (a systematic rise and fall in solar wind daily average velocity) were able to be identified for six of the seven five-channel events; satellite data gaps precluded identifying a seventh trigger. The average solar wind trigger velocity was 567.86 km/sec, an average velocity of more than two standard deviations above the mean (See Table I). Table V presents the results of the five-channel event identification for the 1979 data set.

TABLE V

1979-1981 DATA
FIVE-CHANNEL EVENT IDENTIFICATION RESULTS
(NOTE: "Data Gap" indicates missing satellite data)

EVENT #	DATE	TRIGGER VELOCITY	VELOCITY NET RISE	TRIGGER OCCURRENCE
1	790614	Data Gap		
2	790625	473.54	150.44	2-Days Prior
3	790805	454.43	98.34	2-Days Prior
4	800107	632.15	227.94	3-Days Prior
5	800210	477.47	149.24	3-Days Prior
6	800301	561.24	253.53	3-Days Prior
7	810425	808.33	378.91	2-Days Prior
	AVERAGE	567.86	209.72	2-3-Days Prior

Also of note is the net solar wind velocity rise and trigger occurrence. A net velocity rise from event minimum to event maximum of an average 209.72 km/sec indicates that the solar wind experienced dramatic velocity increases over a relatively short time. These adrupt velocity changes

reached their maximum amplitudes, as evidenced by trigger occurrence, approximately two to three days prior to all five-channel events. These results show that as solar wind velocity dramatically increases, high energy electron count rates are also driven higher with an approximately two to three day lag period.

1983 Data Set

Approach 1 (Original Data)

The correlation analysis done on the 1983 data set revealed across-the-board increases in R-Squared values over the results for the 1979 data set. Table VI presents the SAS calculated R-Squared values for all five electron channels versus various solar wind lag days.

TABLE VI

1983-1985 DATA
R-SQUARED VALUES OF SOLAR WIND LAGS vs HIGH ENERGY ELECTRONS
(NOTE: Results are for Original Data)

SOLAR WIND	SEESSD	SEE1	SEE2	SEE3	SEE4
0-DAY LAG	0.05791	0.02046	0.02022	0.03929	0.02982
1-DAY LAG	0.24540	0.10244	0.08966	0.18713	0.13242
2-DAY LAG	0.36196	0.23563	0.21149	0.30818	0.20439
3-DAY LAG	0.26707	0.20013	0.17205	0.23653	0.15417
4-DAY LAG	0.12930	0.10242	0.08860	0.09049	0.07573

Admittedly, the maximum R-Squared achieved of 0.362 is still somewhat small by statistical standards, however it is an

increase of almost forty-five percent over the maximum R-Squared value documented from the 1979-1981 data.

As with the 1979 data set, the SEESSD channel showed the highest R-Squared value. An R-Squared value of 0.362 was achieved when SEESSD count rate was correlated with two-day old solar wind data. An easy way of showing the visual significance of a 0.362 determination coefficient is to construct a scatter plot of the two variables. Figure 13 is such a scatter plot. It plots SEESSD count rate versus two-day old solar wind velocity.

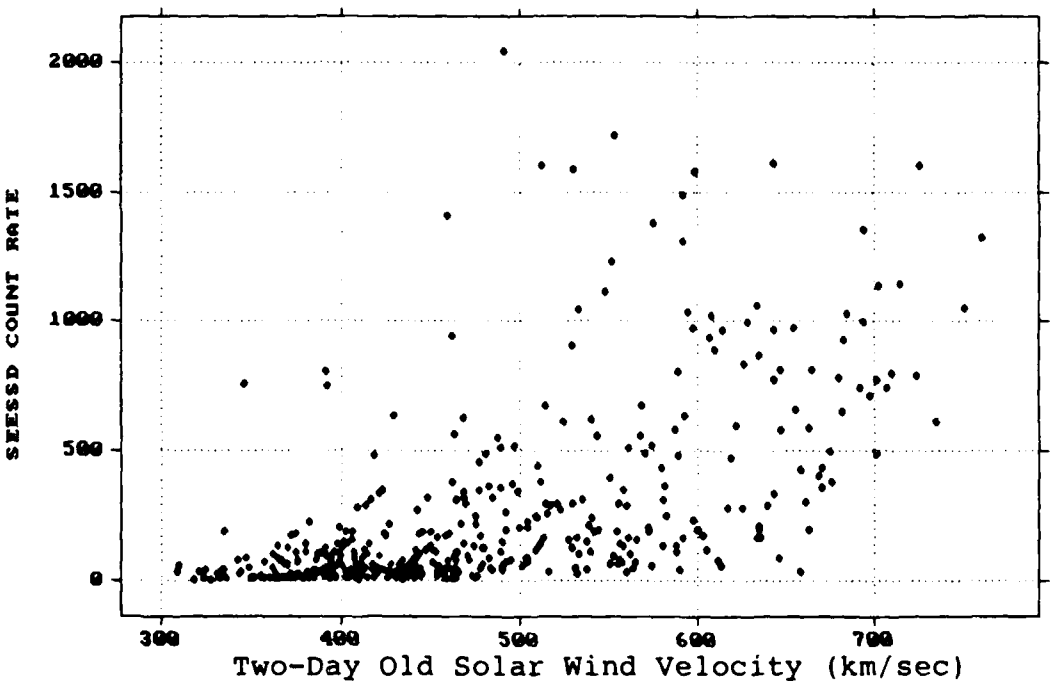

Figure 13: Scatter Plot of 2-Day Old Solar Wind Velocity vs SEESSD Count Rate for 1983-1985 Data Set

SEE1 and SEE2 also showed stronger correlations with solar wind for the 1983-1985 time period. SEE1's R-Squared

value with the two-day old solar wind increased to 0.236 from its 1979 value of 0.131. SEE2's determination coefficient rose sharply as well, rising from 0.042 to 0.211, an increase of over 400 percent.

Showing the most significant and dramatic difference in correlation results were the two upper energy channels, SEE3 and SEE4. For the 1979 data set, both SEE3 and SEE4 exhibited their best correlations with current solar wind velocity. This was not the case with the 1983-1985 data. Just as for the lower three energy channels, SEE3's and SEE4's maximum R-Squared value occurred with two-day old solar wind data. SEE4's determination coefficient rose from 0.041 to 0.204 while SEE3's R-Squared value showed a spectacular increase, rising from 0.014 to 0.308, a twenty-two fold advance.

Also of significance were the R-values themselves. For the 1979 data the R-values for both SEE3 and SEE4 were negative indicating an inverse relationship with solar wind velocity. That trend was completely reversed for the 1983-1985 data. R-values were positive for all energy channels. These positive correlation coefficients show that the solar wind had a direct relationship with electron count rates for the 1983-1985 time period.

Approach 2 (Percentiled Data)

Just as for the 1979 data set, the percentiling of electron count rates and solar wind velocity significantly changed the R-Squared values recorded for the original data. Table VII shows the R-Squared values calculated from the percentiled data. These results can be broken into two categories.

The first category encompasses those high energy electron channels which showed increased R-Squared values

TABLE VII

1983-1985 DATA
R-SQUARED VALUES OF SOLAR WIND LAGS vs HIGH ENERGY ELECTRONS
(NOTE: Results are for Percentiled Data)

SOLAR WIND	SEESSD	SEE1	SEE2	SEE3	SEE4
0-DAY LAG	0.11076	0.06215	0.03179	0.01942	0.01261
1-DAY LAG	0.41560	0.33013	0.25661	0.14590	0.08281
2-DAY LAG	0.46089	0.43407	0.35257	0.19297	0.11314
3-DAY LAG	0.29460	0.32677	0.26008	0.13080	0.07667
4-DAY LAG	0.15381	0.20273	0.16719	0.06512	0.03209

for percentiled data. SEESSD and SEE2 had R-Squared increases of 0.099 and 0.142 respectively. Similar to its 1979 results, SEE1 showed the largest increase in R-Squared value. SEE1 determination coefficient for percentiled data of two-day old solar wind versus SEE1 count rate rose from 0.236 to 0.434. Figure 14 shows the R-Squared trend of SEE1 original and percentiled data versus various solar wind lag

days. The remaining plots of R-Squared values for both original and percentiled data can be found in Appendix E.

Both SEE3 and SEE4, on the other hand, showed across-the-board decreases in coefficients of determination for percentiled data. SEE3's maximum R-Squared value, occurring with two-day old solar wind velocity, decreased to 0.193 from 0.308. SEE4 showed a similar reduction with its maximum R-Squared value decreasing to 0.113 from 0.204.

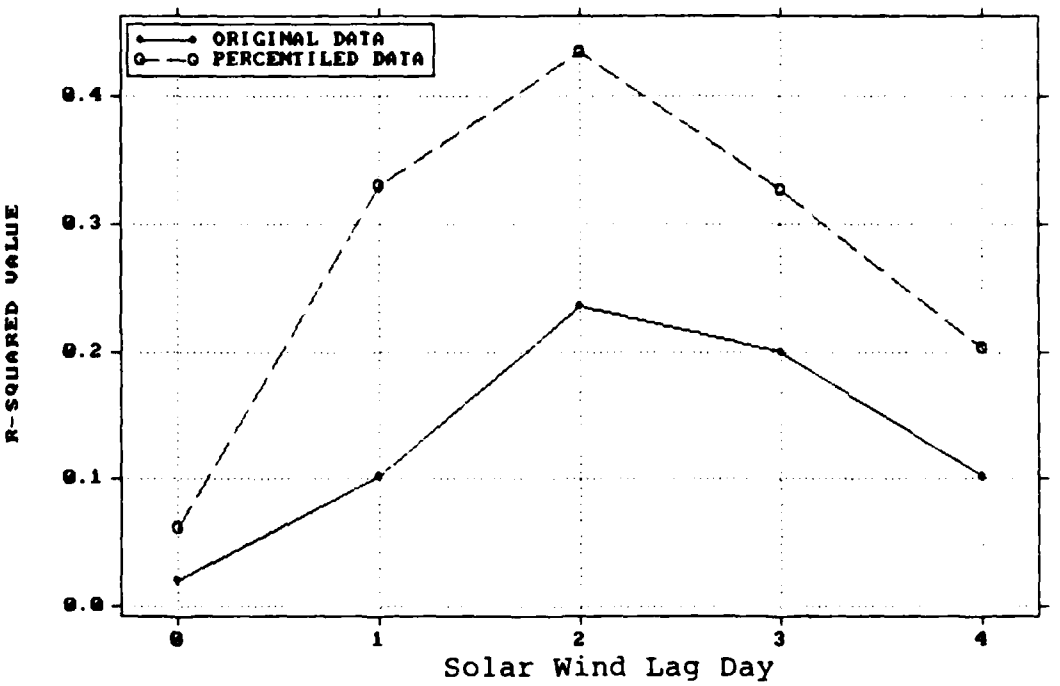

Figure 14: Plot of R-Squared Values for Both Original and Percentiled SEE1 Data vs Solar Wind Lags for 1983-1985 Data

Even though both upper energy channels exhibited decreases in R-Squared values for percentiled data, the correlation results for the 1983 data set did indicate that

the solar wind does appear to modulate all five high energy electron channels. The plots of R-Squared values versus solar wind lags for all five electron channels show that the solar wind's ability to predict electron count rate modulation is strongest for the SEESSD channel and decreases as electron energy increases.

Approach 3 (Event Analysis)

The results of the event analysis on the 1983 data set reinforced the event results of the 1979 data set. Of the twenty-five independently identified events, seventeen occurred simultaneously forming "five-channel" events. This equates to a sixty-eight percent probability that any one event was part of a larger five-channel event. From these seventeen events, ten had sufficient satellite data to show the occurrence of a solar wind trigger. The other seven five-channel events very likely had solar wind triggers of their own, however these events occurred at such a time that solar wind velocity data was not available from the IMP-8 satellite. The identified solar wind triggers for these seventeen events had an average velocity of 661.3 km/sec which is 1.81 standard deviations above the mean solar wind velocity of 480.84 km/sec (See Table II). The results of Approach 3 for the 1983 data set are shown in Table VIII.

The net velocity rise and trigger occurrence say something about solar wind behavior prior to all

five-channel events. The average rise in velocity for each solar wind trigger was 247.4 km/sec. This is almost twenty percent larger than the average velocity rise for the 1979-1981 solar wind triggers. Just as for the 1979 data set, solar wind triggers occurred roughly two to three days prior to the occurrence of five-channel electron events.

TABLE VIII

1983-1985 DATA
FIVE-CHANNEL EVENT IDENTIFICATION RESULTS
(NOTE: "Data Gap" indicates missing satellite data)

EVENT #	DATE	TRIGGER VELOCITY	VELOCITY NET RISE	TRIGGER OCCURRENCE
1	831123	Data Gap		
2	831208	610.7	189.0	2-Days Prior
3	831217	Data Gap		
4	840305	681.7	295.2	3-Days Prior
5	840406	Data Gap		
6	840428	Data Gap		
7	840721	Data Gap		
8	840806	607.1	214.7	4-Days Prior
9	840925	751.4	291.2	1-Day Prior
10	841014	Data Gap		
11	841025	Data Gap		
12	841119	576.0	134.3	3-Days Prior
13	841208	707.1	331.1	3-Days Prior
14	841220	598.7	230.2	2-Days Prior
15	850114	655.5	230.9	3-Days Prior
16	850213	665.0	259.2	3-Days Prior
17	850310	760.6	298.2	3-Days Prior
	AVERAGE	661.3	247.4	2-3-Days Prior

These event analysis results show that dramatic increases in solar wind activity culminating in a solar wind velocity approximately two standard deviations above its

mean do signal significant increases in high energy electron count rates, two to three days after peak solar wind event occurrence.

VI. Conclusions and Recommendations

Conclusions

The results of this study revealed several interesting facts about high energy electron count rate and solar wind activity. Many of these findings were the by-product of using two data sets: one at solar maximum (the 1979-1981 data set) and the other at solar minimum (the 1983-1985 data set). First, the plots of original data for both the 1979 and 1983 data sets showed that all five electron channels and solar wind velocity experienced much more modulation during the 1983-1985 time period (near solar minimum). Mean amplitude and standard deviation were higher for all six variables in the 1983 data set. Second, the upper two electron energy channels, SEE3 and SEE4, exhibited decidedly different behavior. For the 1979 data set, both showed very little modulation with their respective baseline count rates decreasing throughout the period. The 1983 data set showed a definate turnaround in SEE3 and SEE4 behavior. The modulation of both channels increased dramatically. Also of importance was the fact that for this time period (1983-1985), the baseline count rate for both SEE3 and SEE4 trended upward. In general, the analysis indicated that both SEE3 and SEE4 exhibit some type of cyclical rise and fall pattern, not in phase with the solar cycle. Third, the frequency and probability plots showed that all variables

with the exception of SEE3 and SEE4 exhibited similar distribution behavior for both the 1979 and 1983 data sets. In general, the frequency and probability plots indicated that it may be possible to classify all variable activity as being lognormally distributed.

The analysis of the extent of the correlation between solar wind velocity and high energy electron count rate also revealed some noteworthy findings. First, the filling-in of all solar wind data gaps, as was recommended in McCormick's thesis, did not significantly change the correlation results obtained by both Smith (1983) and McCormick (1984) in their respective theses. Maximum R-Squared for the 1979 data set was 0.249 which occurred for the SEESSD channel with two-day old solar wind values. Exhibiting different behavior from the three lower electron energy channels, SEE3 and SEE4 had negative correlations with solar wind data while both correlated best with current solar wind velocity. The 1983 data set showed significantly stronger correlations between solar wind velocity and all electron count rates. Just as the 1979 data set, the highest R-Squared values were achieved with two-day old solar wind values. For the 1983-1985 time period, the upper two energy channels, SEE3 and SEE4, correlated positively with solar wind velocity and behaved just as the lower three energy channels did (maximum R-Squared values occurring with two-day old solar wind data). Second, the percentiling of

data did increase R-Squared values for all variables with the exception of SEE2 for the 1979 data set and both SEE3 and SEE4 for the 1983 data set. Scatter plots of percentiled data did indicate that high percentile solar wind events do tend to occur with high percentile electron events. Third, the "event" analysis approach indicated that the occurrences of "five-channel" high energy electron events were preceded by dramatic rises in solar wind velocity two to three days prior to the occurrence of the "five-channel" event.

The ultimate goal of this thesis effort was to determine the extent of the correlation between high energy electron count rate and solar wind velocity, and to determine if the solar wind holds promise as a predictor of high energy electron events. This thesis has shown that solar wind velocities do correlate differently with high energy electron count rates depending on where in the solar cycle the solar wind events occur. It was also shown that two to three days prior to a significant rise in electron count rates for all five high energy channels, a significant rise in solar wind velocity occurred. Based on these findings and the results of the linear correlation analysis, solar wind does hold promise as a predictor of high energy electron events. However, due to the low correlation results achieved, it is likely that solar wind velocity is only one of several variables determining the occurrence and

magnitude of high energy electron events at earth geosynchronous altitude.

Recommendations

In the progression of this thesis, the author came across several areas that hold promise for future research. First, the "event" analysis (Approach 3) could be expanded. This expansion would include the construction of an indicator of available energy from solar wind fluctuations. Based on the available energy, this expansion would then determine the likely energy deposition and results thereof in the five high energy electron channels. This recommendation came about by the author's findings that small solar wind events appear to affect only the lower energy channels while large solar wind events affect all electron energy channels, i.e., are there threshold energy levels above which solar wind effects are felt in progressively higher electron energy channels?

The second recommendation concerns that of gamma rays and cosmic rays. From a physics standpoint, it is possible that photons of the gamma ray energy levels could strike molecules in the earth's extreme outer atmosphere and liberate high energy electrons. One gamma ray has sufficient energy for hundreds of these scattering events (where high energy electrons are liberated from their host molecules) to possibly occur. This second recommendation

would be to investigate the relationship between gamma/cosmic rays and high energy electron count rates.

And finally, due to the small R-Squared values encountered in this thesis, an alternative regression model could be investigated. Either a nonlinear model or a multiple regression model that involves more than one independent variable could be attempted to more effectively explain the variation in high energy electron count rates.

Appendix A: Plots of Original Data

Page

1979-1981 Data 70

1983-1985 Data 82

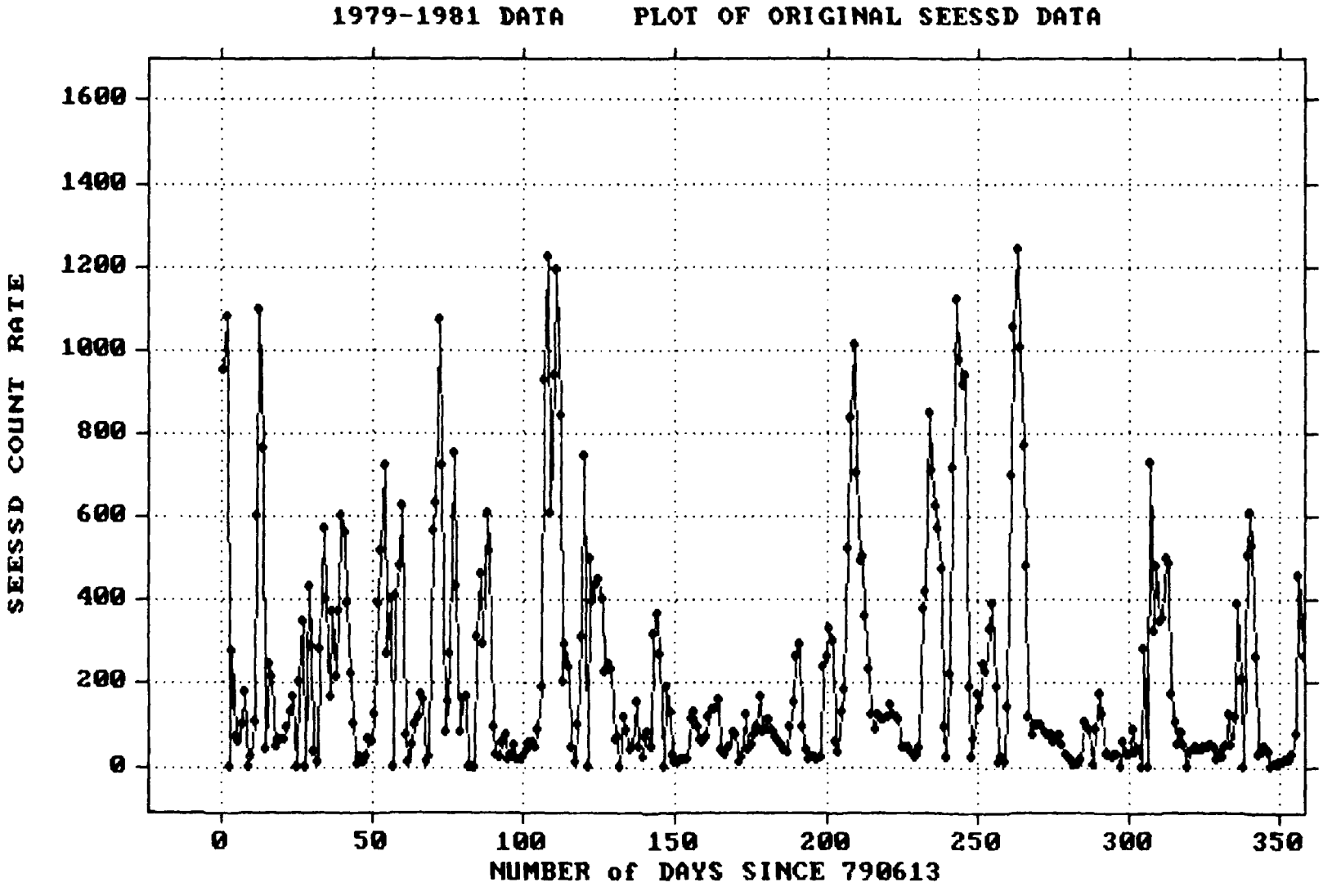
1979-1981 DATA PLOT OF ORIGINAL SEESSD DATA
SEESSD COUNT RATE
1600
1400
1200
1000
800
600
400
200
0
0
50
100
150
200
250
300
350
NUMBER of DAYS SINCE 790613

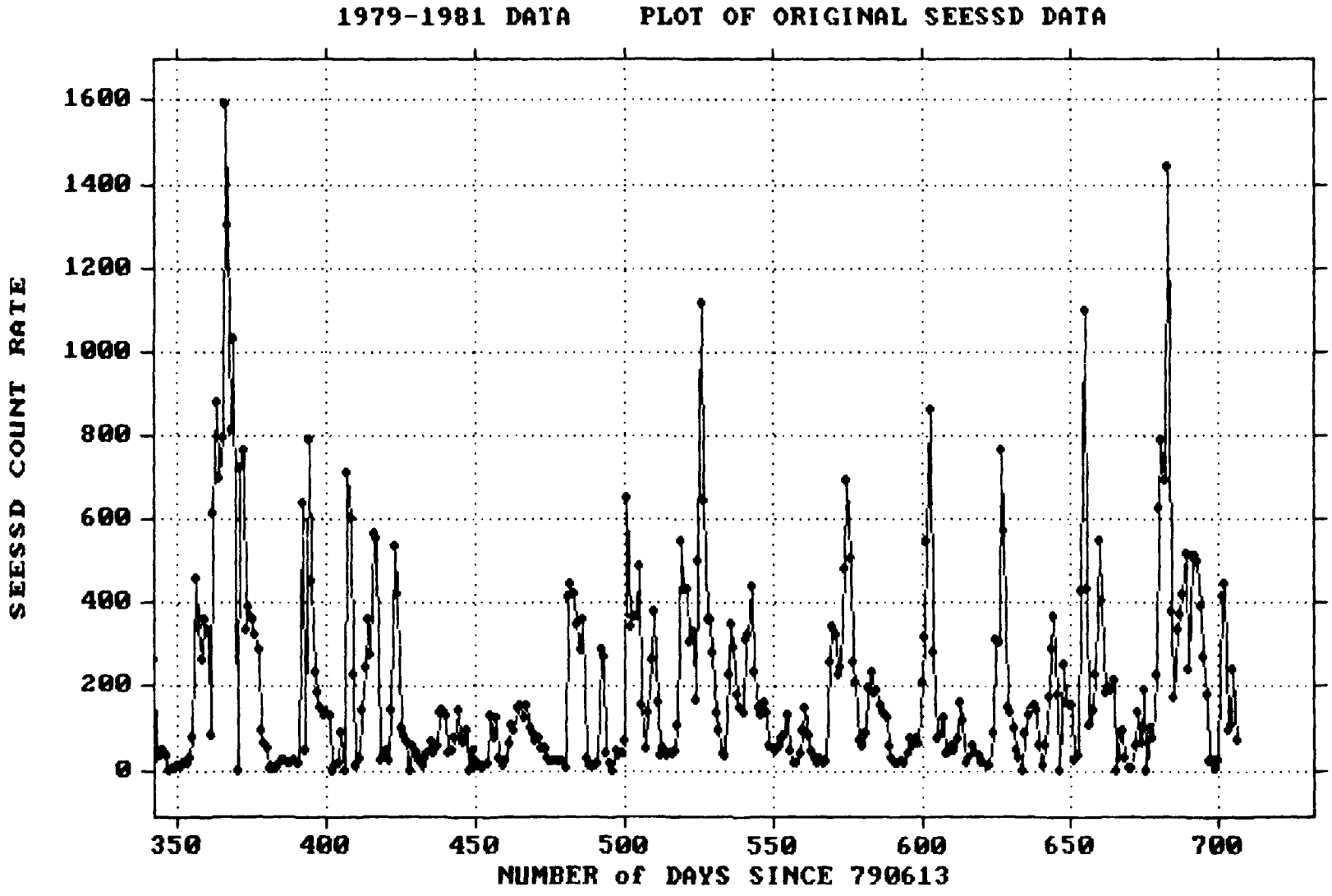
1979-1981 DATA PLOT OF ORIGINAL SEESSD DATA
SEESSD COUNT RATE
1600
1400
1200
1000
800
600
400
200
0
350
400
450
500
550
600
650
700
NUMBER of DAYS SINCE 790613

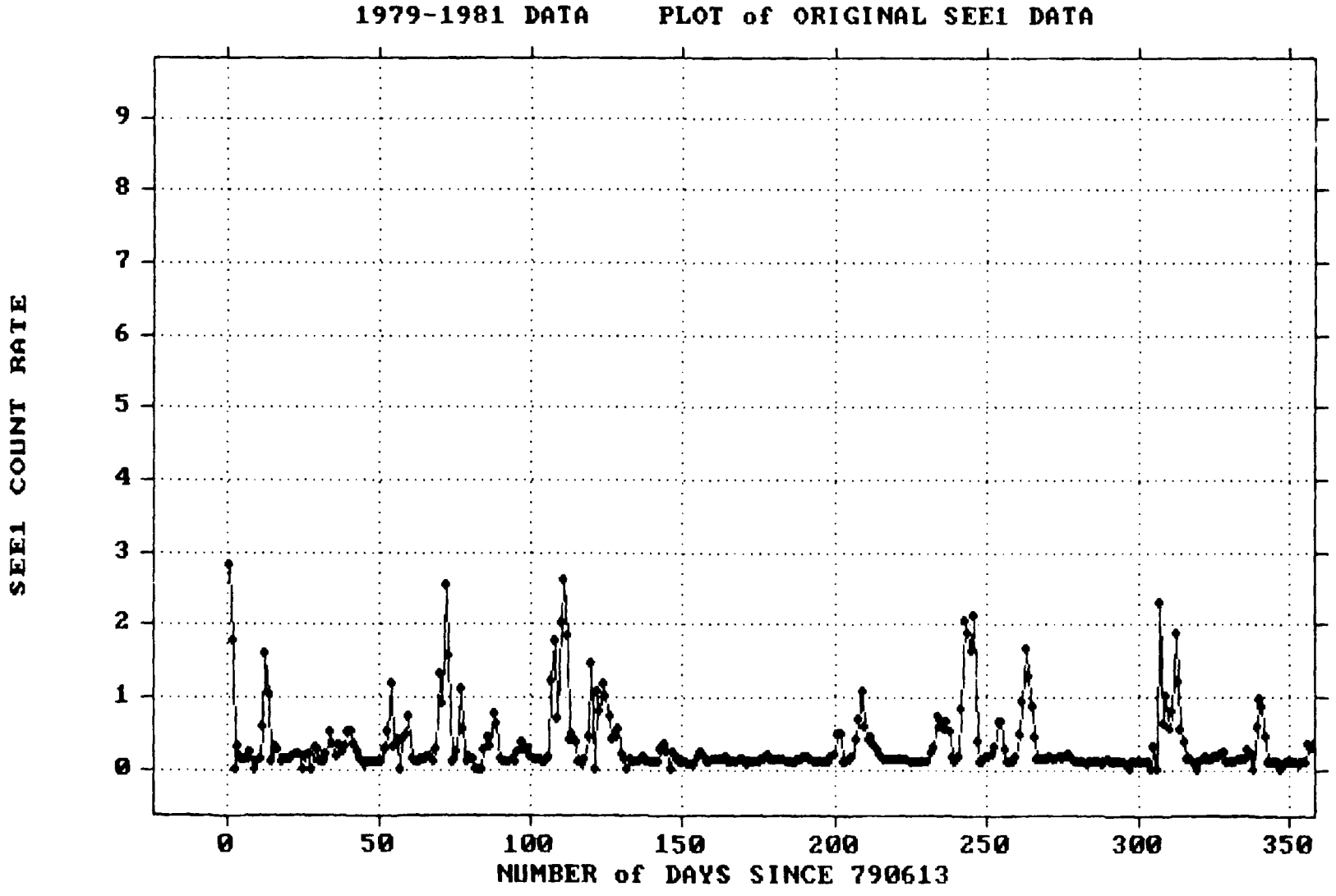
1979-1981 DATA PLOT of ORIGINAL SEE1 DATA
SEE1 COUNT RATE
0
1
2
3
4
5
6
7
8
9
0
50
100
150
200
250
300
350
NUMBER of DAYS SINCE 790613

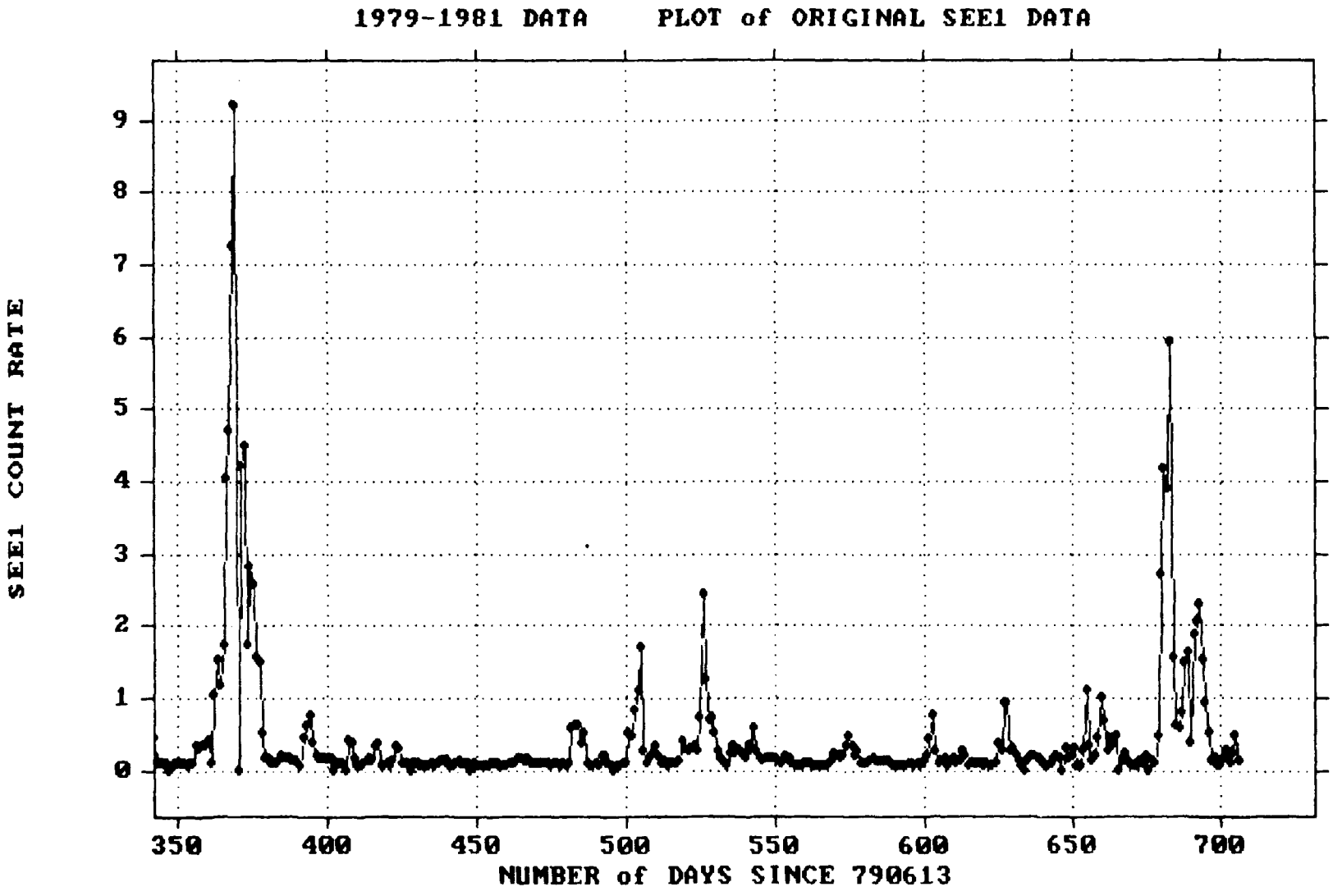
1979-1981 DATA PLOT of ORIGINAL SEE1 DATA
SEE1 COUNT RATE
0
1
2
3
4
5
6
7
8
9
350
400
450
500
550
600
650
700
NUMBER of DAYS SINCE 790613

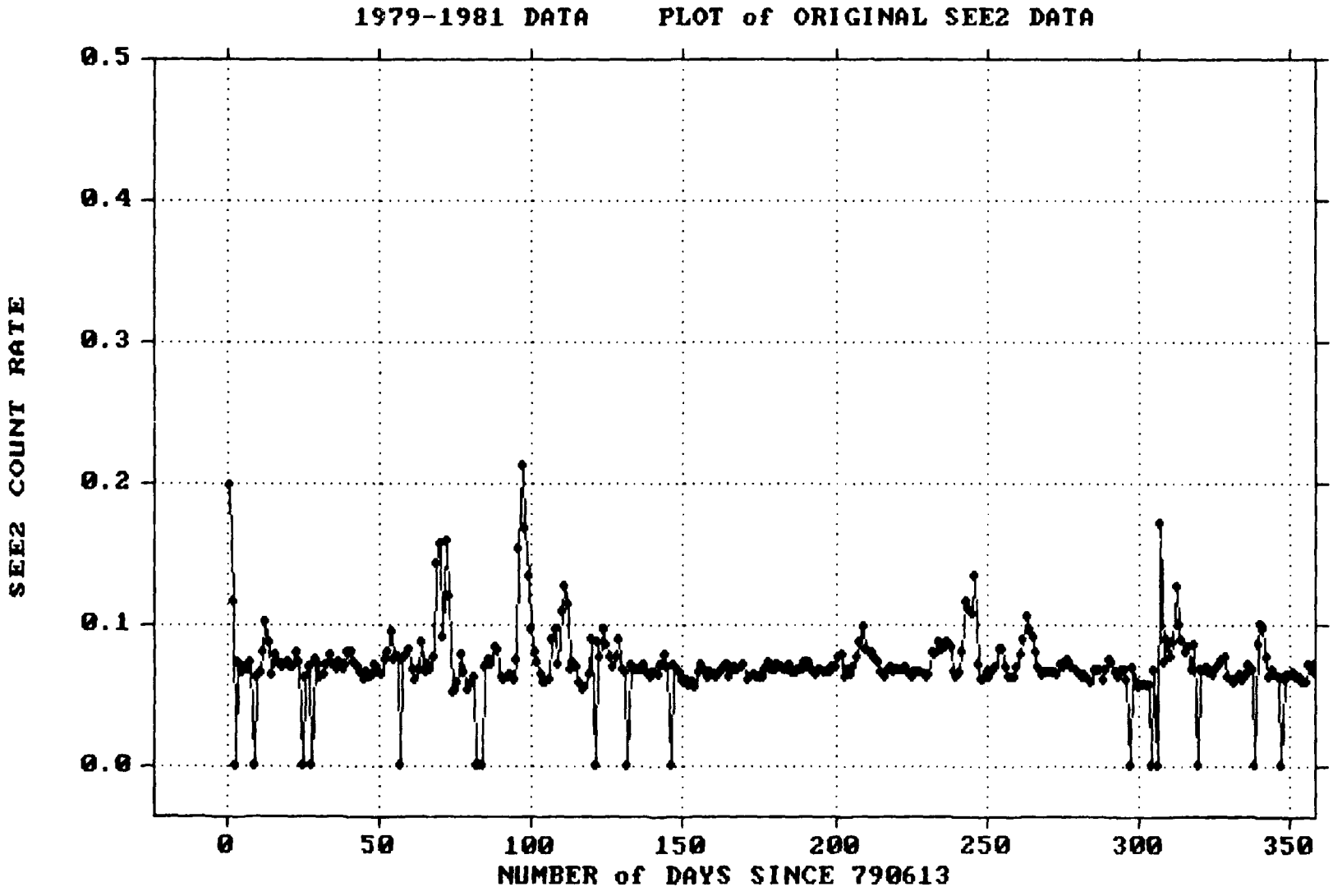
1979-1981 DATA PLOT of ORIGINAL SEE2 DATA
SEE2 COUNT RATE
0.5
0.4
0.3
0.2
0.1
0.0
0
50
100
150
200
250
300
350
NUMBER of DAYS SINCE 790613

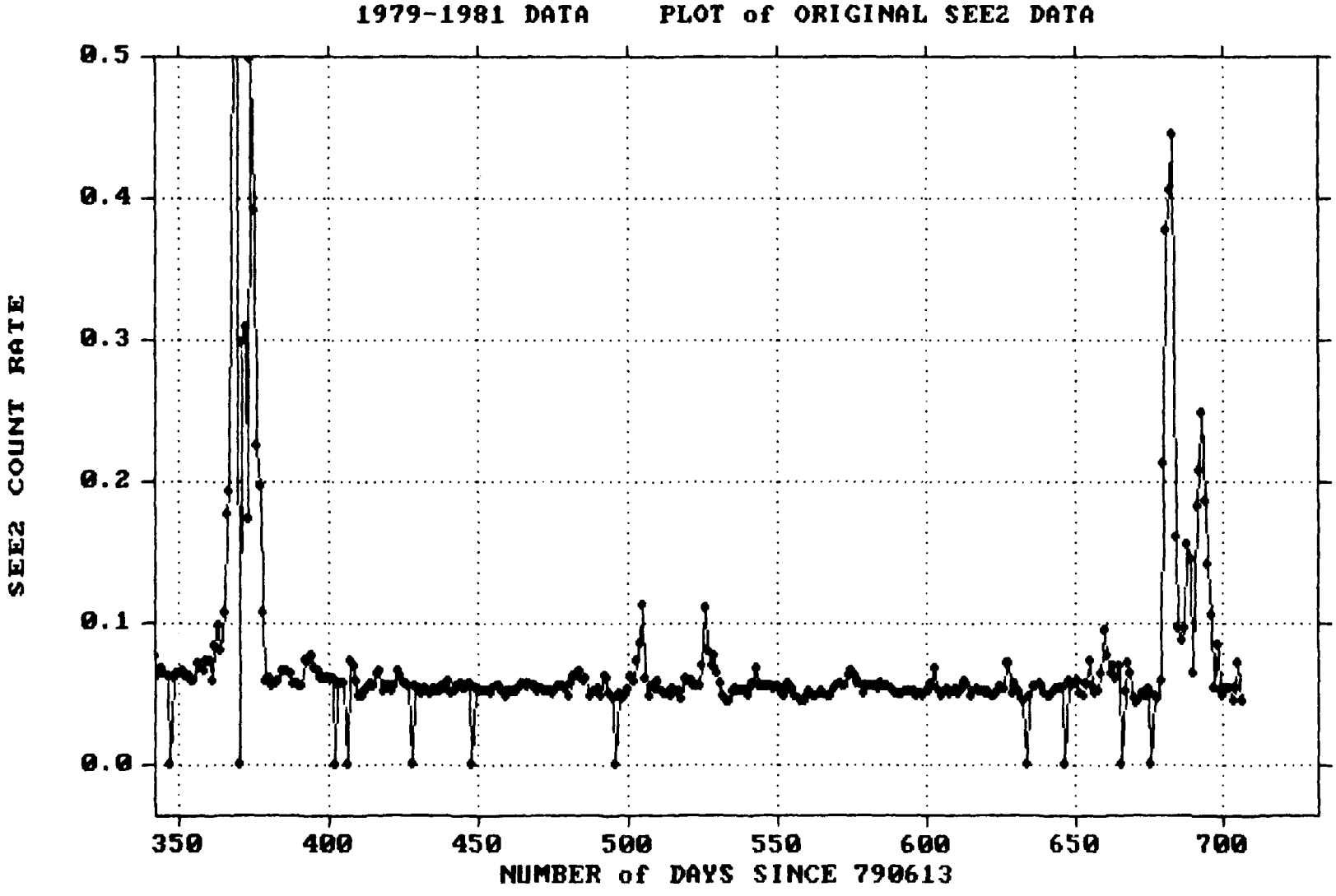
1979-1981 DATA PLOT of ORIGINAL SEE2 DATA
SEE2 COUNT RATE
0.5
0.4
0.3
0.2
0.1
0.0
350
400
450
500
550
600
650
700
NUMBER of DAYS SINCE 790613

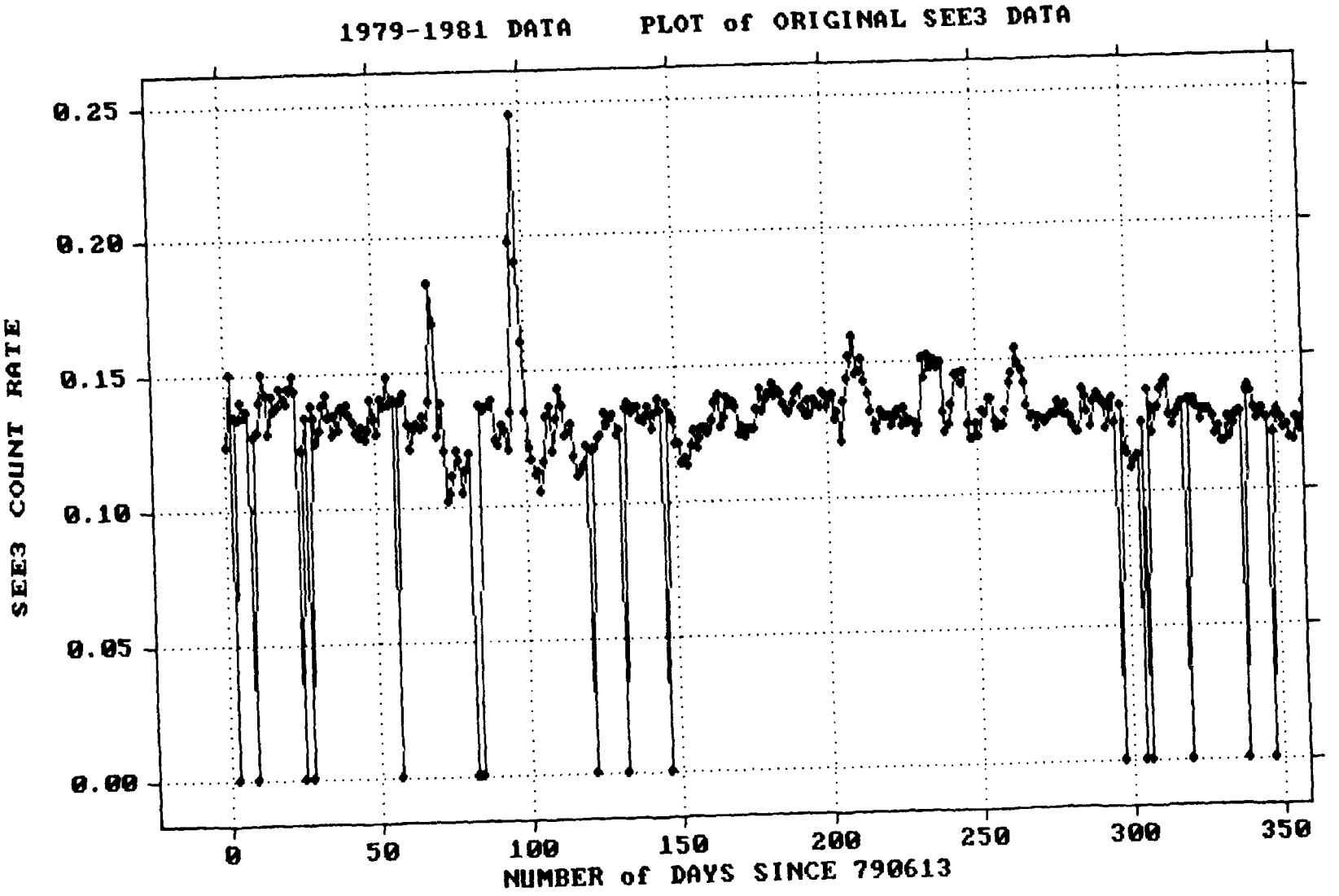
1979-1981 DATA PLOT of ORIGINAL SEE3 DATA
SEE3 COUNT RATE
0.25
0.20
0.15
0.10
0.05
0.00
0
50
100
150
200
250
300
350
NUMBER of DAYS SINCE 790613

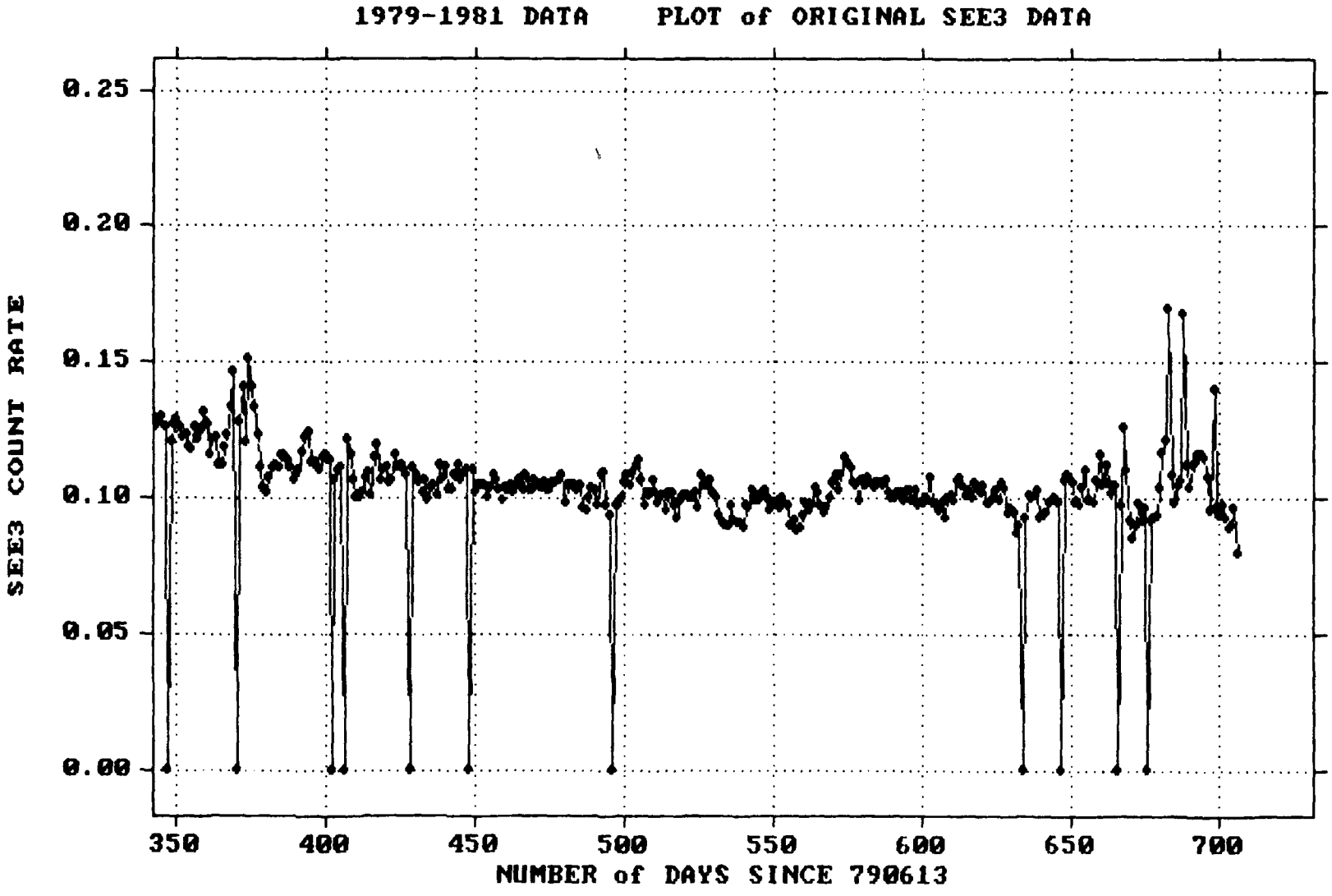
1979-1981 DATA PLOT of ORIGINAL SEE3 DATA
SEE3 COUNT RATE
0.25
0.20
0.15
0.10
0.05
0.00
350
400
450
500
550
600
650
700
NUMBER of DAYS SINCE 790613

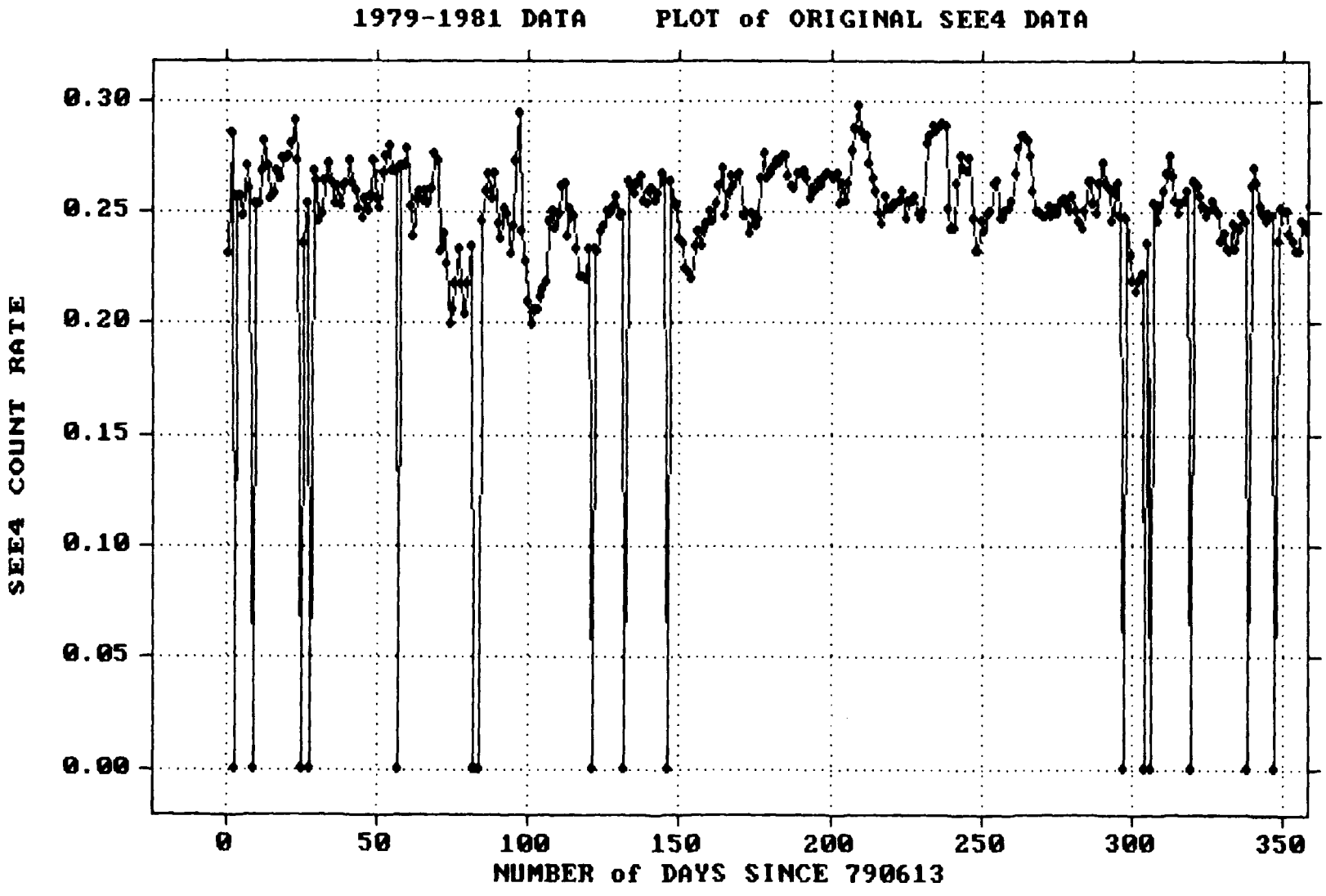
1979-1981 DATA PLOT of ORIGINAL SEE4 DATA
SEE4 COUNT RATE
0.30
0.25
0.20
0.15
0.10
0.05
0.00
0
50
100
150
200
250
300
350
NUMBER of DAYS SINCE 790613

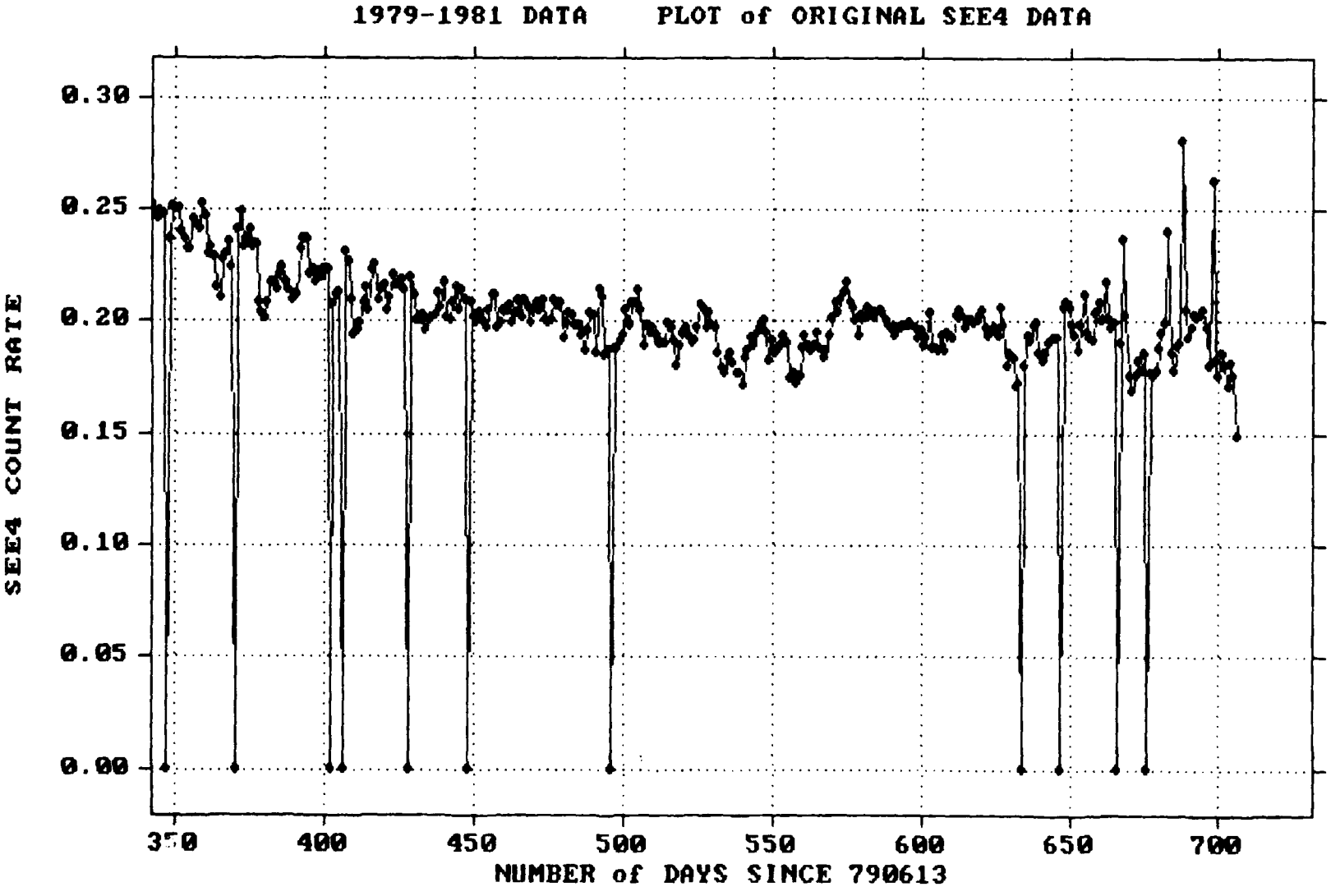
1979-1981 DATA PLOT of ORIGINAL SEE4 DATA
SEE4 COUNT RATE
0.30
0.25
0.20
0.15
0.10
0.05
0.00
350
400
450
500
550
600
650
700
NUMBER of DAYS SINCE 790613

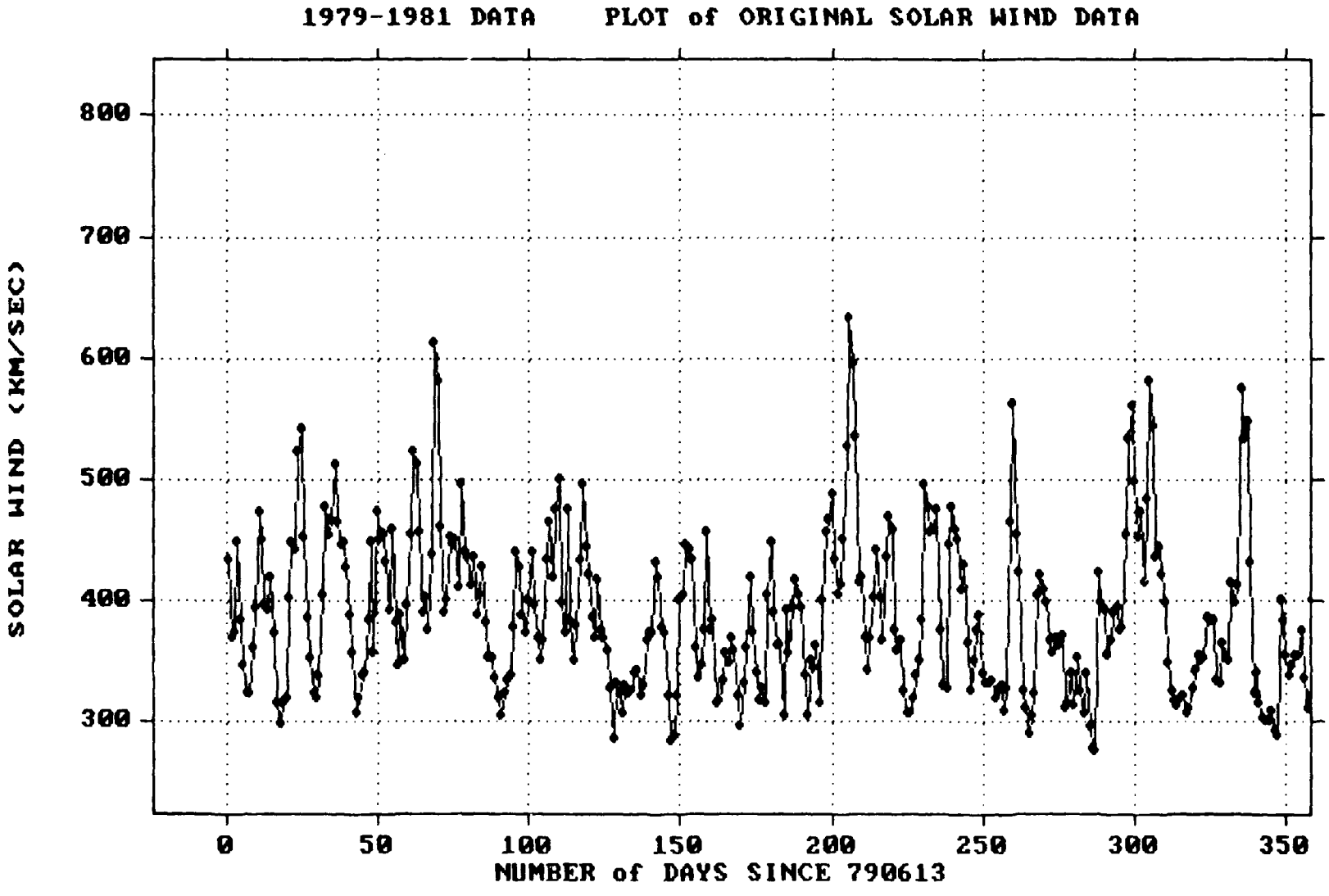
1979-1981 DATA PLOT of ORIGINAL SOLAR WIND DATA
SOLAR WIND (KM/SEC)
800
700
600
500
400
300
0
50
100
150
200
250
300
350
NUMBER of DAYS SINCE 790613

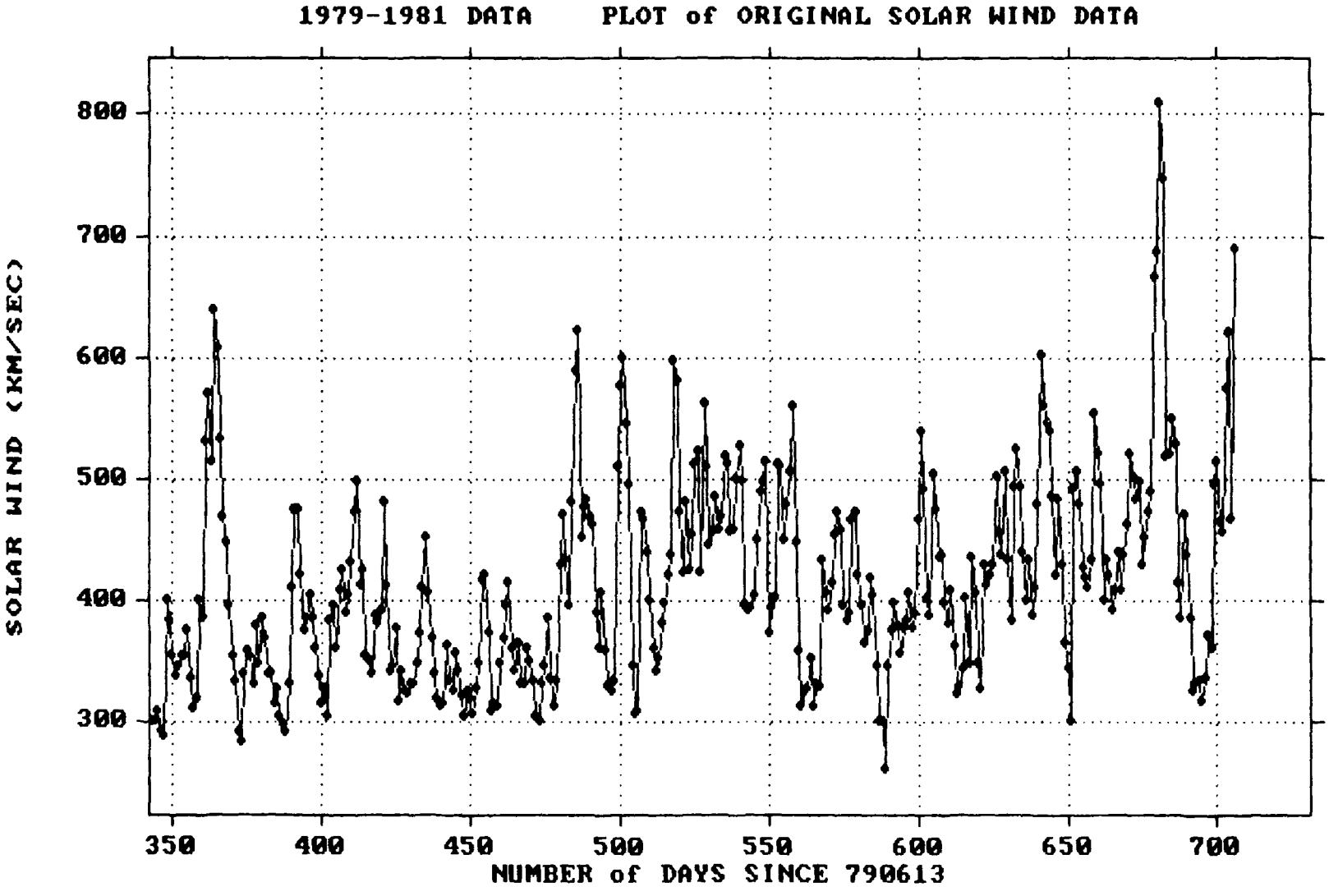
1979-1981 DATA PLOT of ORIGINAL SOLAR WIND DATA
SOLAR WIND (KM/SEC)
800
700
600
500
400
300
350
400
450
500
550
600
650
700
NUMBER of DAYS SINCE 790613

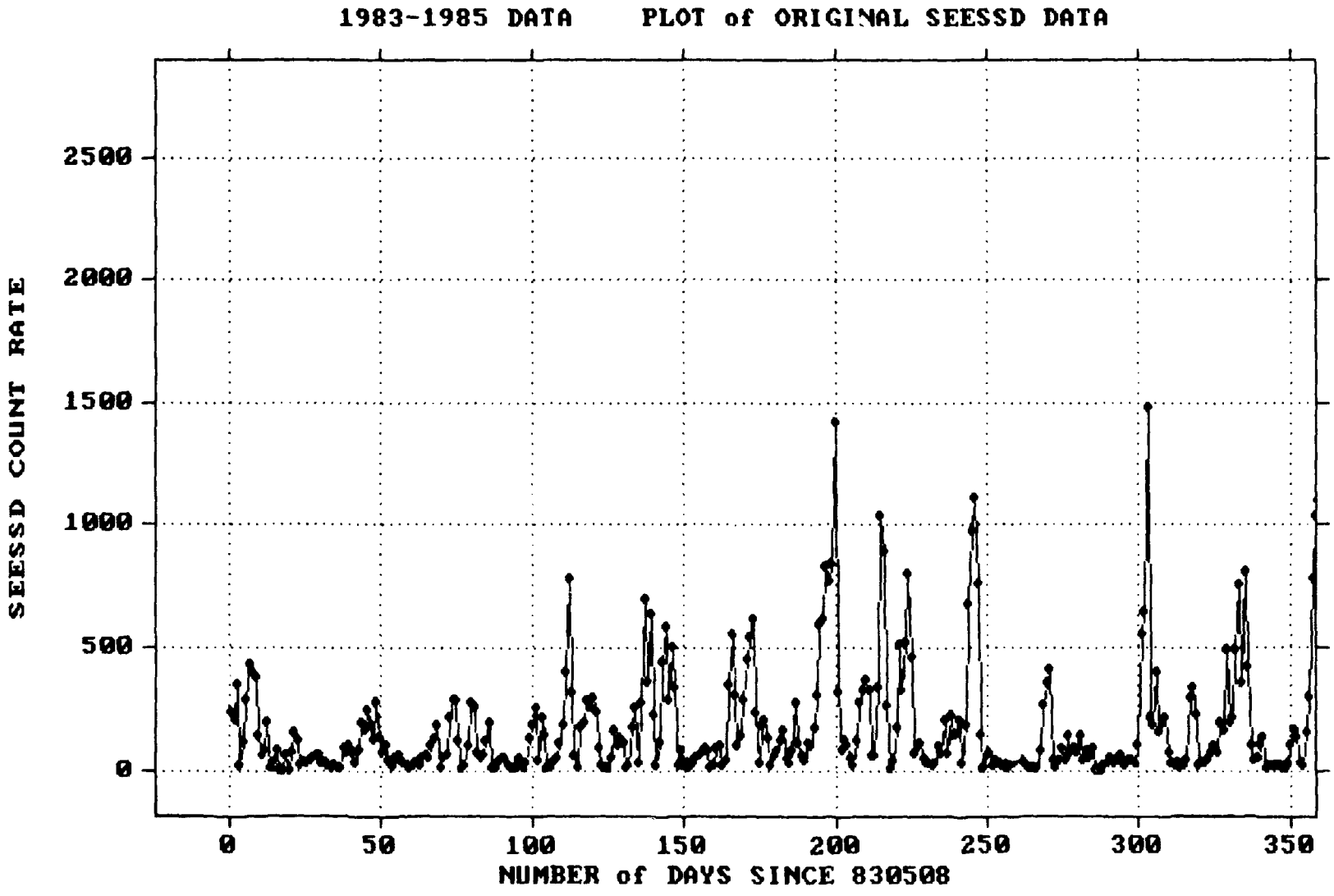
1983-1985 DATA PLOT of ORIGINAL SEESSD DATA
SEESSD COUNT RATE
2500
2000
1500
1000
500
0
0
50
100
150
200
250
300
350
NUMBER of DAYS SINCE 830508

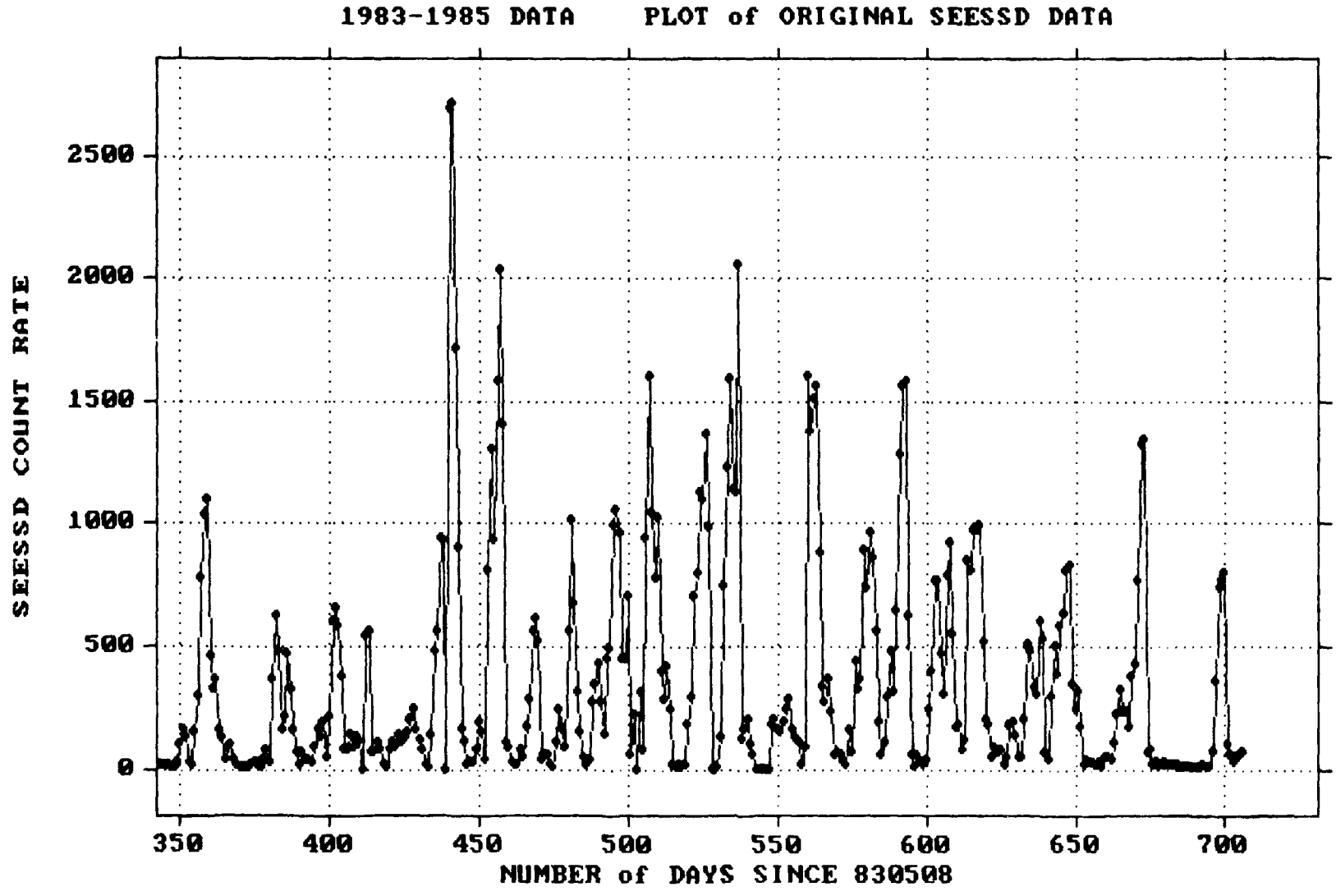
1983-1985 DATA PLOT of ORIGINAL SEESSD DATA
SEESSD COUNT RATE
2500
2000
1500
1000
500
0
350
400
450
500
550
600
650
700
NUMBER of DAYS SINCE 830508

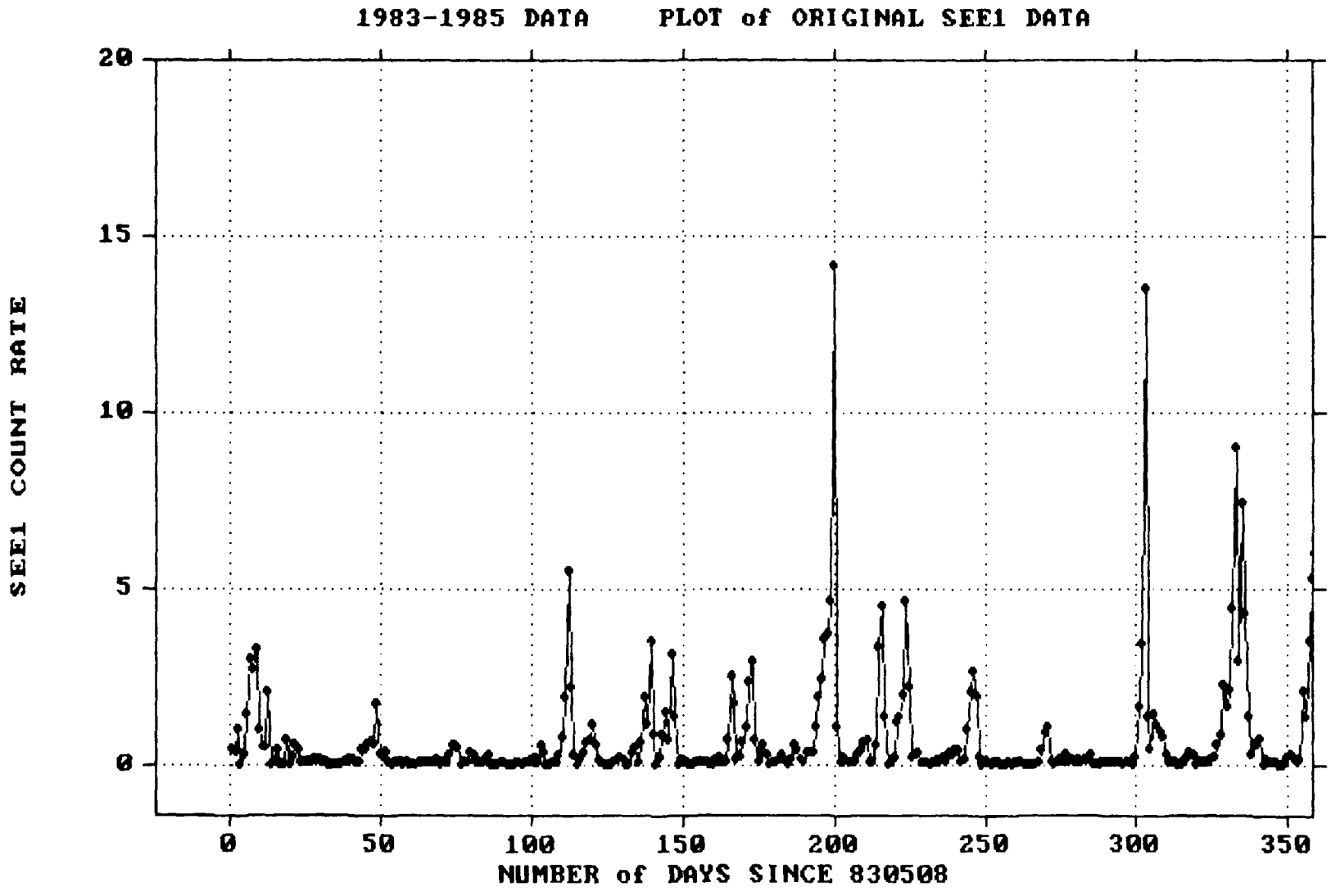
1983-1985 DATA PLOT of ORIGINAL SEE1 DATA
SEE1 COUNT RATE
20
15
10
5
0
0
50
100
150
200
250
300
350
NUMBER of DAYS SINCE 830508

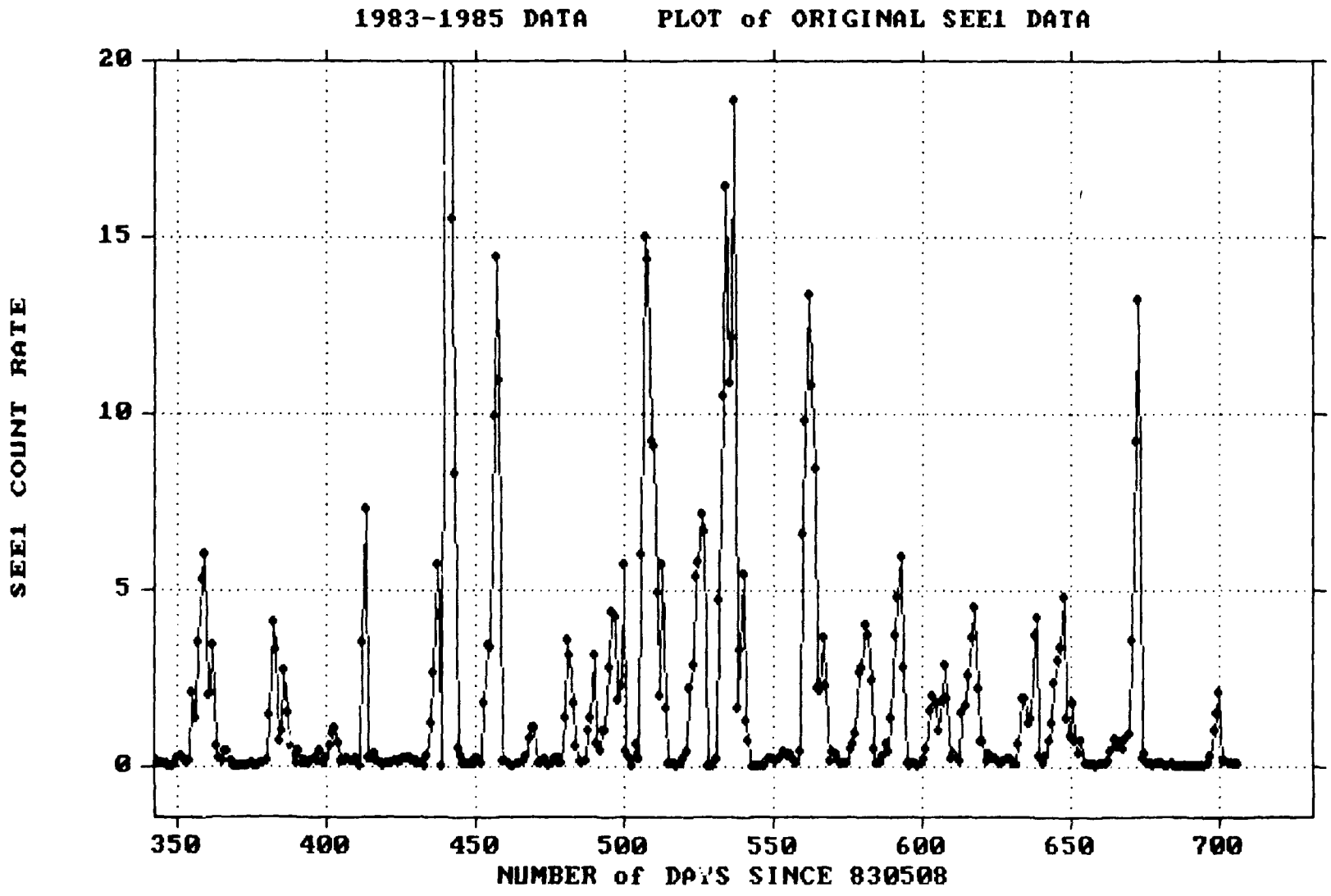
1983-1985 DATA PLOT of ORIGINAL SEE1 DATA
SEE1 COUNT RATE
20
15
10
5
0
350
400
450
500
550
600
650
700
NUMBER of DAYS SINCE 830508

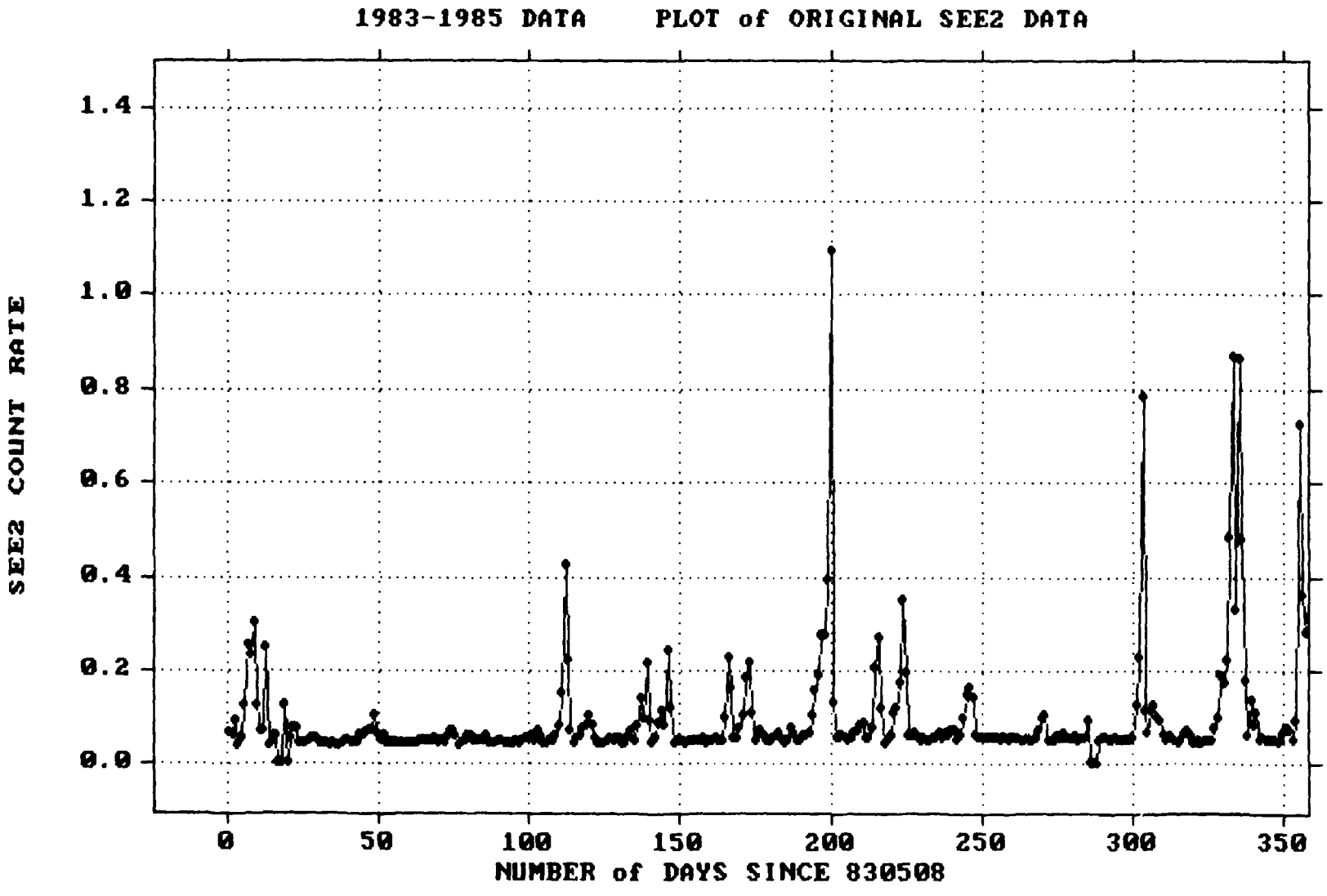
1983-1985 DATA PLOT of ORIGINAL SEE2 DATA
SEE2 COUNT RATE
1.4
1.2
1.0
0.8
0.6
0.4
0.2
0.0
0
50
100
150
200
250
300
350
NUMBER of DAYS SINCE 830508

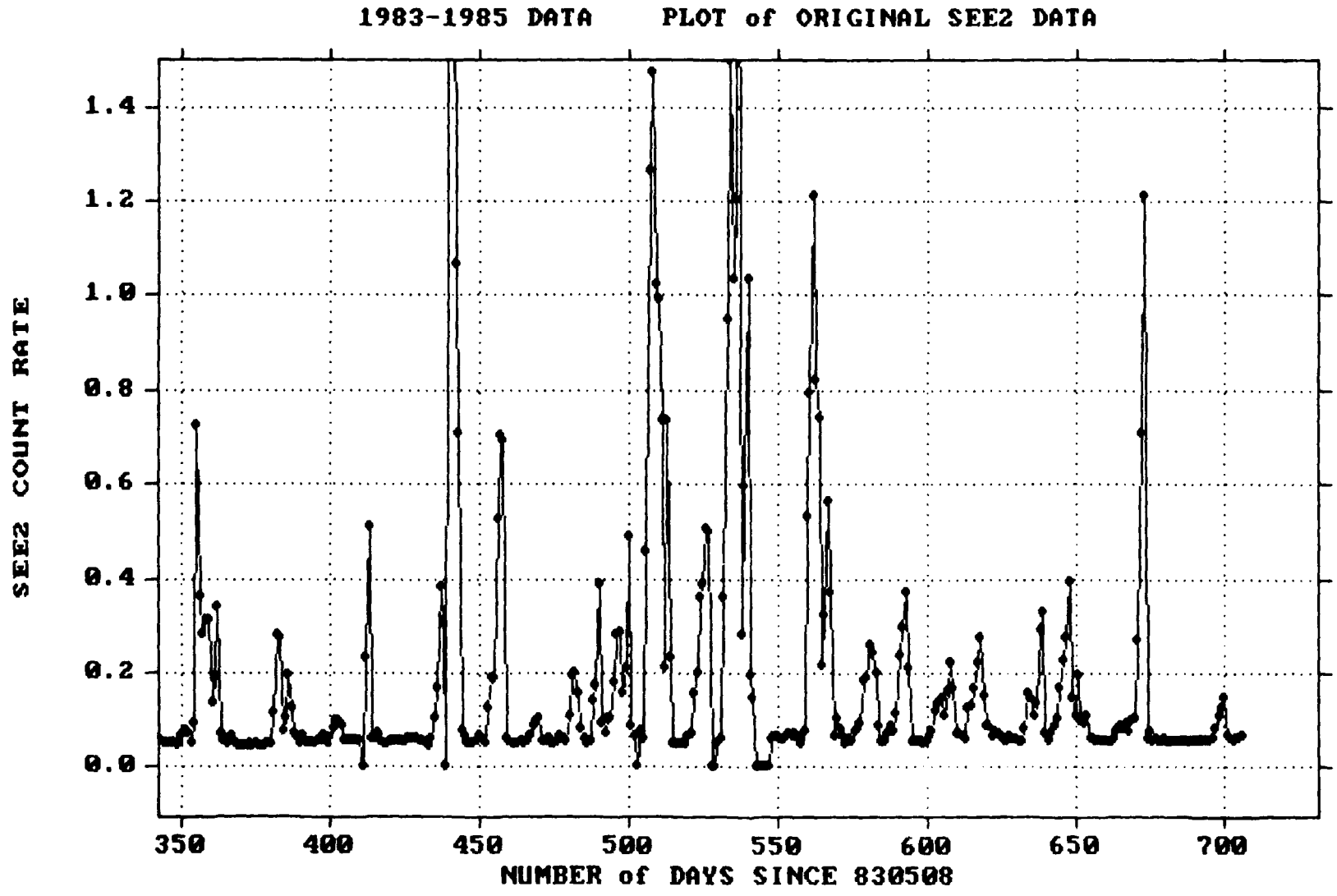
1983-1985 DATA PLOT of ORIGINAL SEE2 DATA
SEE2 COUNT RATE
1.4
1.2
1.0
0.8
0.6
0.4
0.2
0.0
350
400
450
500
550
600
650
700
NUMBER of DAYS SINCE 830508

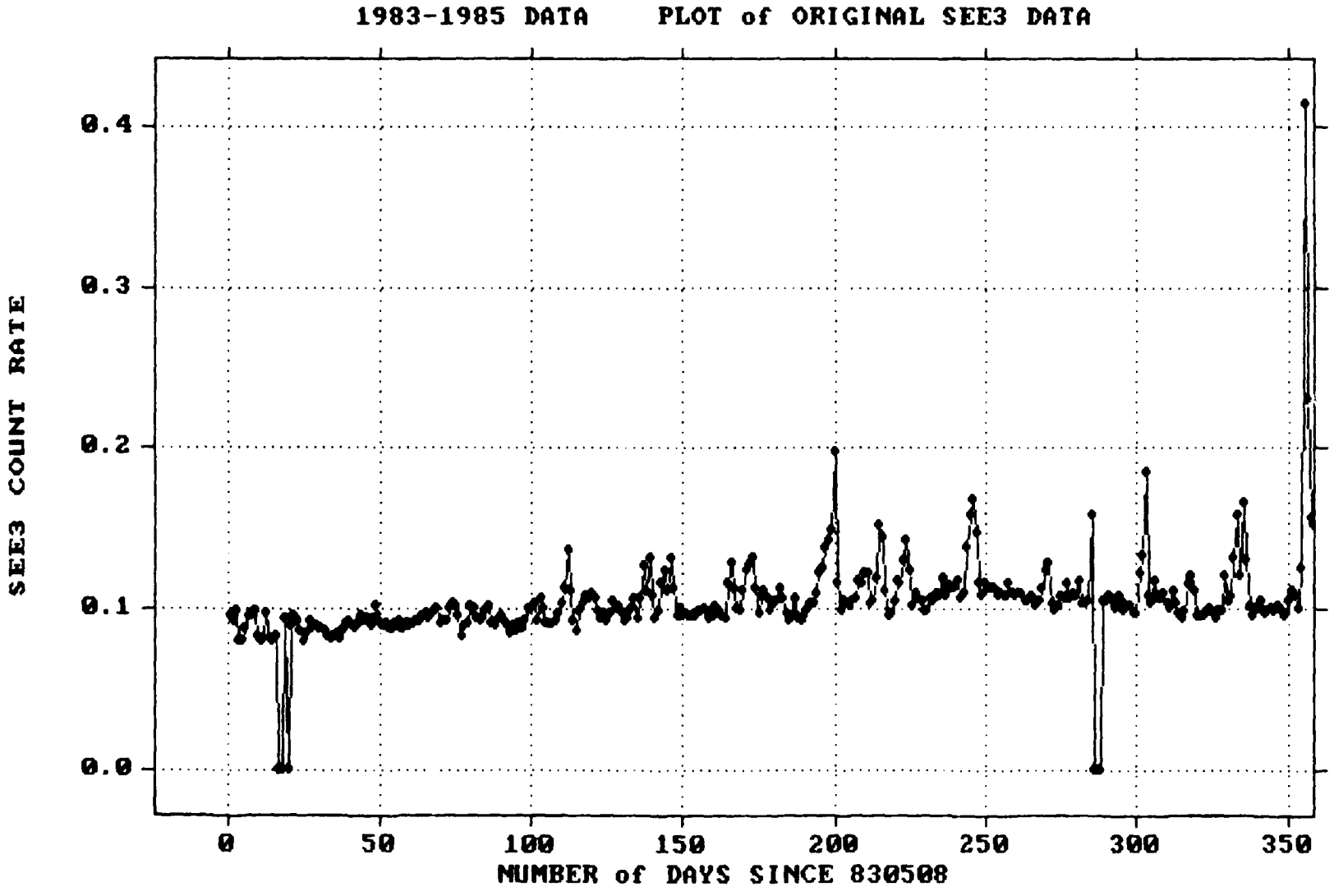
1983-1985 DATA PLOT of ORIGINAL SEE3 DATA
SEE3 COUNT RATE
0.4
0.3
0.2
0.1
0.0
0
50
100
150
200
250
300
350
NUMBER of DAYS SINCE 830508

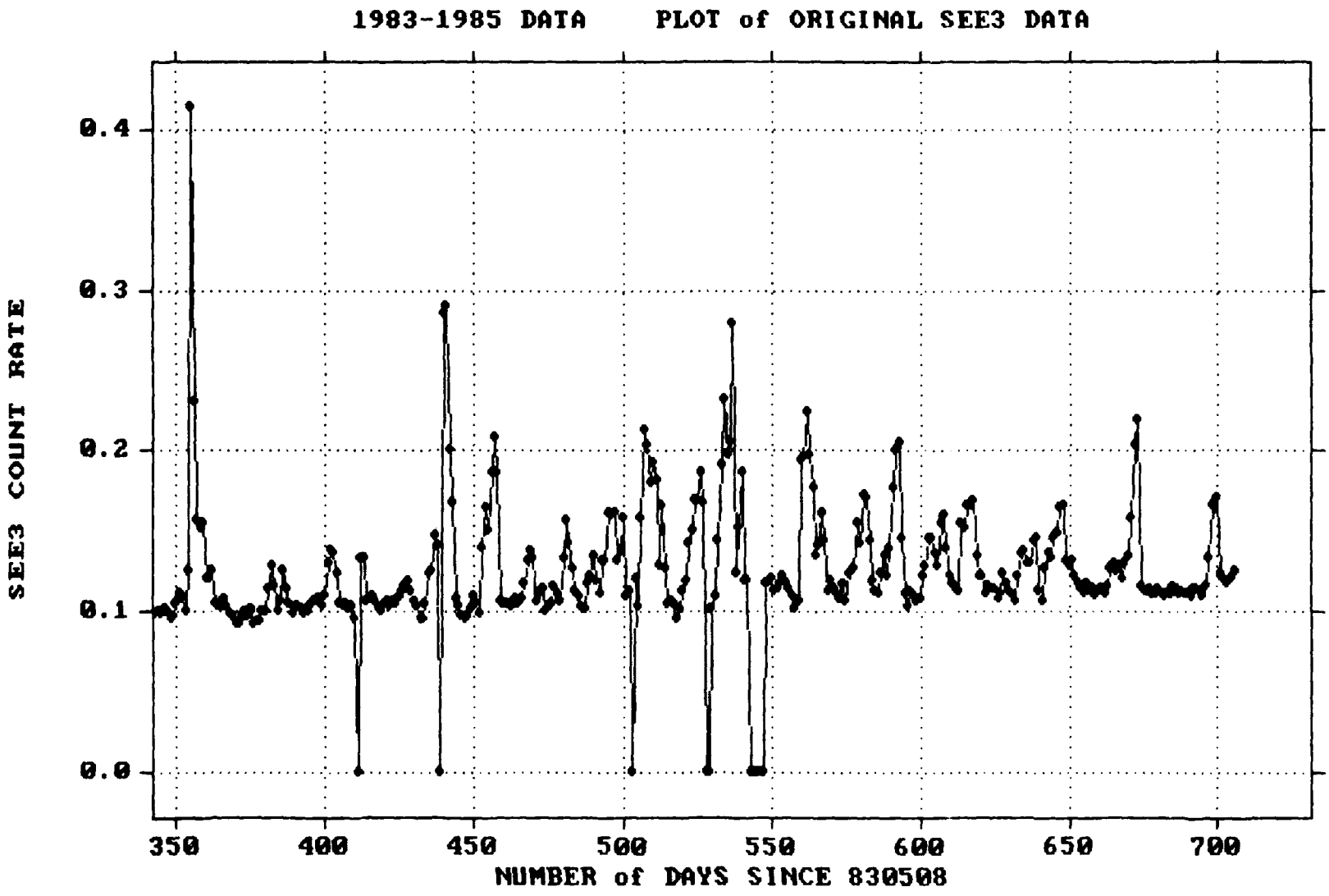
1983-1985 DATA PLOT of ORIGINAL SEE3 DATA
SEE3 COUNT RATE
0.4
0.3
0.2
0.1
0.0
350
400
450
500
550
600
650
700
NUMBER of DAYS SINCE 830508

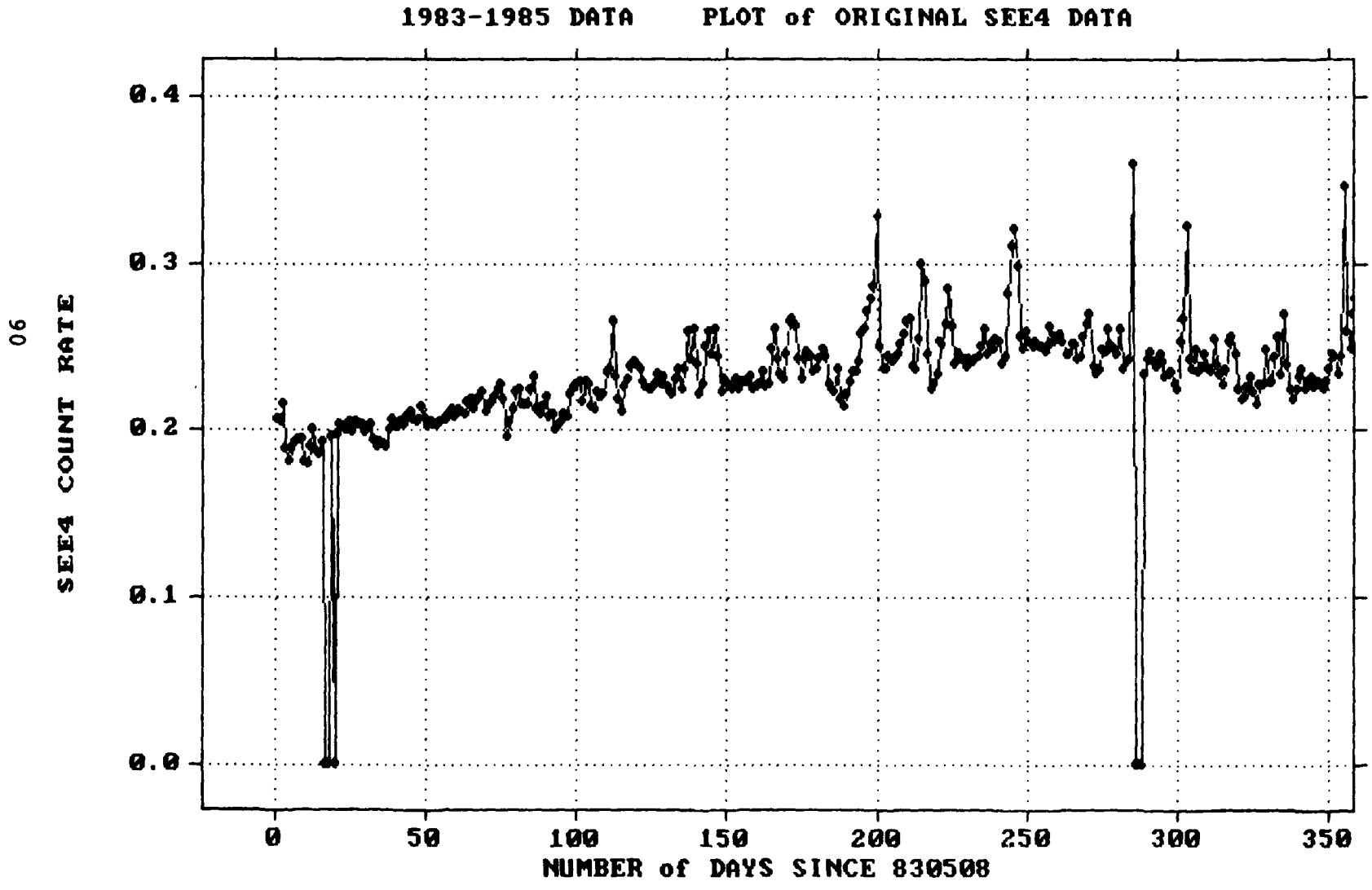
1983-1985 DATA PLOT of ORIGINAL SEE4 DATA
SEE4 COUNT RATE
0.4
0.3
0.2
0.1
0.0
0
50
100
150
200
250
300
350
NUMBER of DAYS SINCE 830508

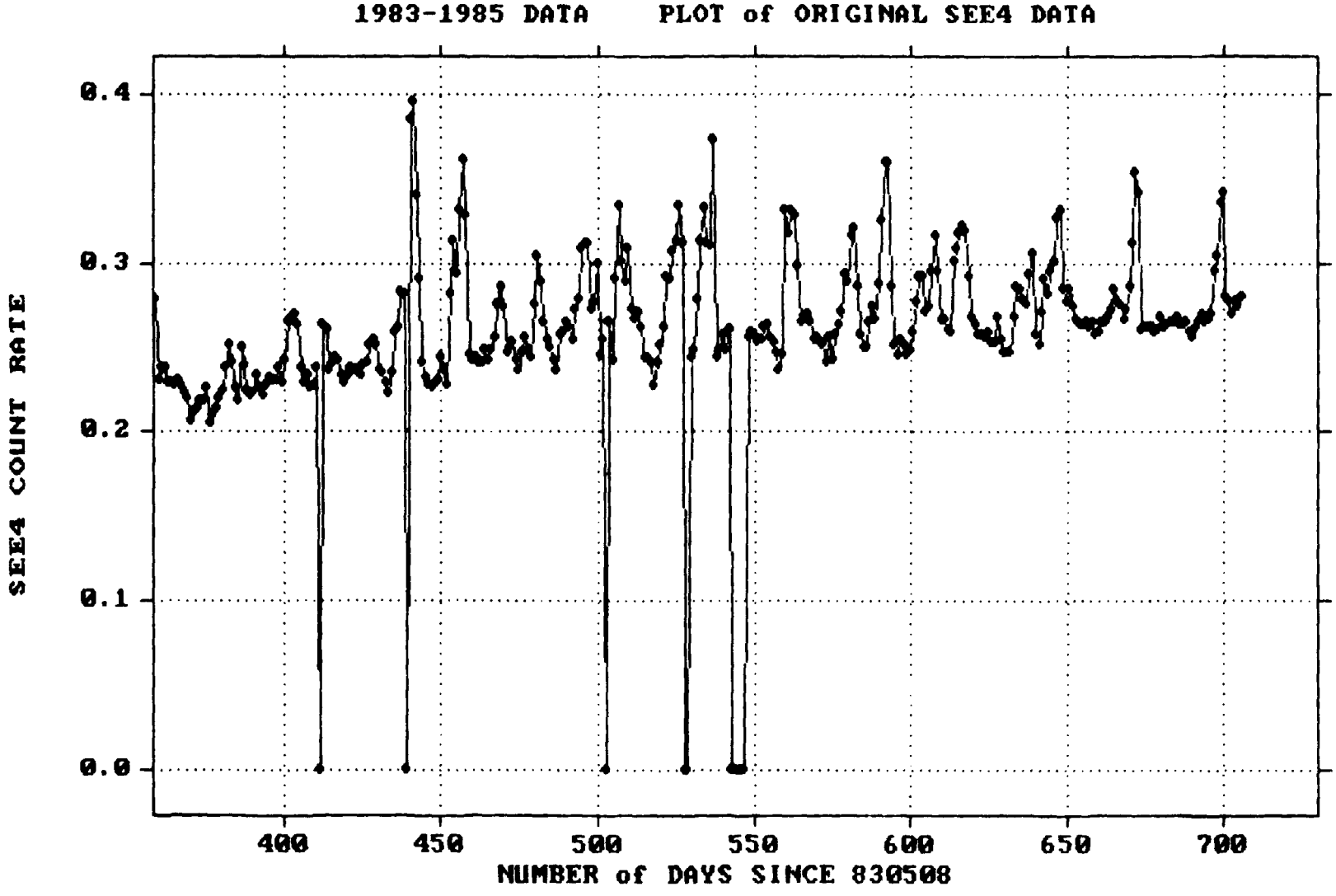
1983-1985 DATA PLOT of ORIGINAL SEE4 DATA
SEE4 COUNT RATE
0.4
0.3
0.2
0.1
0.0
400
450
500
550
600
650
700
NUMBER of DAYS SINCE 830508

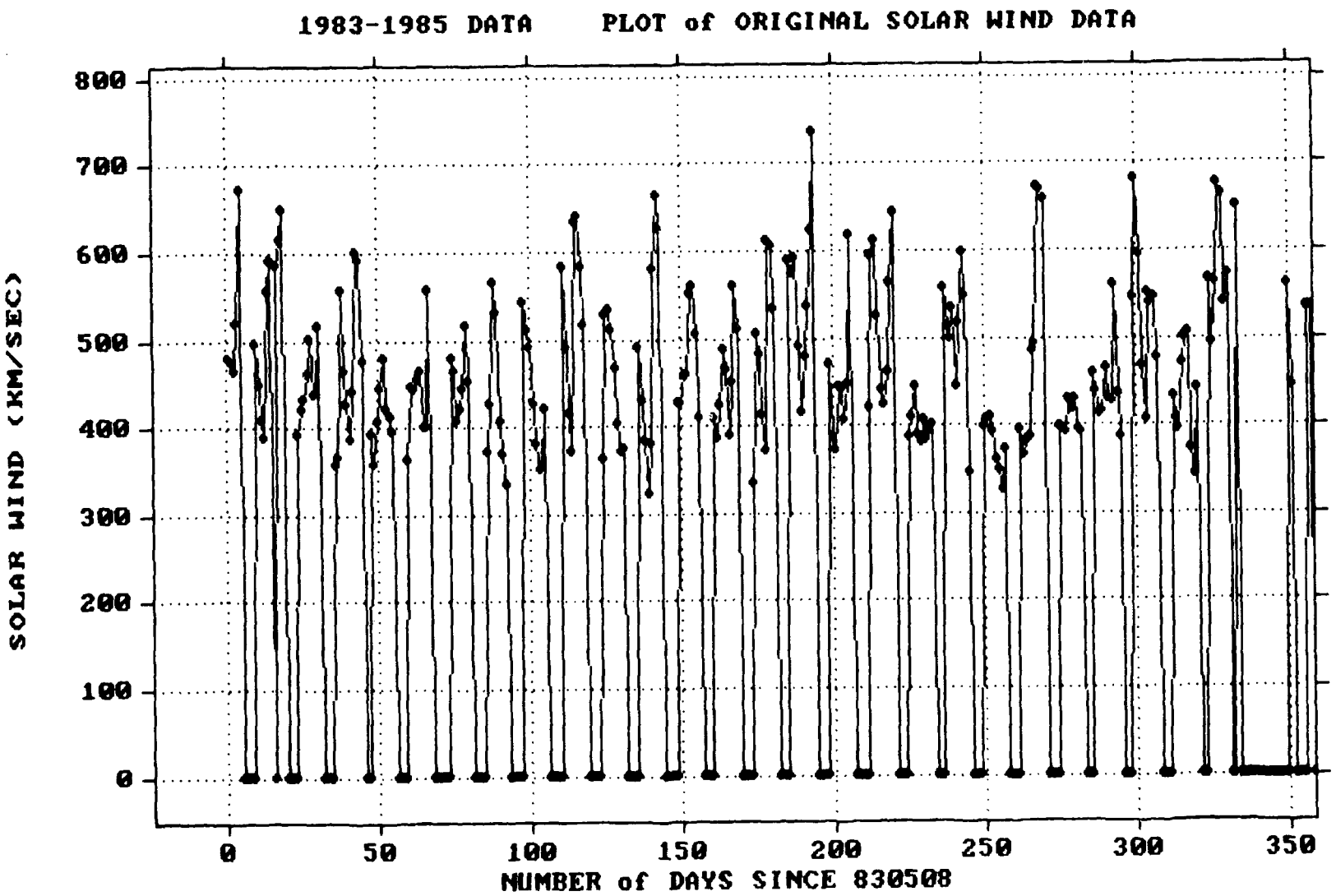
1983-1985 DATA PLOT of ORIGINAL SOLAR WIND DATA
SOLAR WIND (KM/SEC)
800
700
600
500
400
300
200
100
0
0
50
100
150
200
250
300
350
NUMBER of DAYS SINCE 830508

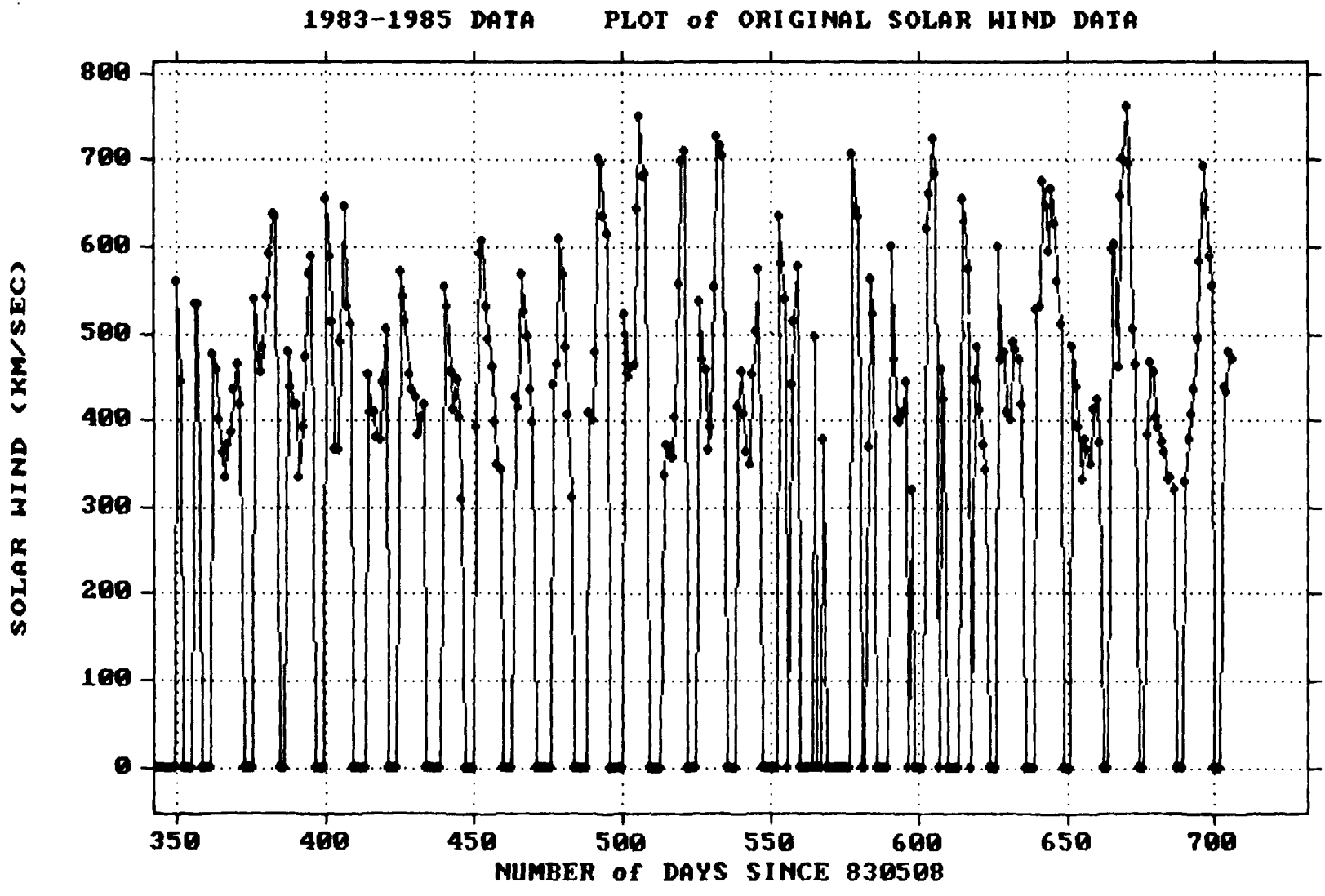
1983-1985 DATA PLOT of ORIGINAL SOLAR WIND DATA
SOLAR WIND (KM/SEC)
800
700
600
500
400
300
200
100
0
350
400
450
500
550
600
650
700
NUMBER of DAYS SINCE 830508

Appendix B: Frequency Plots

Page

1979-1981 Data 95

1983-1985 Data 101

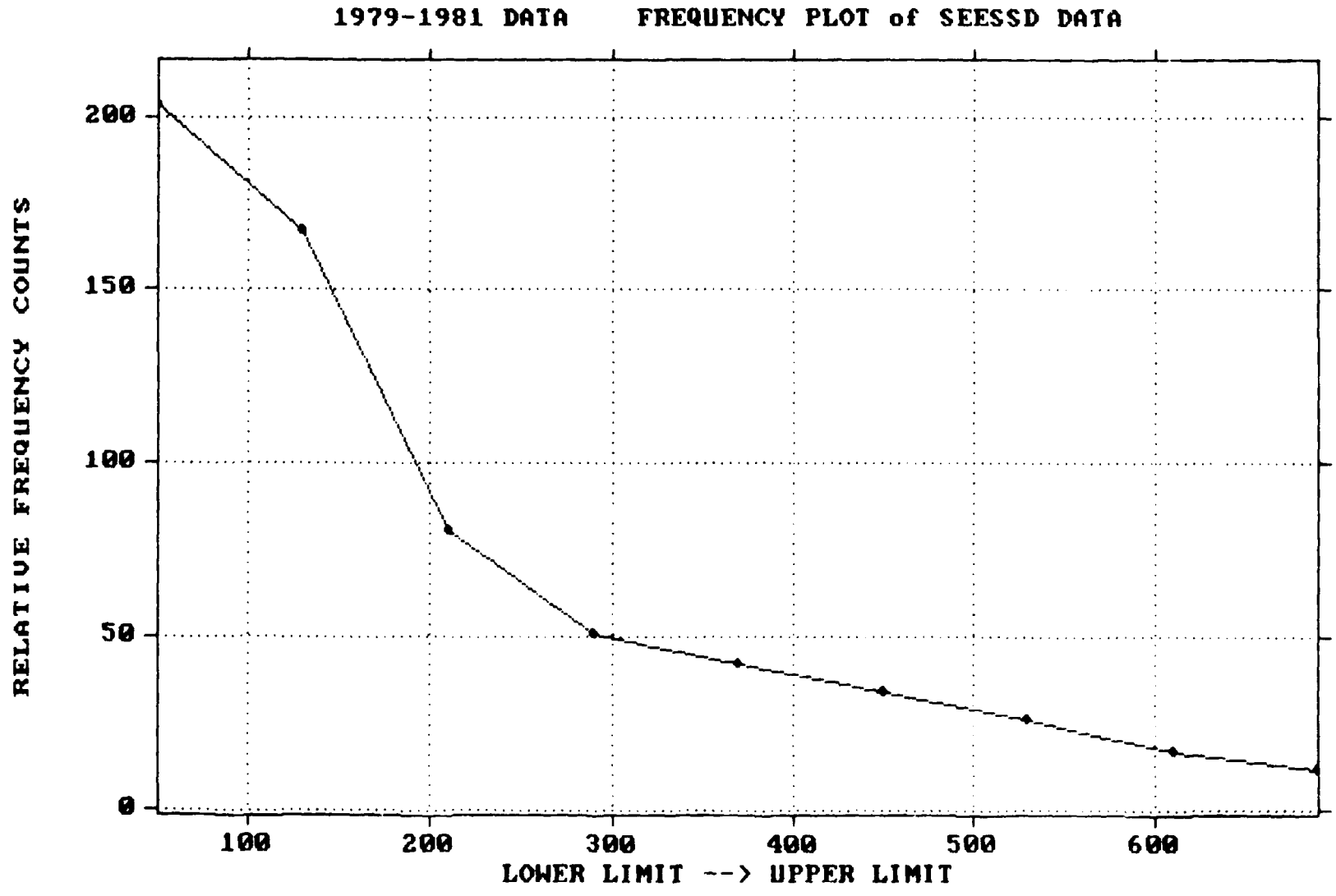
1979-1981 DATA FREQUENCY PLOT of SEESSD DATA
RELATIVE FREQUENCY COUNTS
200
150
100
50
0
100
200
300
400
500
600
LOWER LIMIT --> UPPER LIMIT

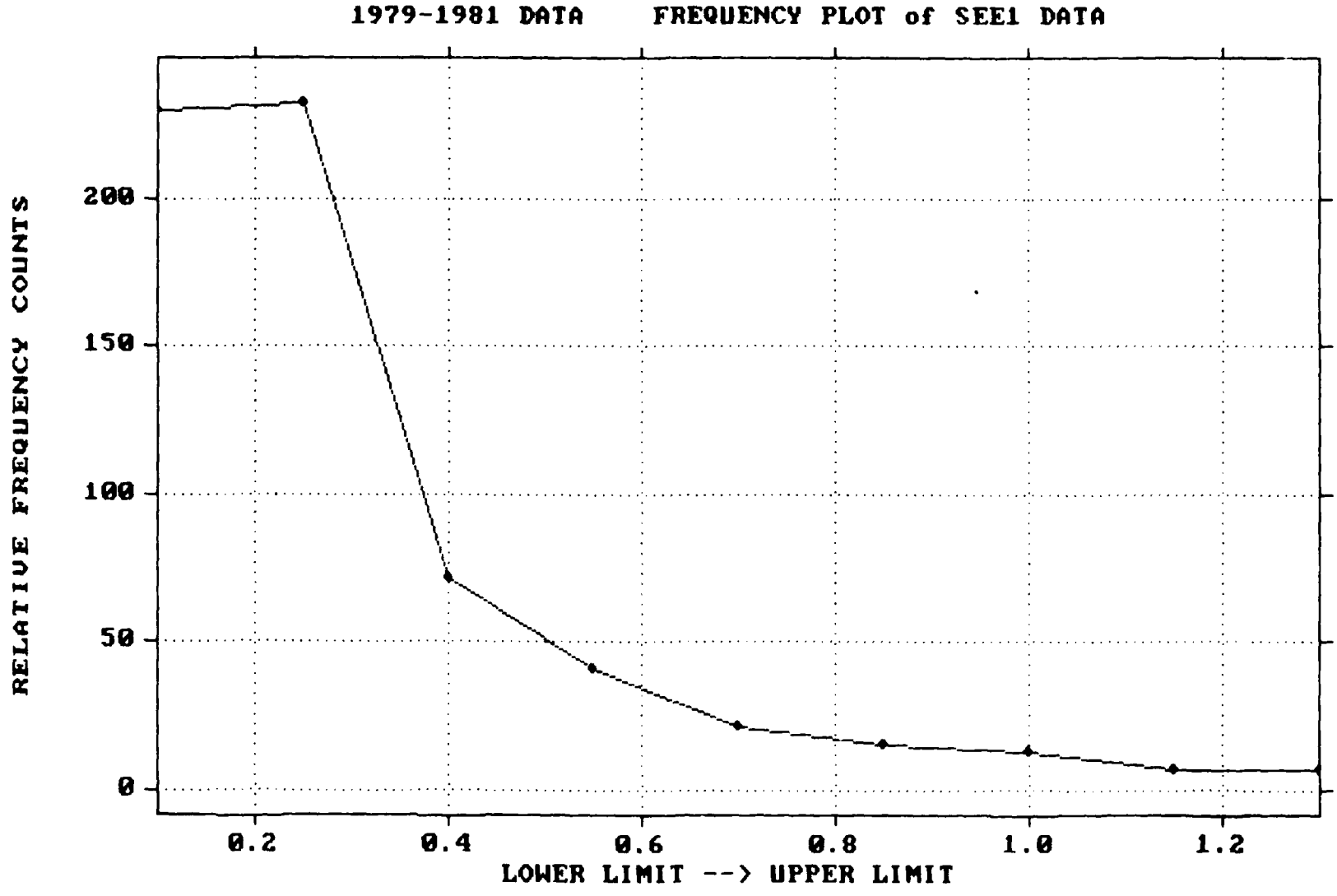
1979-1981 DATA FREQUENCY PLOT of SEE1 DATA
RELATIVE FREQUENCY COUNTS
200
150
100
50
0
0.2
0.4
0.6
0.8
1.0
1.2
LOWER LIMIT --> UPPER LIMIT

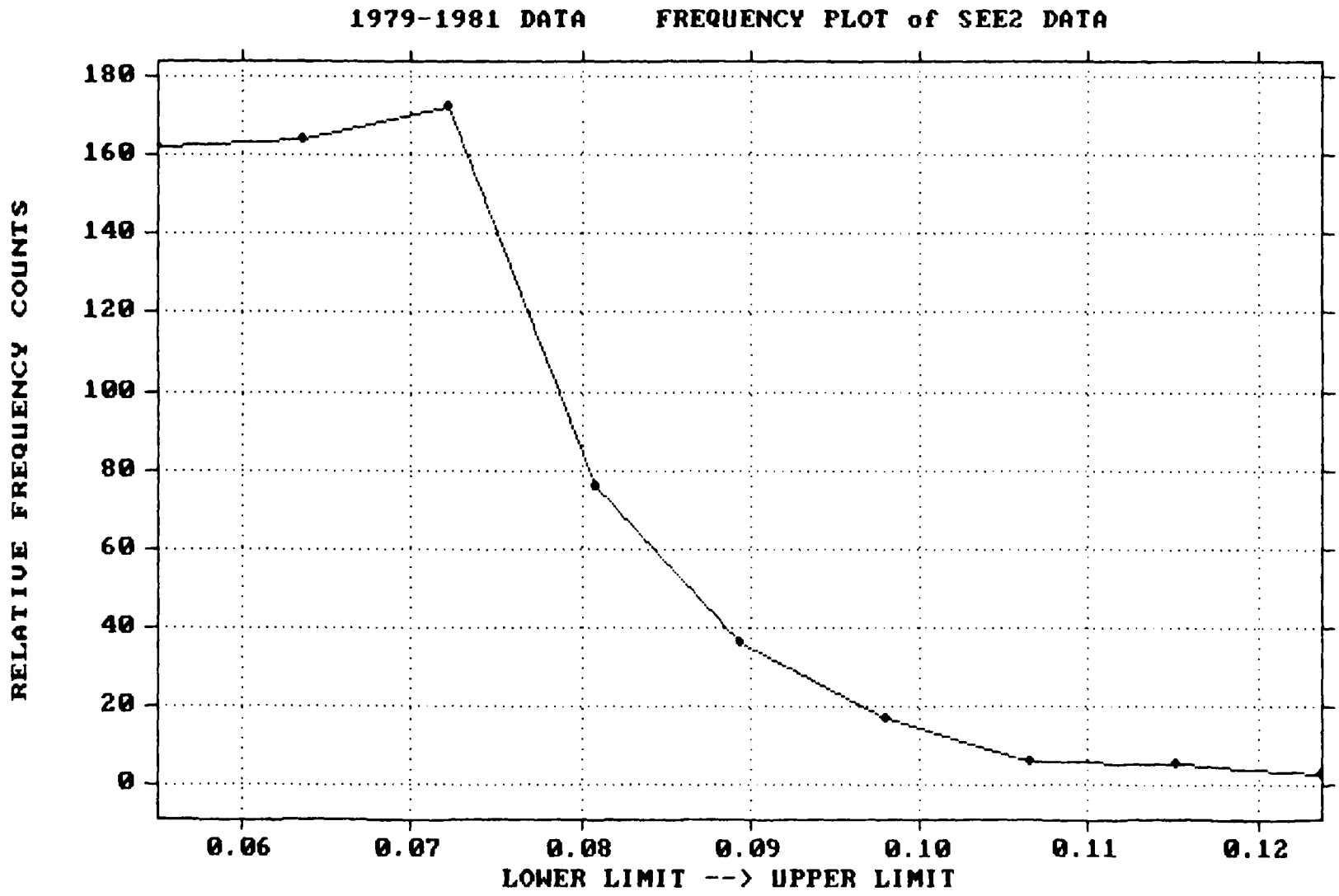
1979-1981 DATA FREQUENCY PLOT of SEE2 DATA
RELATIVE FREQUENCY COUNTS
180
160
140
120
100
80
60
40
20
0
0.06
0.07
0.08
0.09
0.10
0.11
0.12
LOWER LIMIT --> UPPER LIMIT

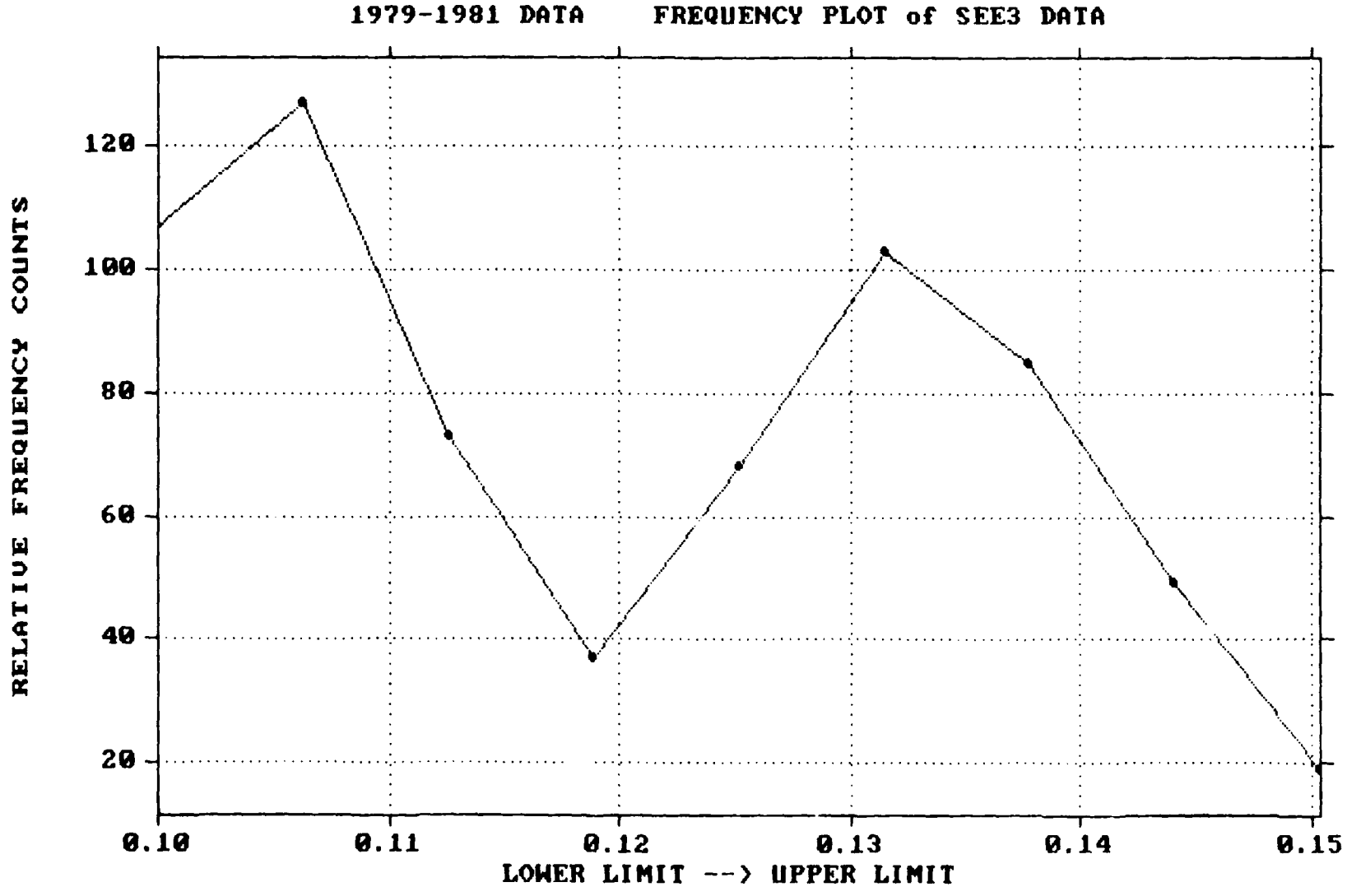
1979-1981 DATA FREQUENCY PLOT of SEE3 DATA
RELATIVE FREQUENCY COUNTS
120
100
80
60
40
20
0.10
0.11
0.12
0.13
0.14
0.15
LOWER LIMIT --> UPPER LIMIT

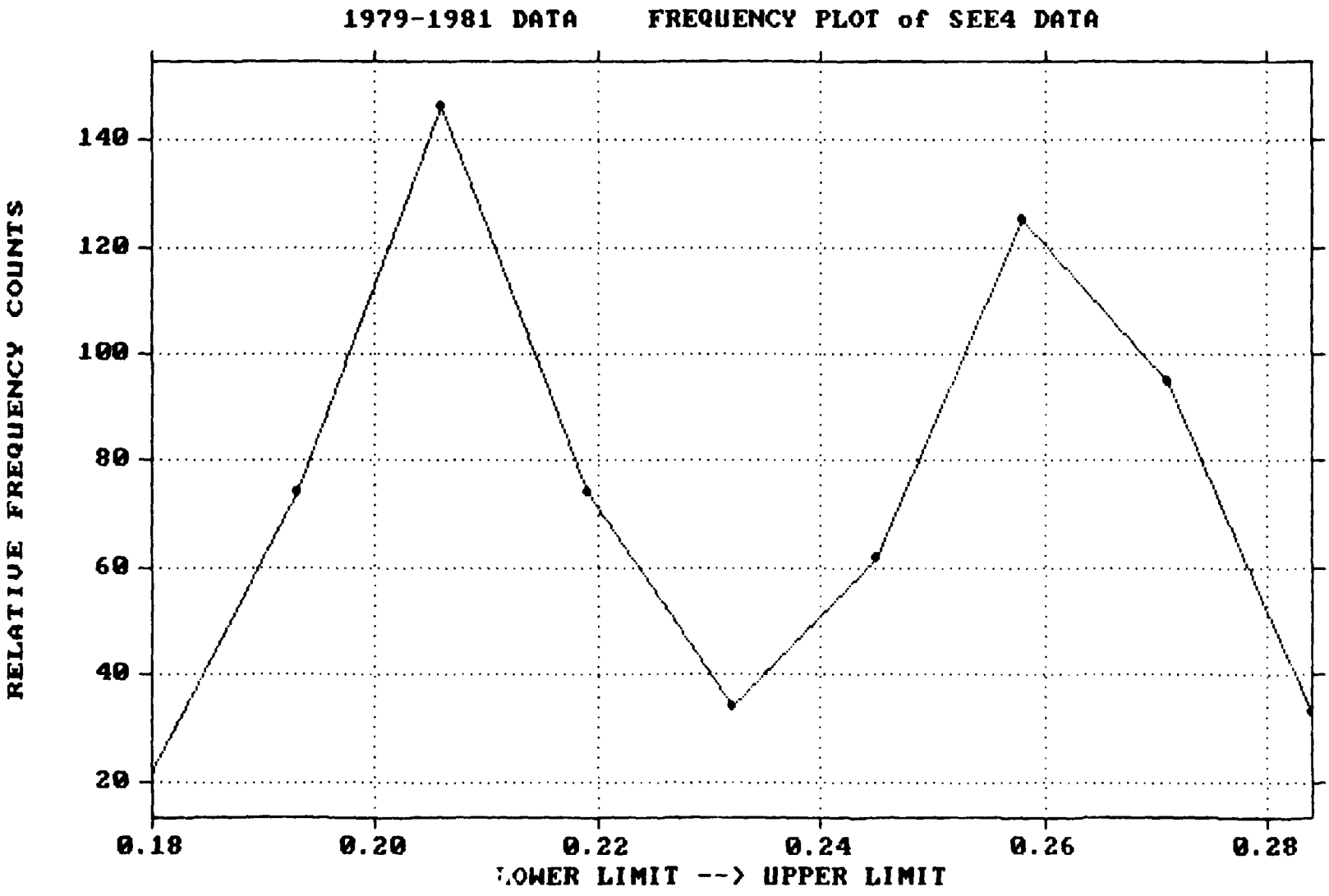
1979-1981 DATA FREQUENCY PLOT of SEE4 DATA
RELATIVE FREQUENCY COUNTS
140
120
100
80
60
40
20
0.18
0.20
0.22
0.24
0.26
0.28
LOWER LIMIT --> UPPER LIMIT

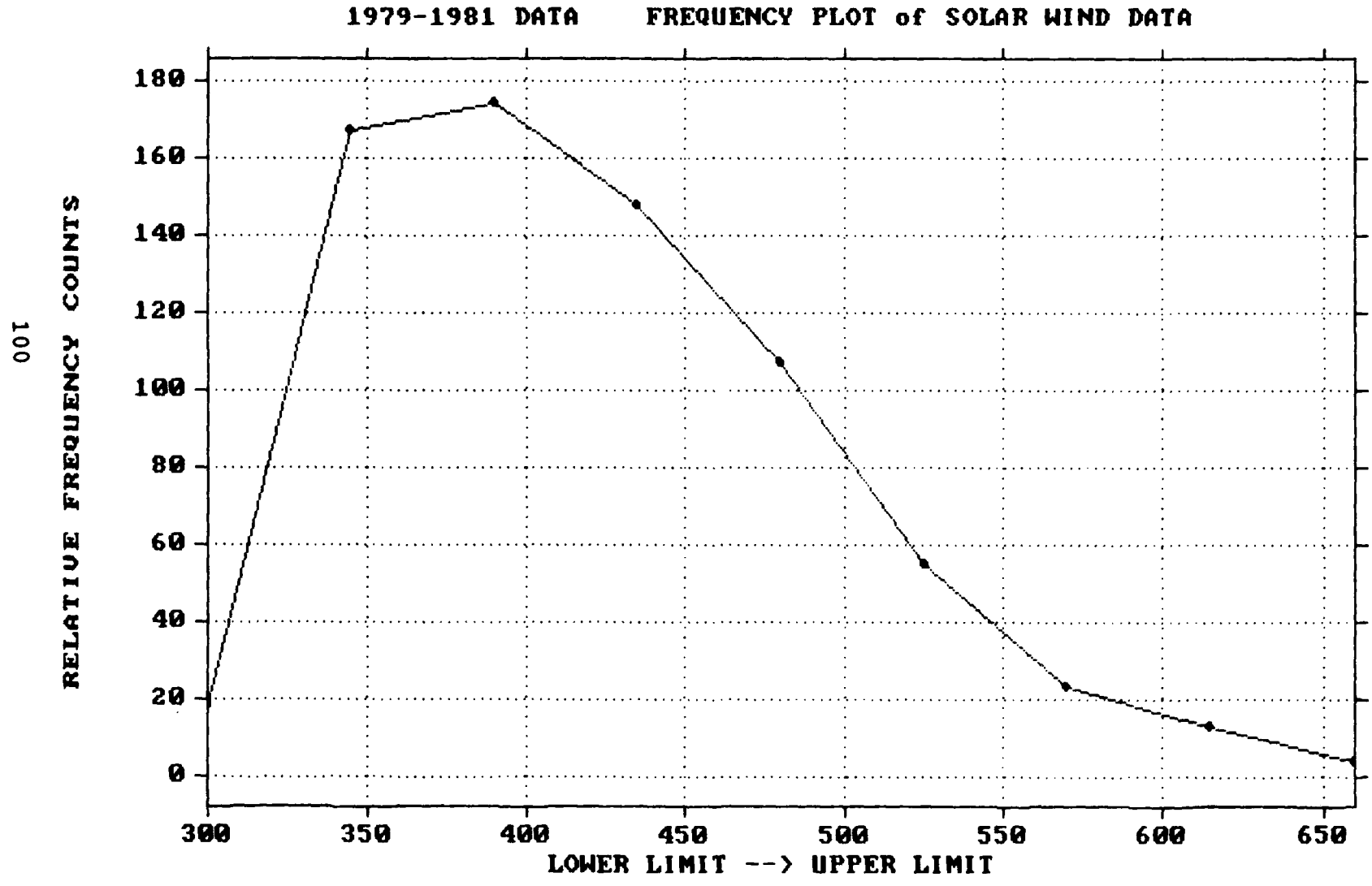
1979-1981 DATA FREQUENCY PLOT of SOLAR WIND DATA
RELATIVE FREQUENCY COUNTS
100
180
160
140
120
100
80
60
40
20
0
300
350
400
450
500
550
600
650
LOWER LIMIT --> UPPER LIMIT

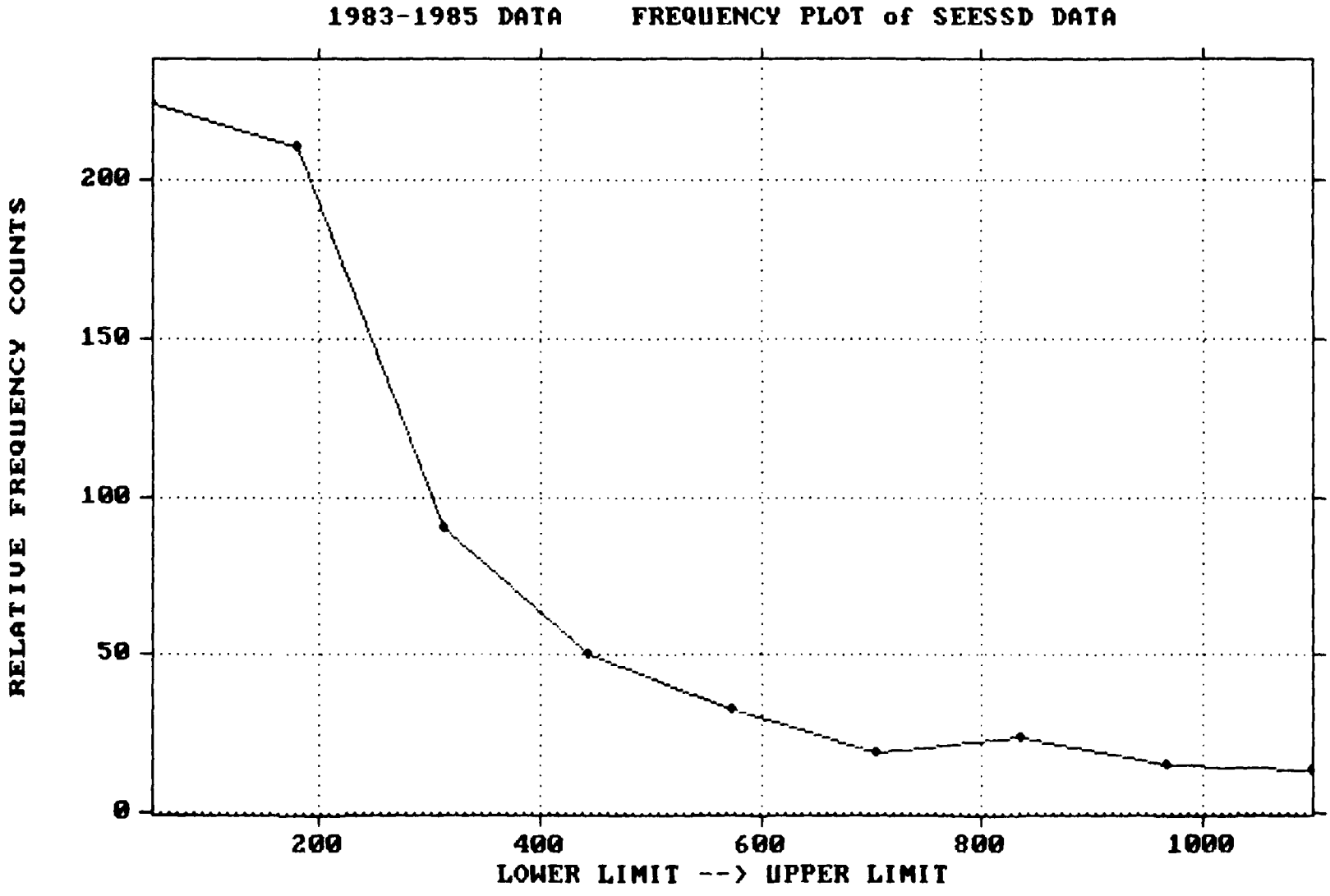
1983-1985 DATA FREQUENCY PLOT of SEESSD DATA
RELATIVE FREQUENCY COUNTS
0
50
100
150
200
200
400
600
800
1000
LOWER LIMIT --> UPPER LIMIT

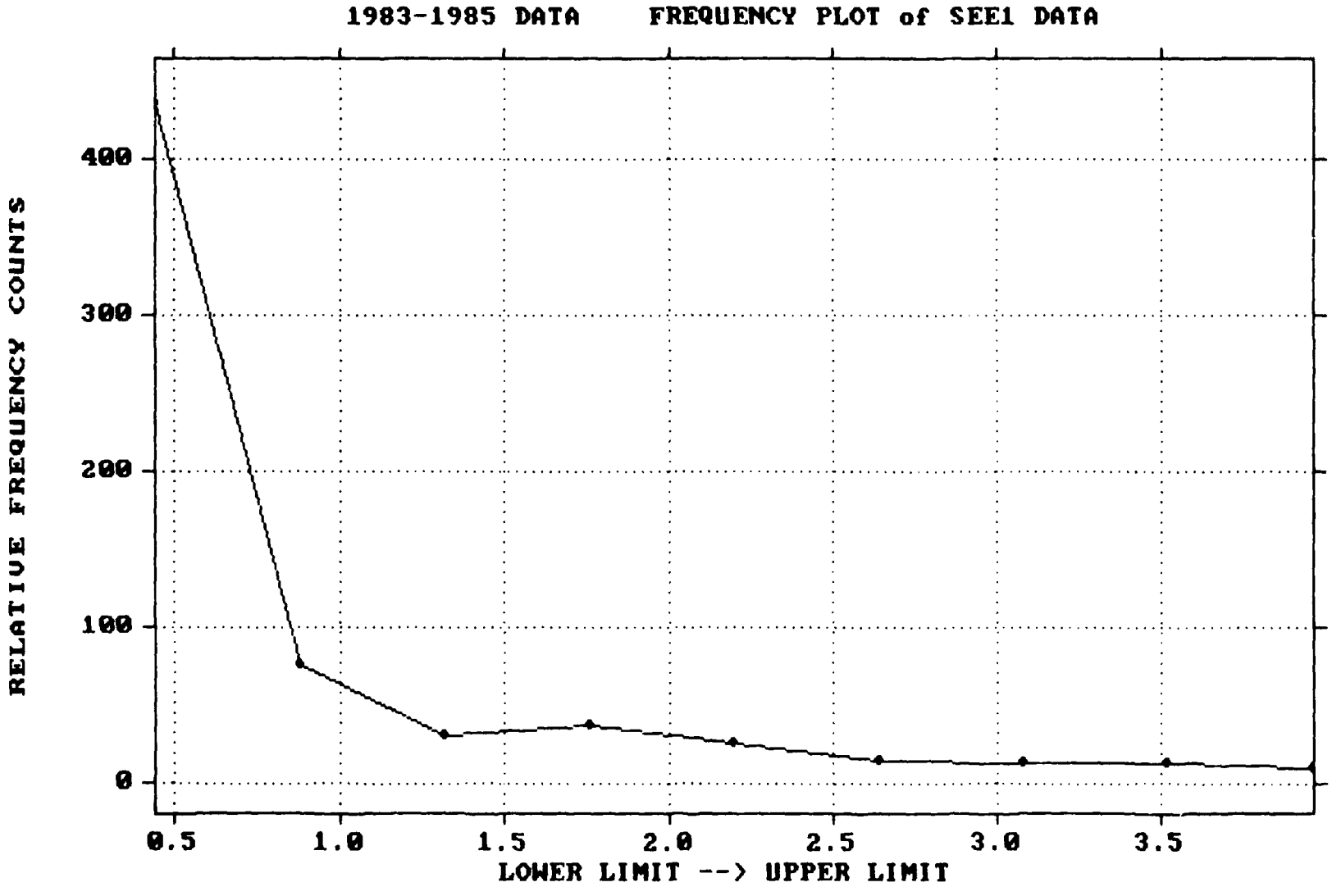
1983-1985 DATA FREQUENCY PLOT of SEE1 DATA
RELATIVE FREQUENCY COUNTS
400
300
200
100
0
0.5
1.0
1.5
2.0
2.5
3.0
3.5
LOWER LIMIT --> UPPER LIMIT

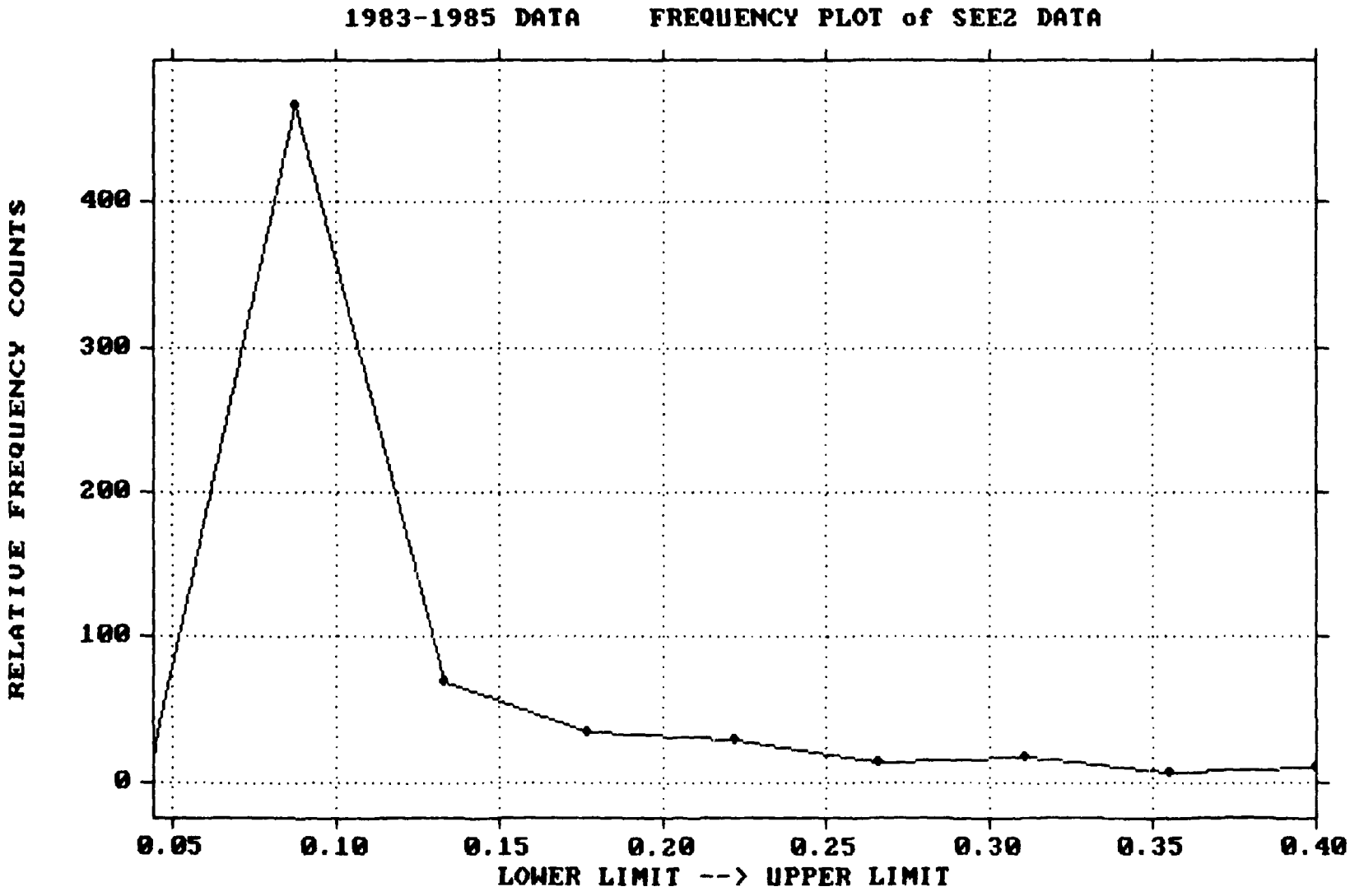
1983-1985 DATA FREQUENCY PLOT of SEE2 DATA
RELATIVE FREQUENCY COUNTS
400
300
200
100
0
0.05
0.10
0.15
0.20
0.25
0.30
0.35
0.40
LOWER LIMIT --> UPPER LIMIT

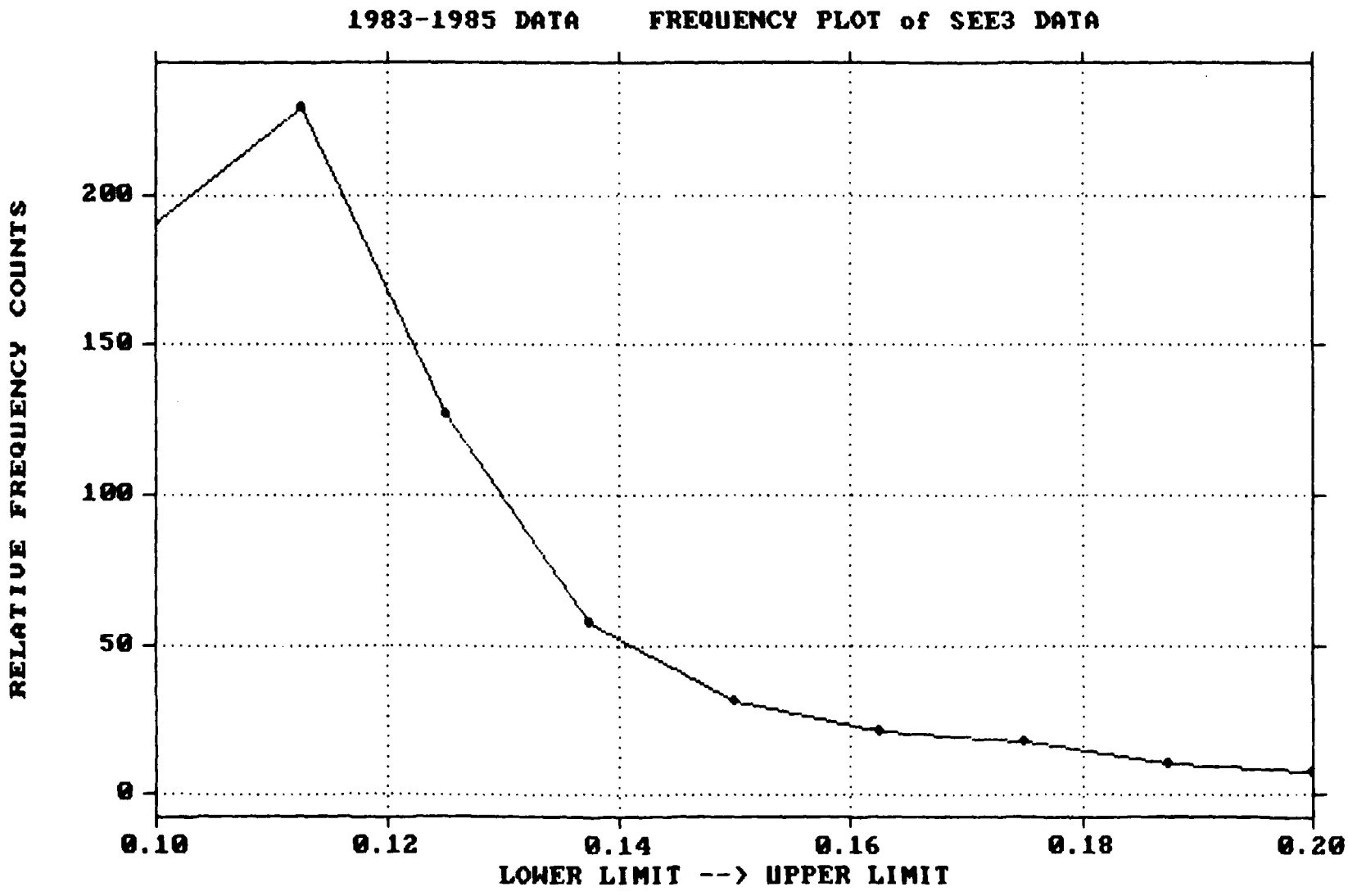
1983-1985 DATA FREQUENCY PLOT of SEE3 DATA
RELATIVE FREQUENCY COUNTS
200
150
100
50
0
0.10
0.12
0.14
0.16
0.18
0.20
LOWER LIMIT --> UPPER LIMIT

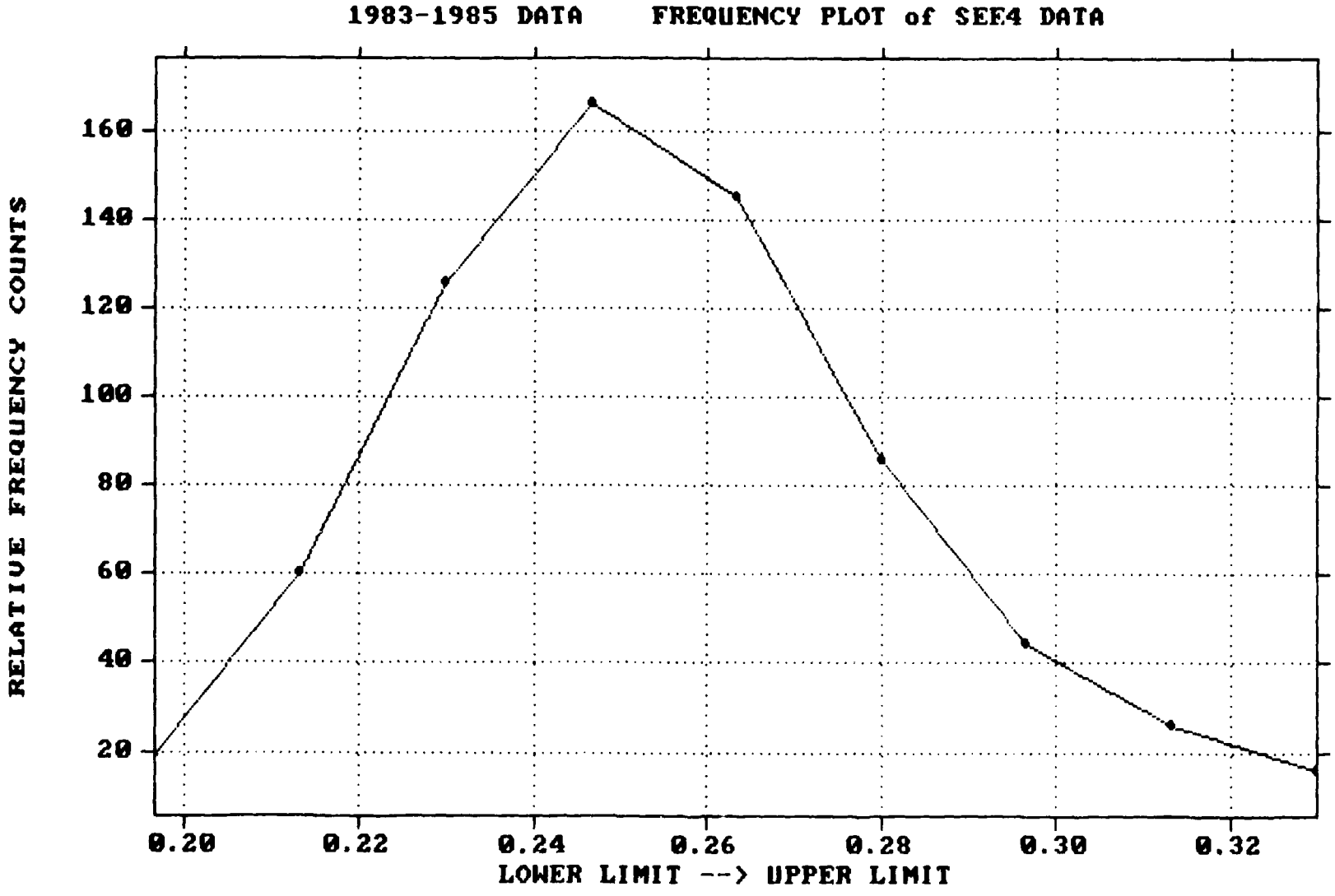
1983-1985 DATA FREQUENCY PLOT of SEE4 DATA
RELATIVE FREQUENCY COUNTS
160
140
120
100
80
60
40
20
0.20
0.22
0.24
0.26
0.28
0.30
0.32
LOWER LIMIT --> UPPER LIMIT

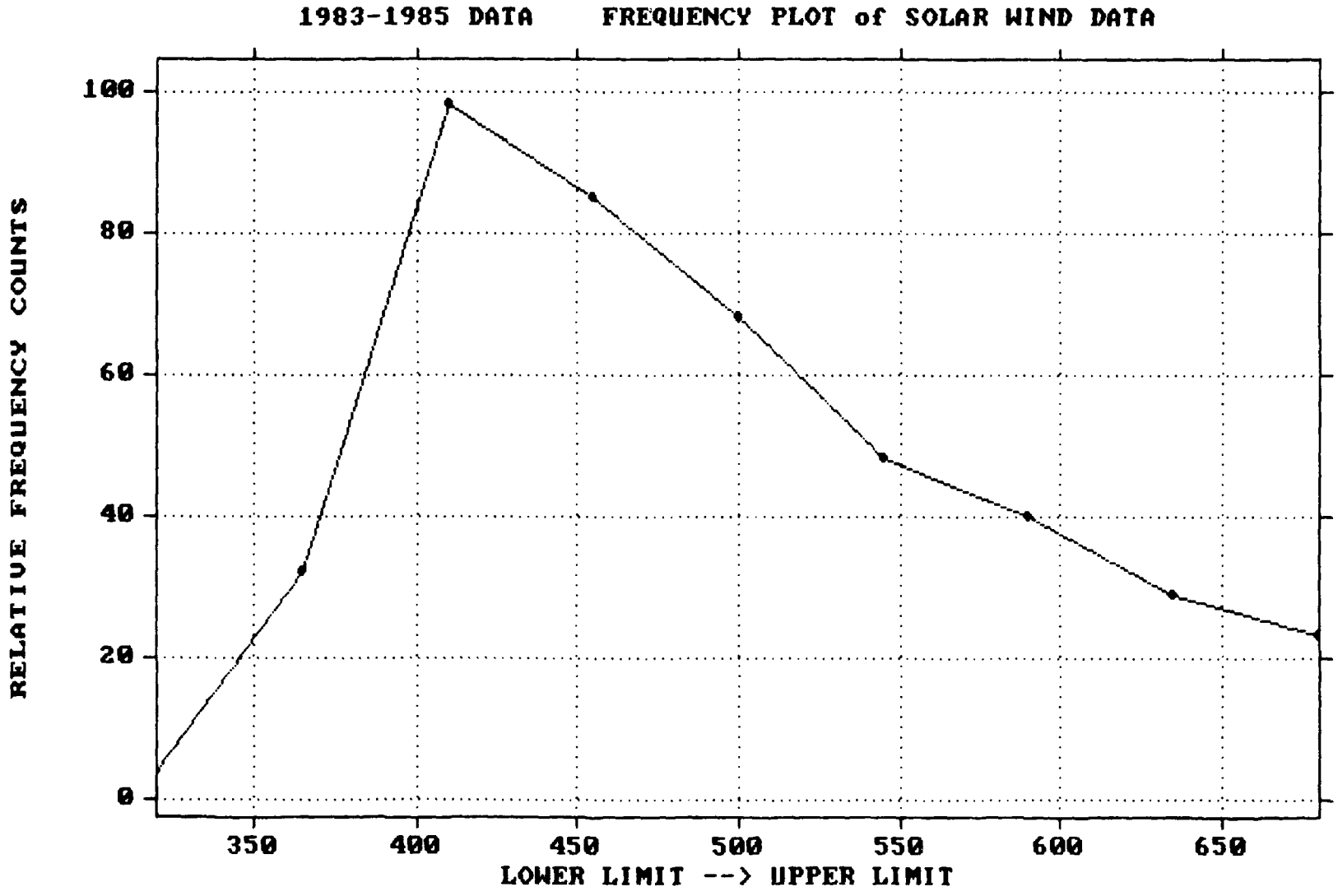
1983-1985 DATA FREQUENCY PLOT of SOLAR WIND DATA
RELATIVE FREQUENCY COUNTS
100
80
60
40
20
0
350
400
450
500
550
600
650
LOWER LIMIT --> UPPER LIMIT

Appendix C: Normal Probability Plots of Ln(Data)

Page

1979-1981 Data 108

1983-1985 Data 114

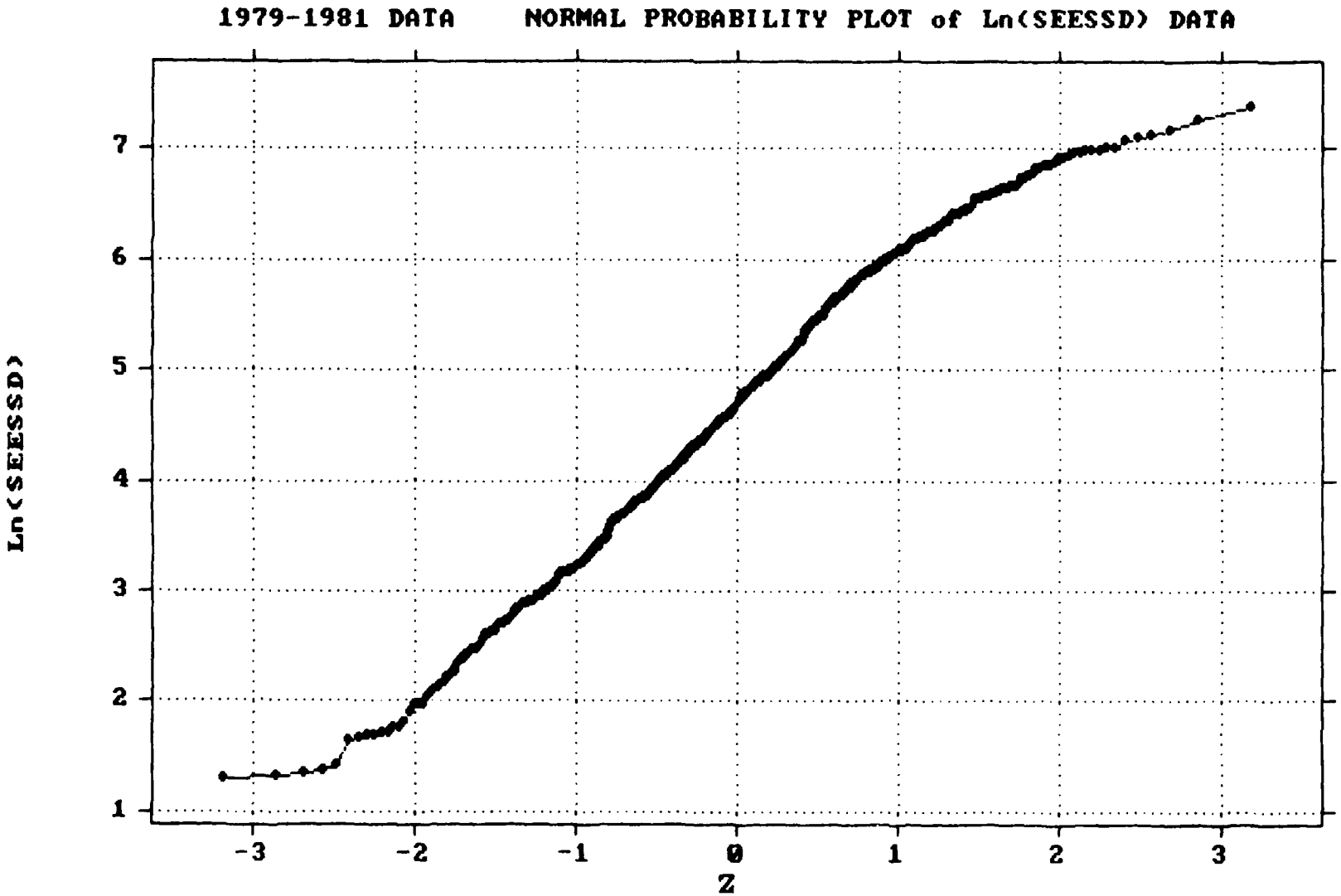
1979-1981 DATA NORMAL PROBABILITY PLOT of Ln(SEESSD) DATA
Ln(SEESSD)
7
6
5
4
3
2
1
-3
-2
-1
0
1
2
3
Z

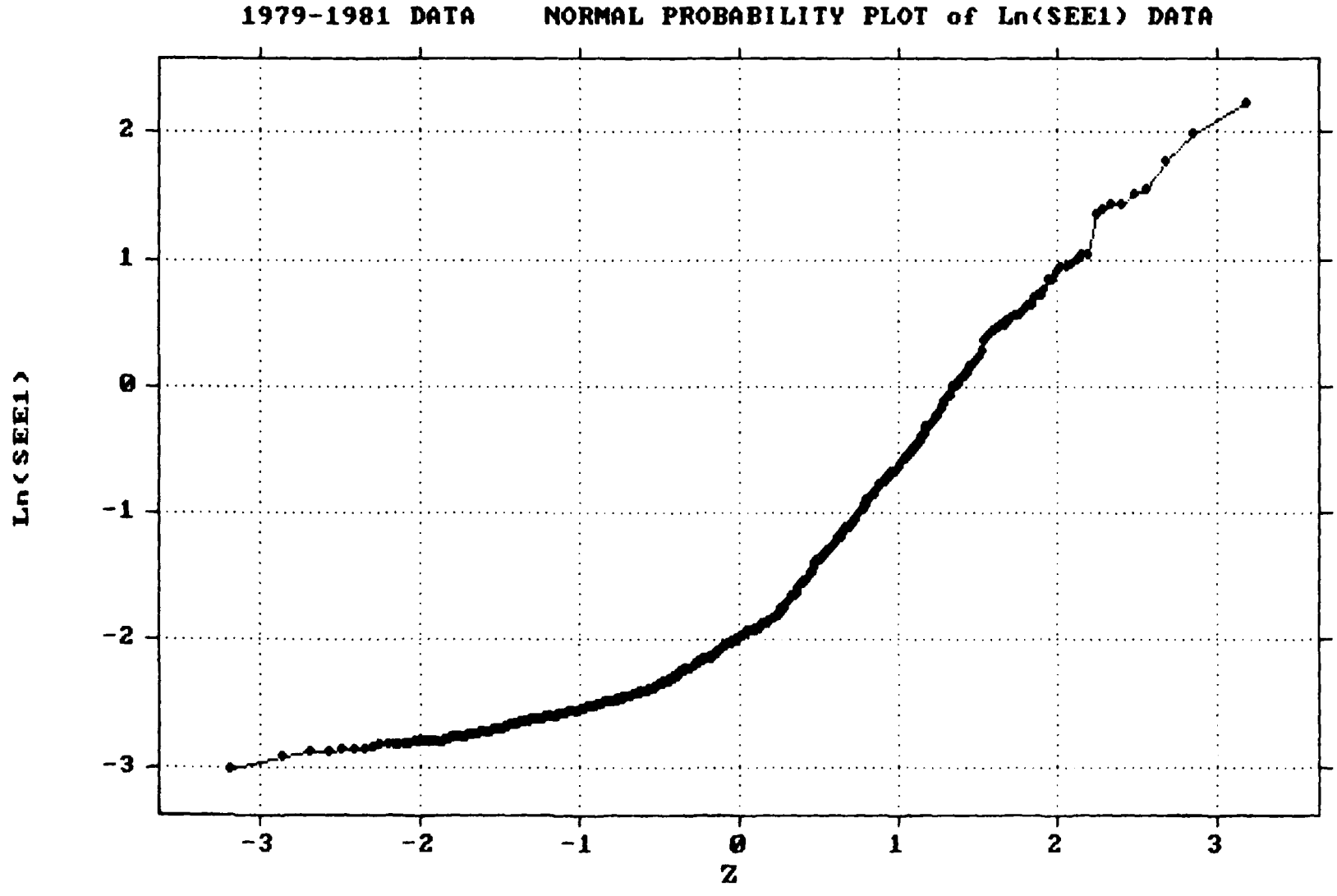
1979-1981 DATA NORMAL PROBABILITY PLOT of Ln(SEE1) DATA
Ln(SEE1)
Z
2
1
0
-1
-2
-3
-3
-2
-1
0
1
2
3

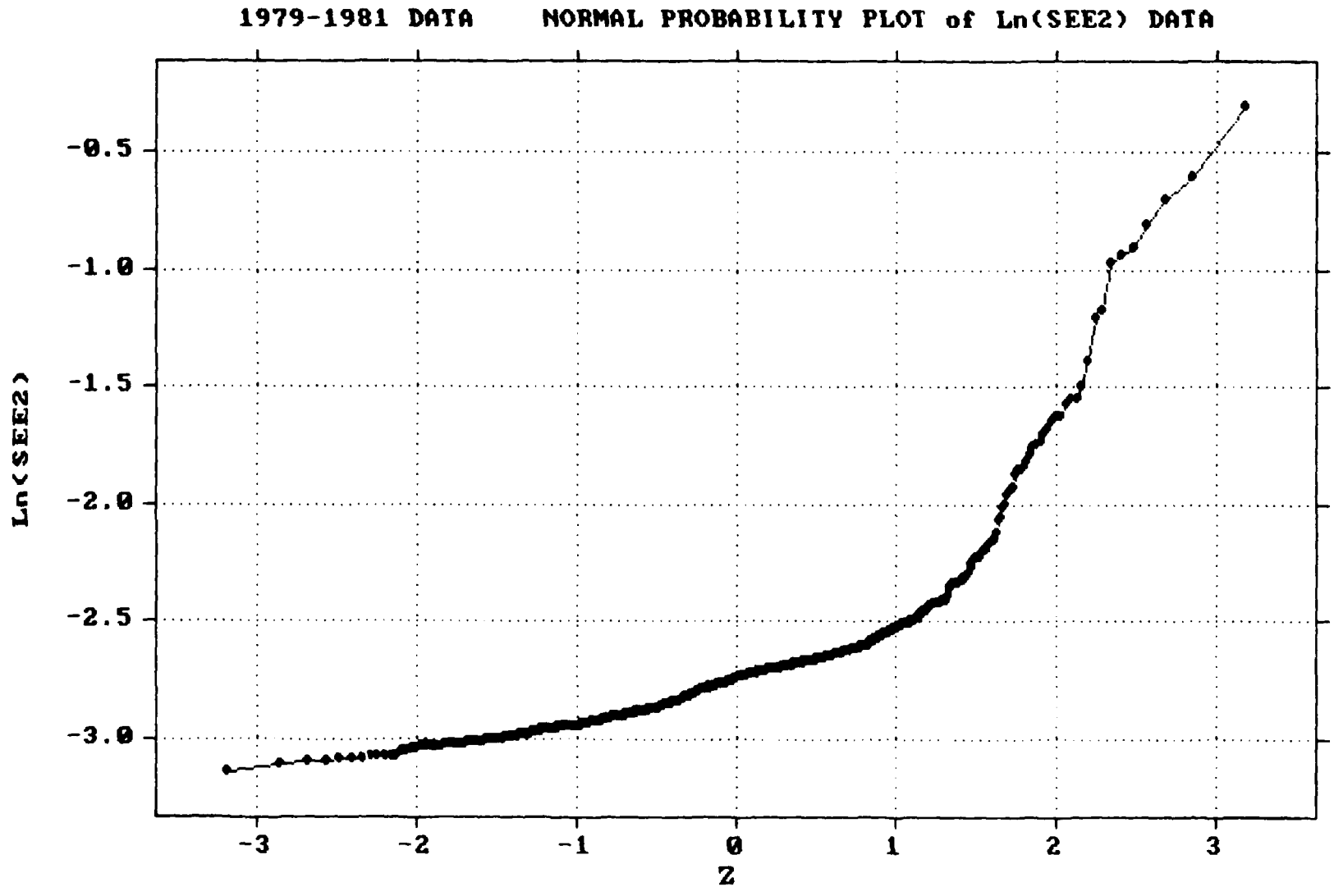
1979-1981 DATA NORMAL PROBABILITY PLOT of Ln(SEE2) DATA
-0.5
-1.0
-1.5
-2.0
-2.5
-3.0
Ln(SEE2)
-3
-2
-1
0
1
2
3
Z

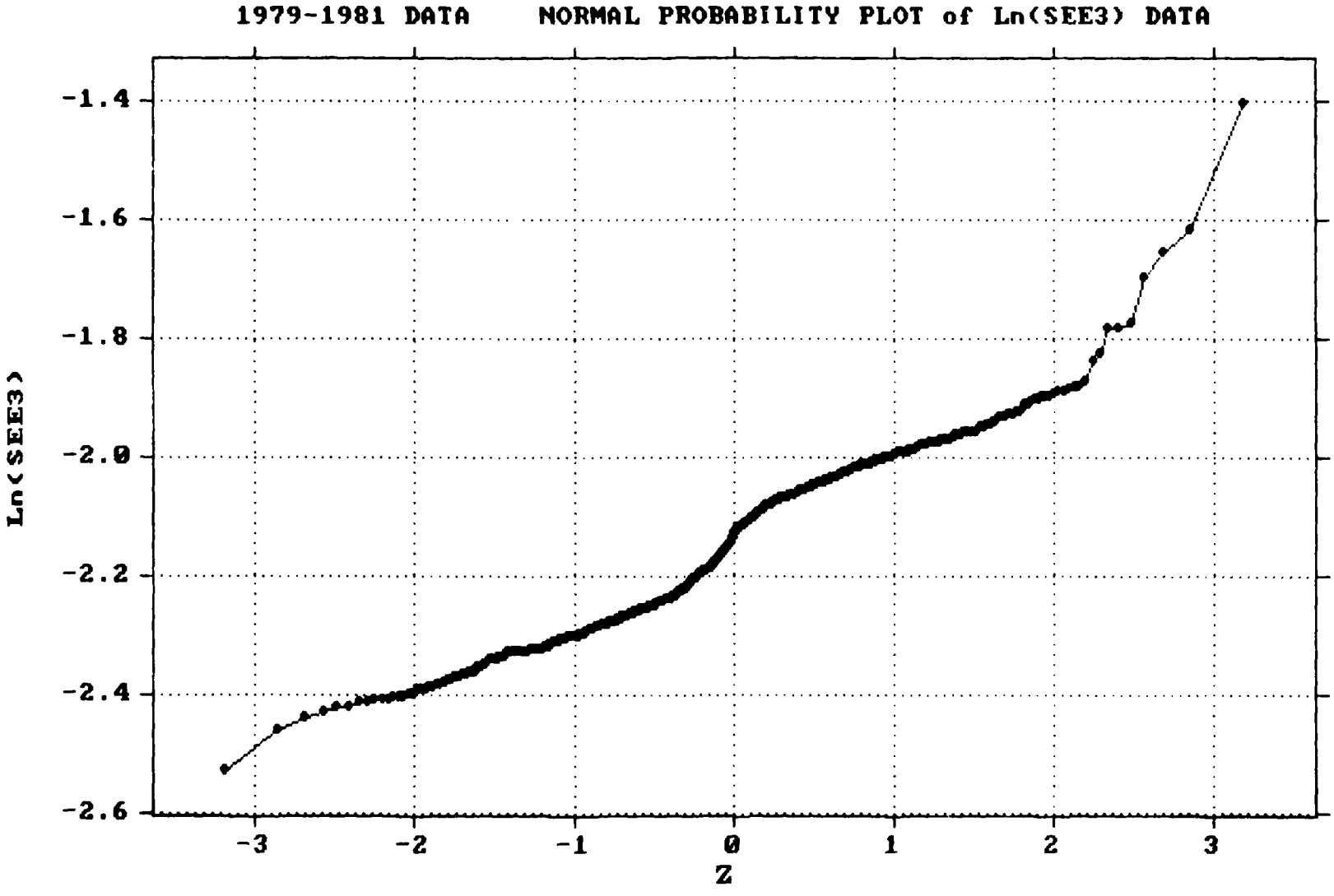
1979-1981 DATA NORMAL PROBABILITY PLOT of Ln(SEE3) DATA
Ln(SEE3)
-1.4
-1.6
-1.8
-2.0
-2.2
-2.4
-2.6
-3
-2
-1
0
1
2
3
Z

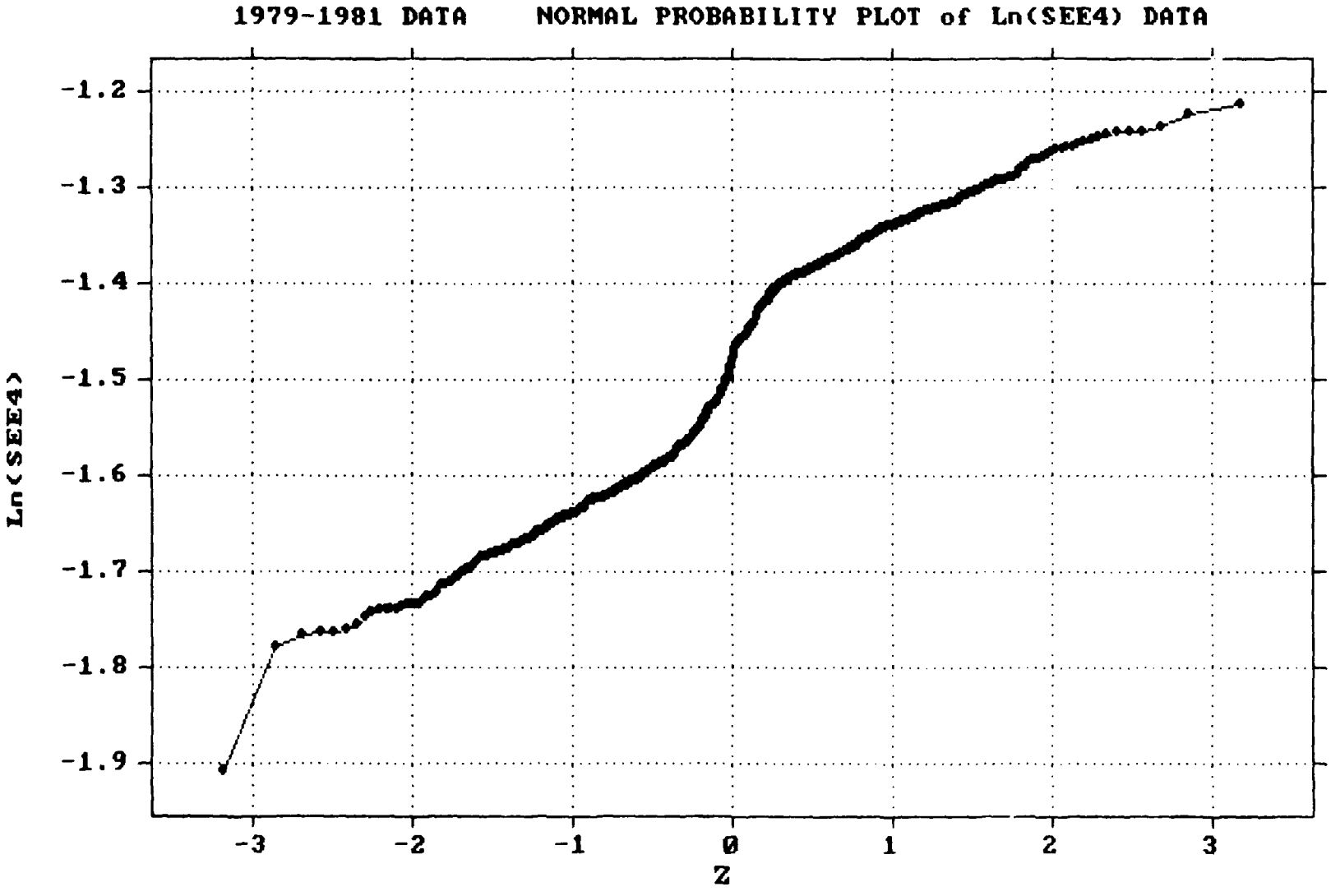
1979-1981 DATA NORMAL PROBABILITY PLOT of Ln(SEE4) DATA
Ln(SEE4)
-1.2
-1.3
-1.4
-1.5
-1.6
-1.7
-1.8
-1.9
-3
-2
-1
0
1
2
3
Z

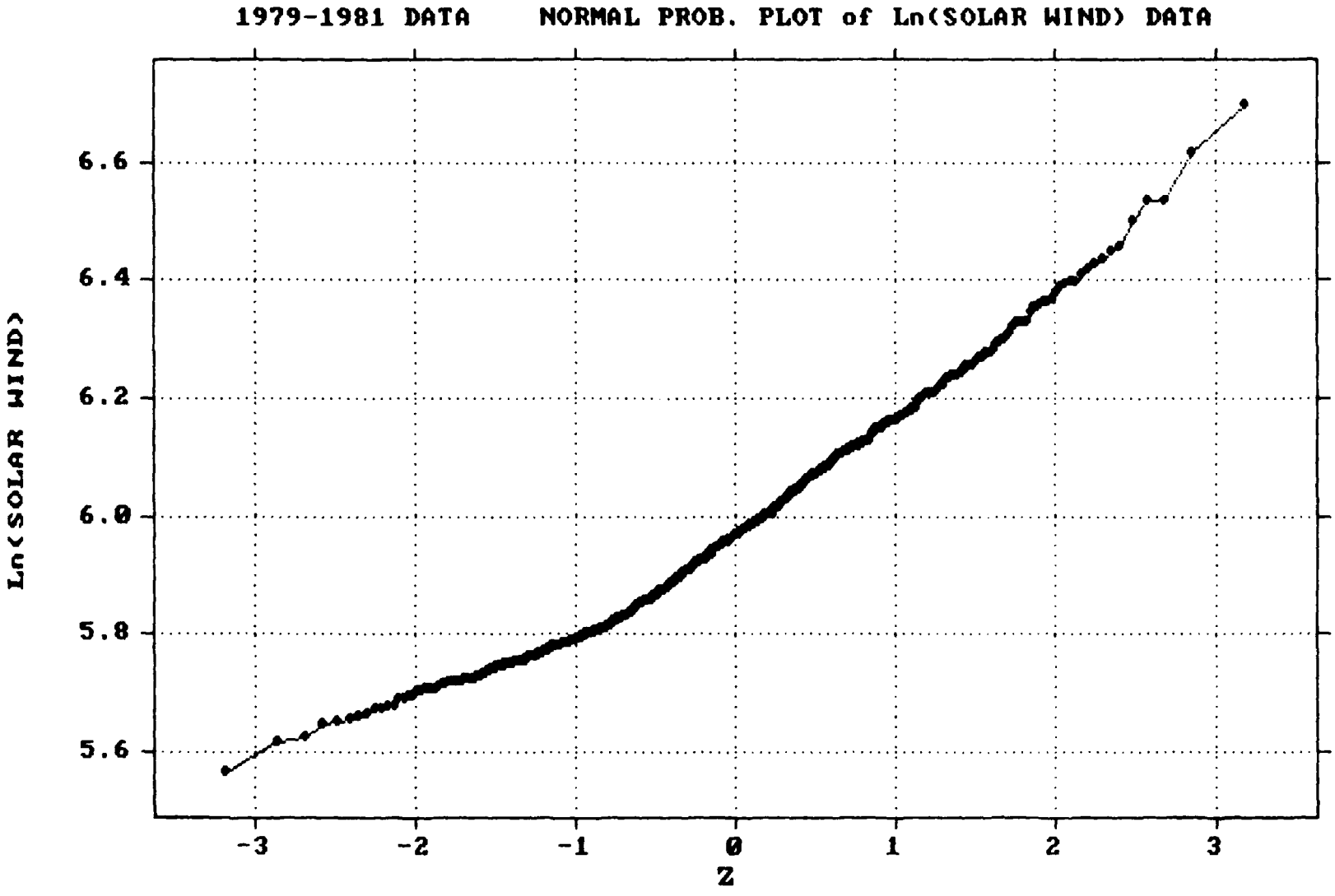
1979-1981 DATA NORMAL PROB. PLOT of Ln(SOLAR WIND) DATA
Ln(SOLAR WIND)
6.6
6.4
6.2
6.0
5.8
5.6
-3
-2
-1
0
1
2
3
Z

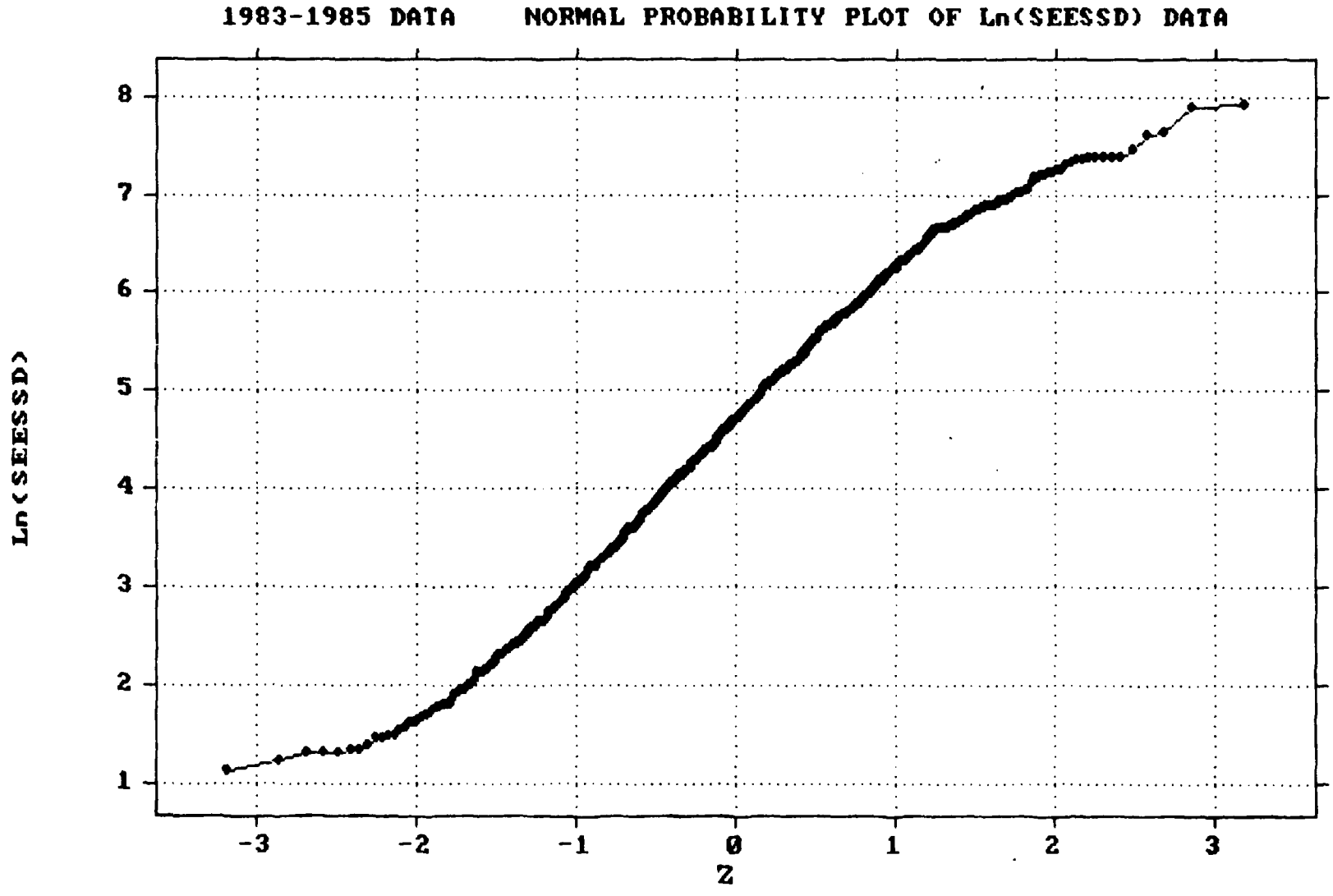
1983-1985 DATA NORMAL PROBABILITY PLOT OF Ln(SEESSD) DATA
Ln(SEESSD)
8
7
6
5
4
3
2
1
-3
-2
-1
0
1
2
3
Z

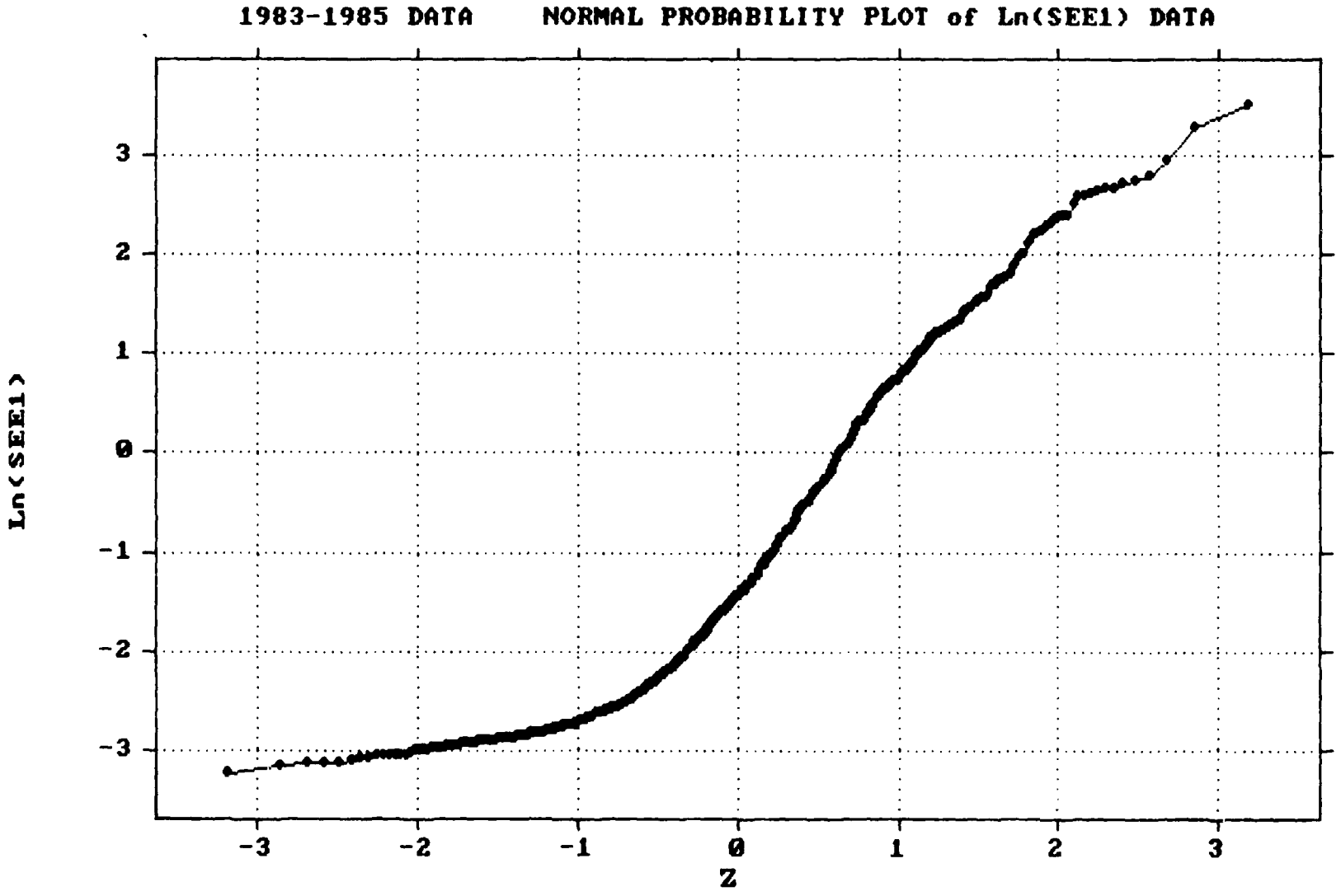
1983-1985 DATA NORMAL PROBABILITY PLOT of Ln(SEE1) DATA
Ln(SEE1)
Z
3
2
1
0
-1
-2
-3
-3
-2
-1
0
1
2
3

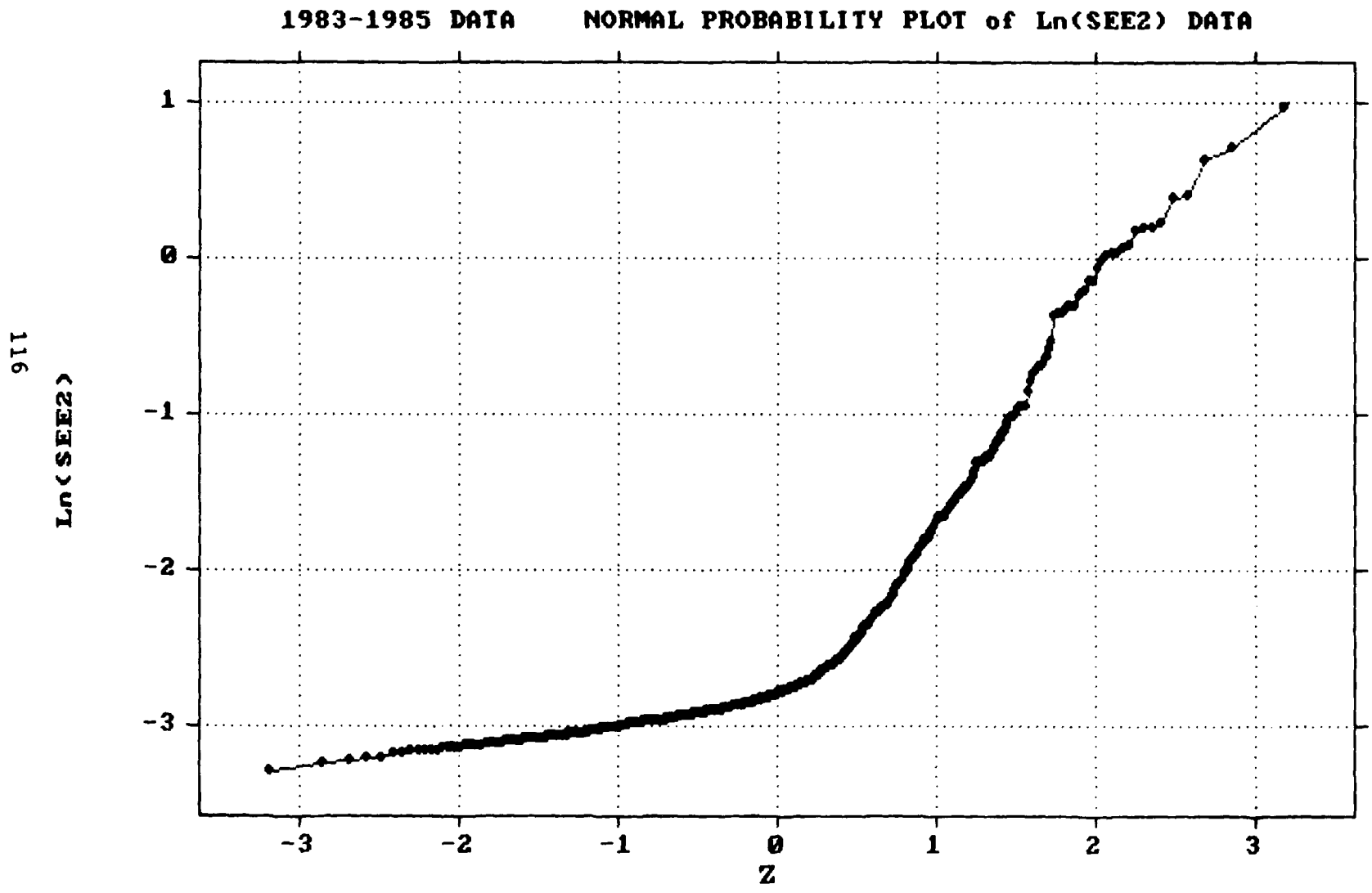
1983-1985 DATA NORMAL PROBABILITY PLOT of Ln(SEE2) DATA
Ln(SEE2)
Z
1
0
-1
-2
-3
-3
-2
-1
0
1
2
3

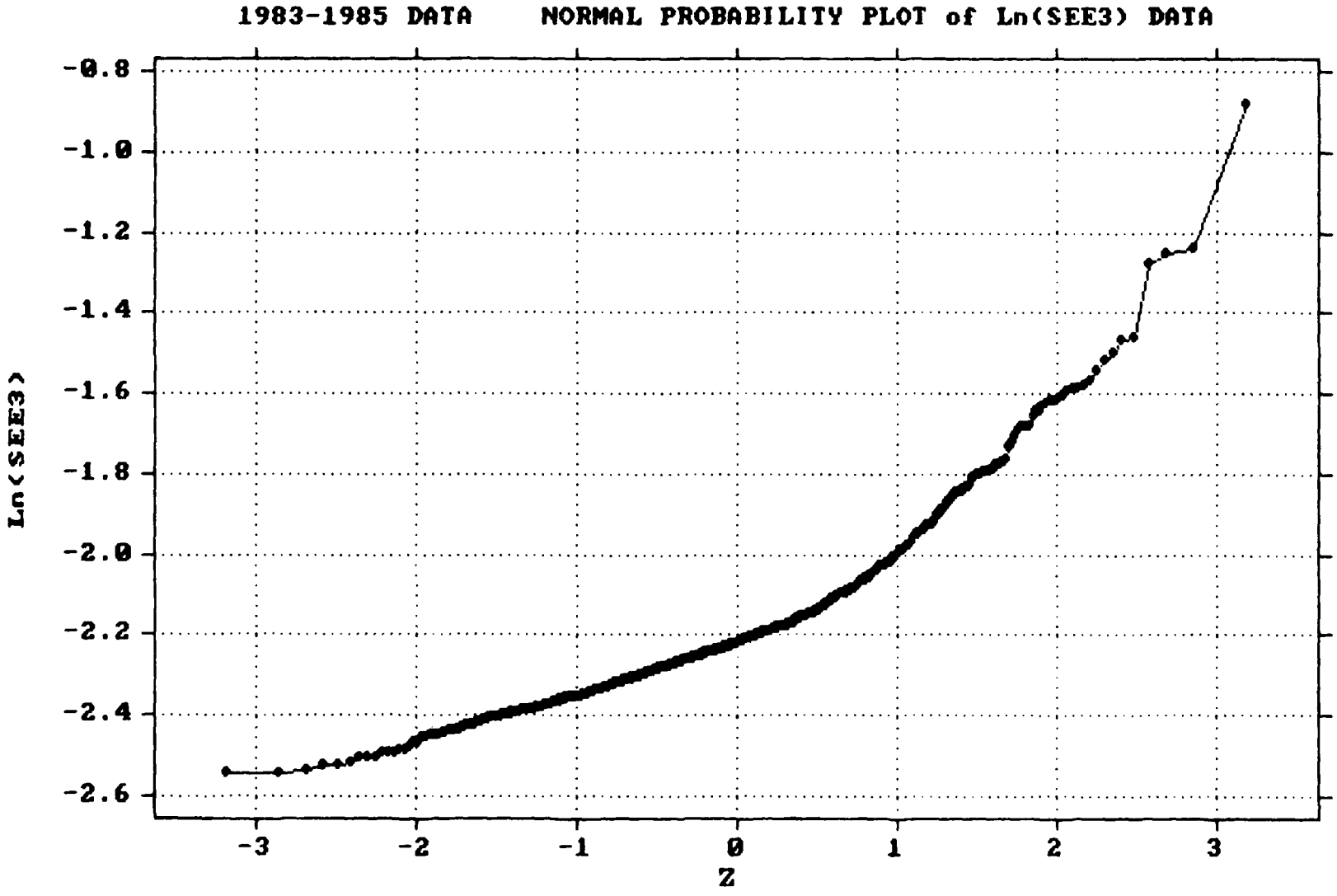
1983-1985 DATA NORMAL PROBABILITY PLOT of Ln(SEE3) DATA
Ln(SEE3)
-0.8
-1.0
-1.2
-1.4
-1.6
-1.8
-2.0
-2.2
-2.4
-2.6
-3
-2
-1
0
1
2
3
Z

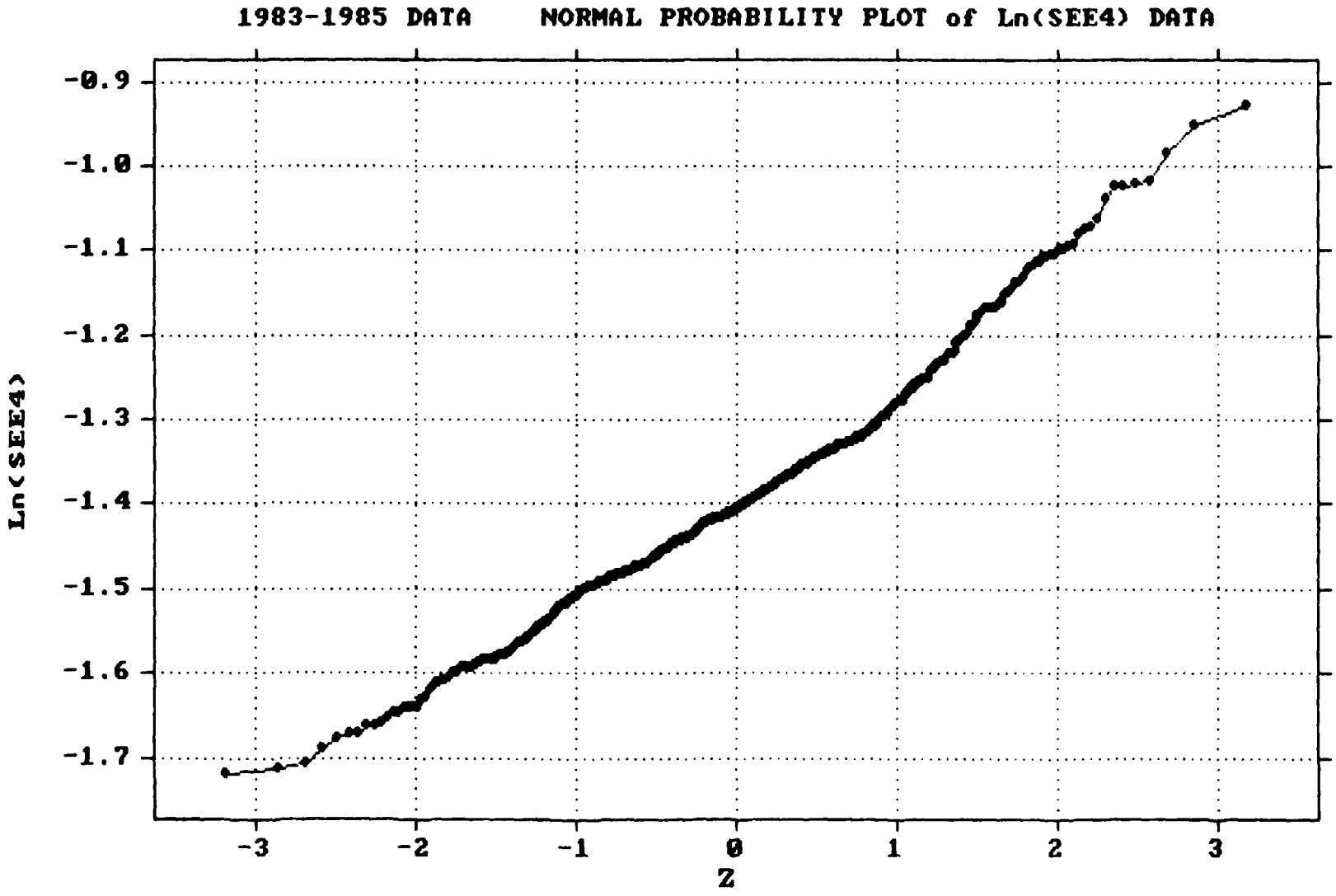
1983-1985 DATA NORMAL PROBABILITY PLOT of Ln(SEE4) DATA
-0.9
-1.0
-1.1
-1.2
-1.3
-1.4
-1.5
-1.6
-1.7
Ln(SEE4)
-3
-2
-1
0
1
2
3
Z

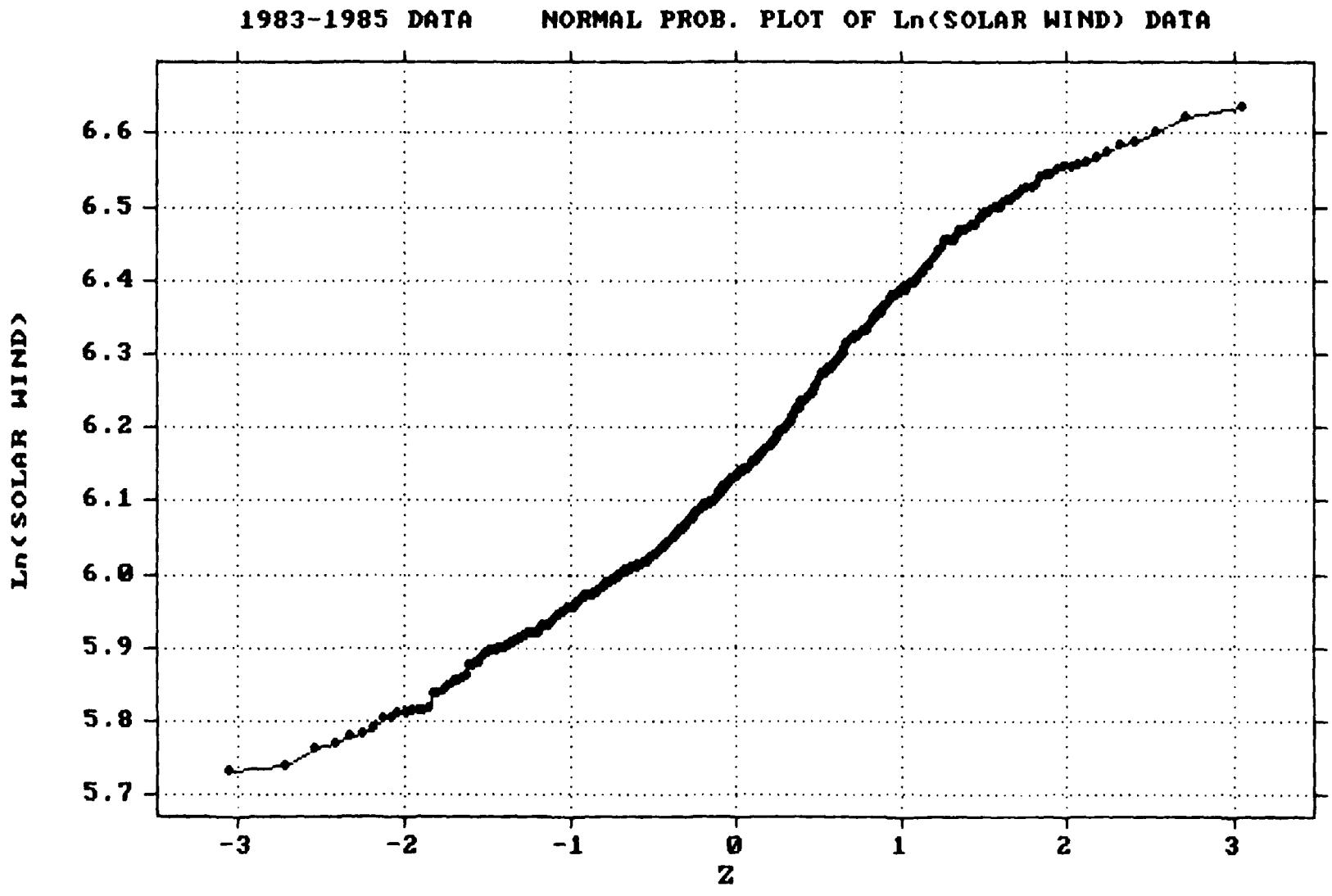
1983-1985 DATA NORMAL PROB. PLOT OF Ln(SOLAR WIND) DATA
Ln(SOLAR WIND)
6.6
6.5
6.4
6.3
6.2
6.1
6.0
5.9
5.8
5.7
-3
-2
-1
0
1
2
3
Z

Appendix D: Scatter Plots of 2-Day Solar Wind Lags verses Electron Count Data for R-Squared Values Greater than .10

Page

1979-1981 Data 121

Original Data 121

Percentiled Data 123

1983-1985 Data 125

Original Data 125

Percentiled Data 130

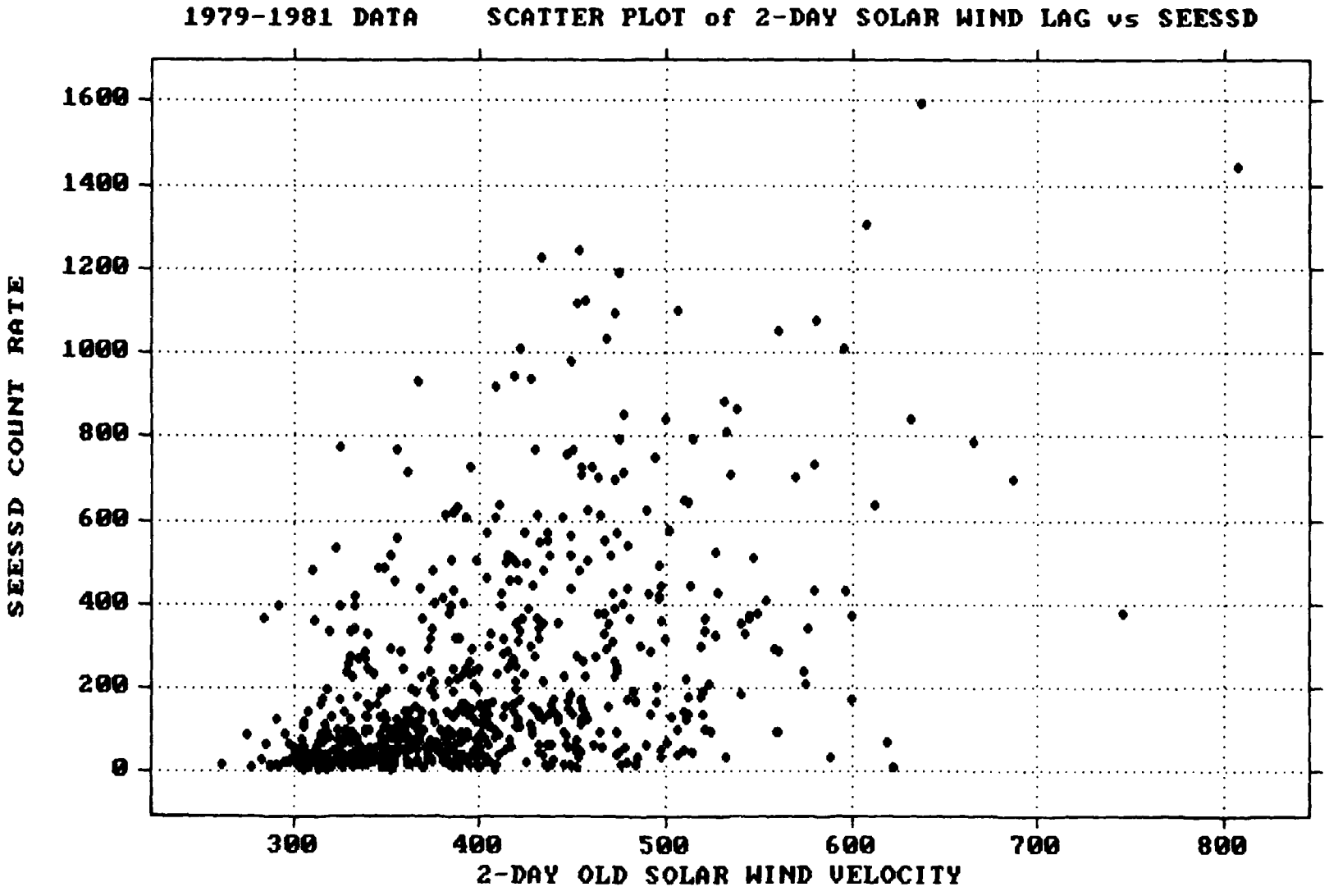
1979-1981 DATA SCATTER PLOT of 2-DAY SOLAR WIND LAG vs SEESSD
SEESSD COUNT RATE
1600
1400
1200
1000
800
600
400
200
0
300
400
500
600
700
800
2-DAY OLD SOLAR WIND VELOCITY

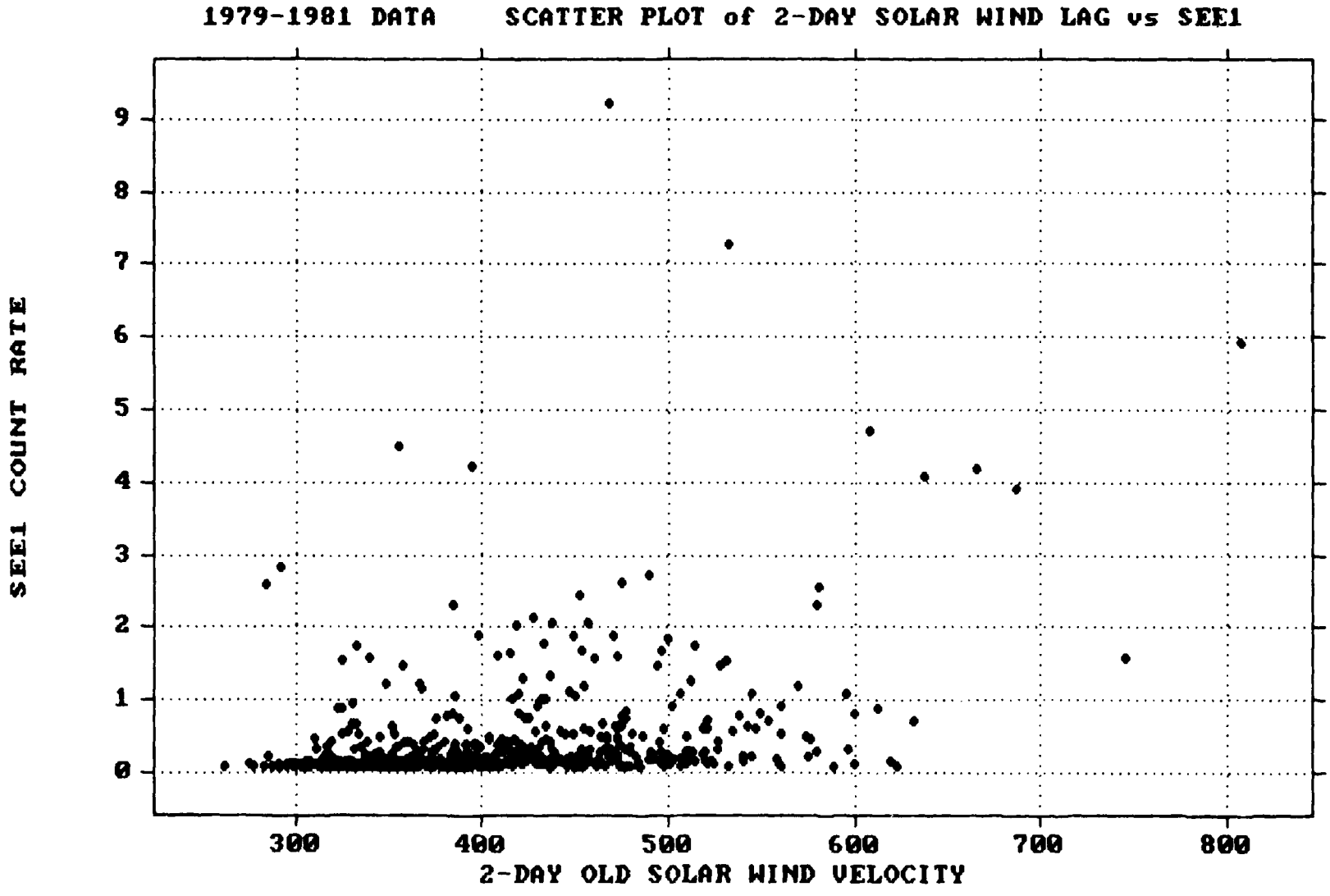
1979-1981 DATA SCATTER PLOT of 2-DAY SOLAR WIND LAG vs SEE1
SEE1 COUNT RATE
0
1
2
3
4
5
6
7
8
9
300
400
500
600
700
800
2-DAY OLD SOLAR WIND VELOCITY

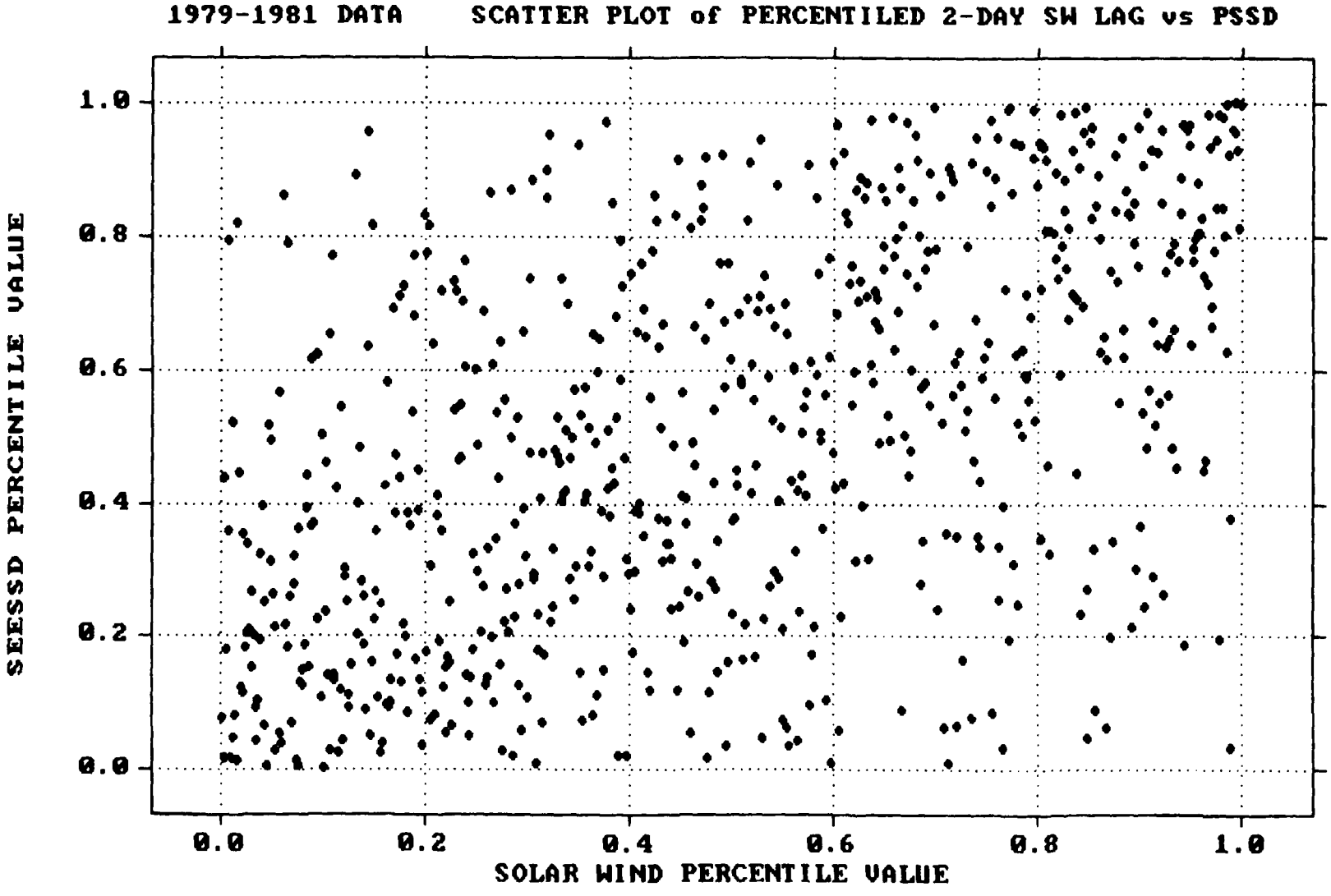
1979-1981 DATA SCATTER PLOT of PERCENTILED 2-DAY SW LAG vs PSSD
SEESSD PERCENTILE VALUE
1.0
0.8
0.6
0.4
0.2
0.0
0.0
0.2
0.4
0.6
0.8
1.0
SOLAR WIND PERCENTILE VALUE

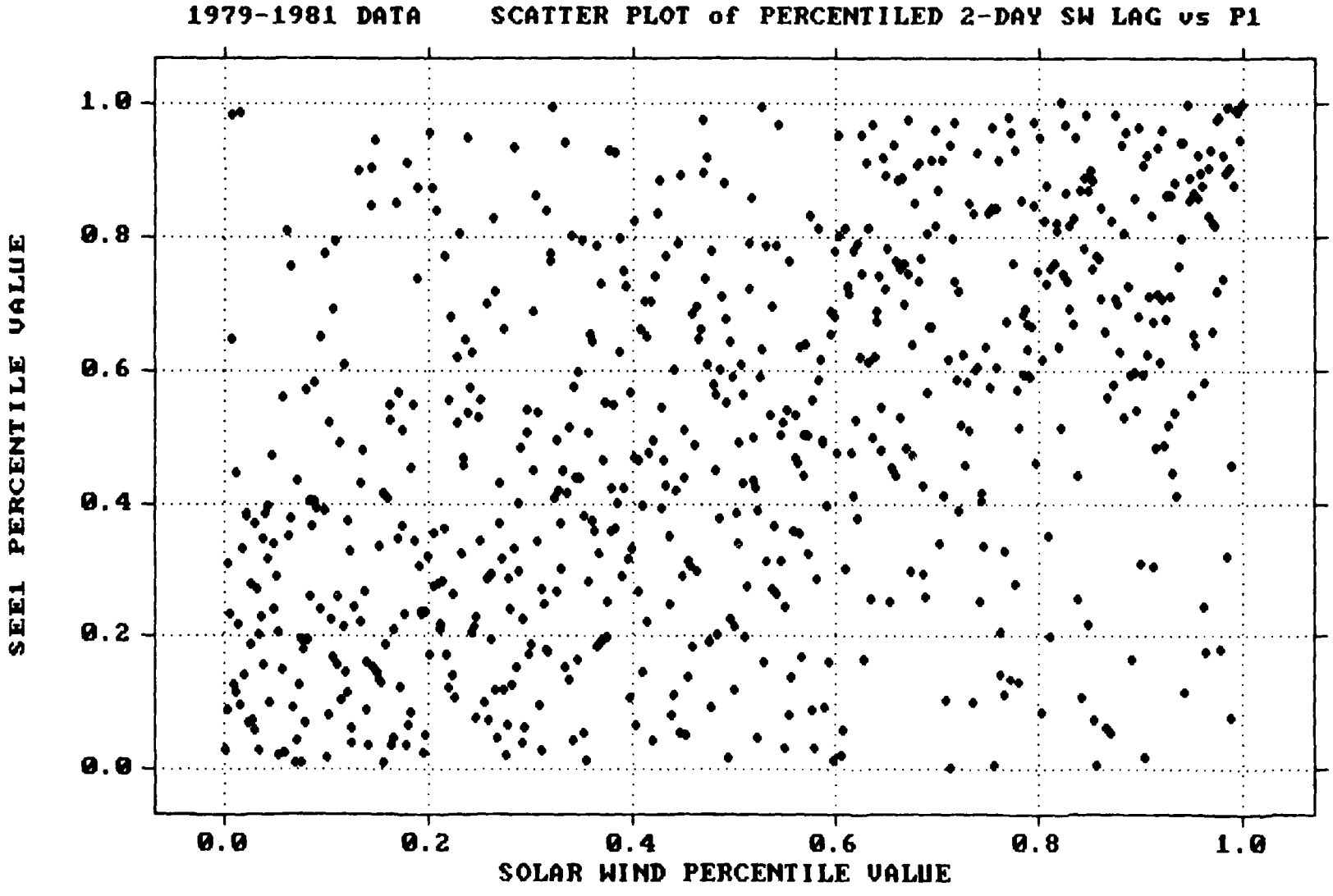
1979-1981 DATA SCATTER PLOT of PERCENTILED 2-DAY SW LAG vs P1
SEE1 PERCENTILE VALUE
1.0
0.8
0.6
0.4
0.2
0.0
0.0
0.2
0.4
0.6
0.8
1.0
SOLAR WIND PERCENTILE VALUE

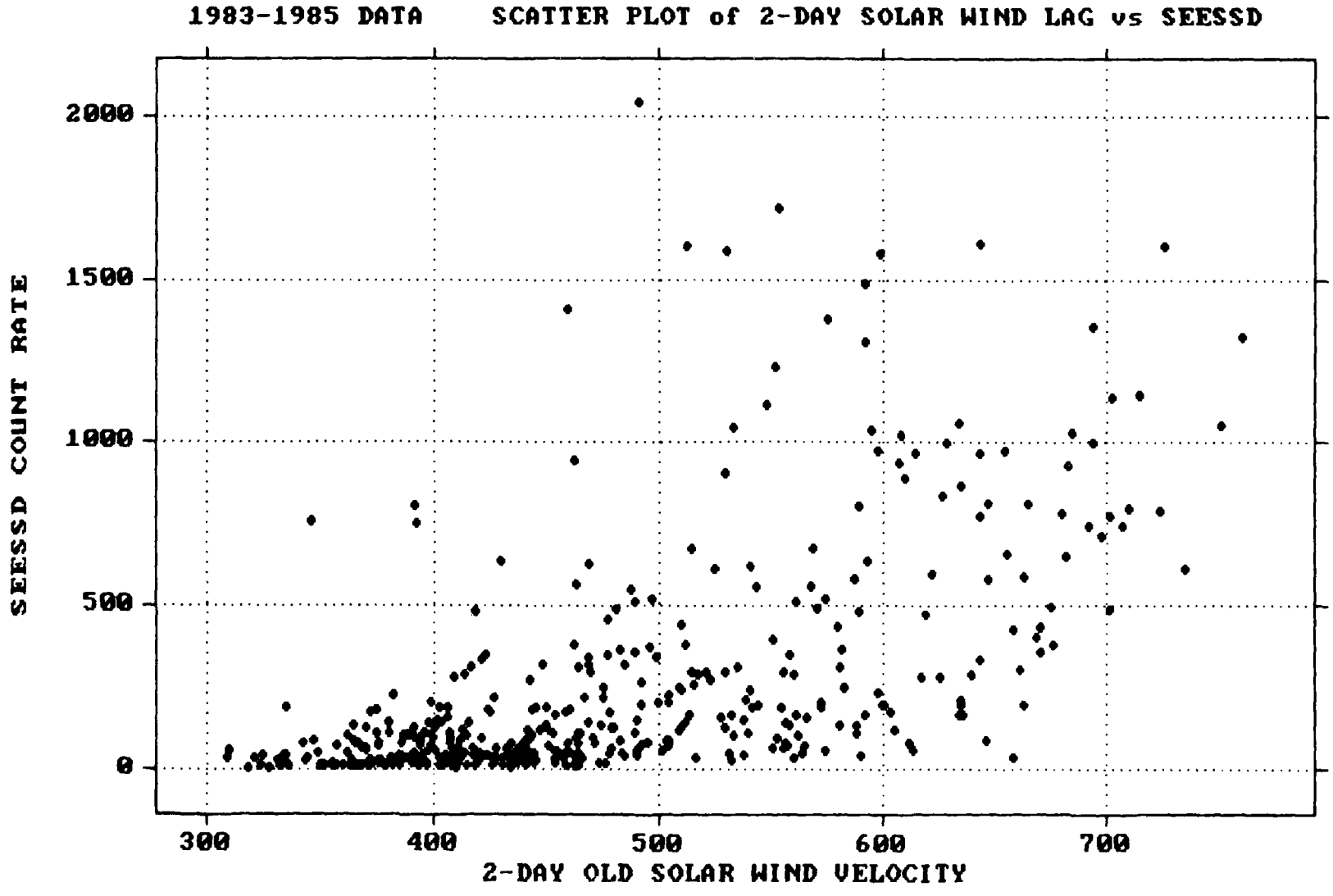
1983-1985 DATA SCATTER PLOT of 2-DAY SOLAR WIND LAG vs SEESSD
SEESSD COUNT RATE
2000
1500
1000
500
0
300
400
500
600
700
2-DAY OLD SOLAR WIND VELOCITY

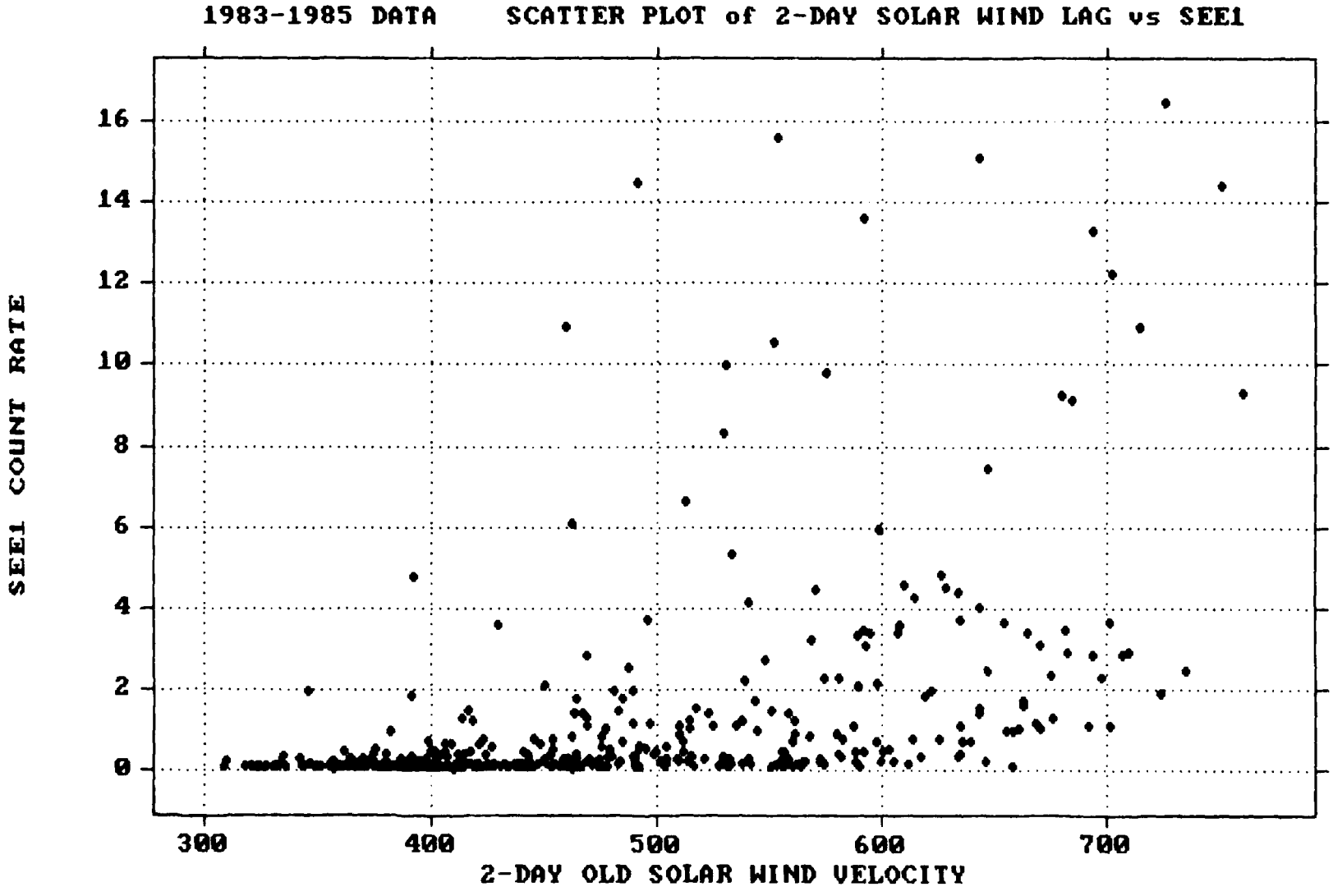
1983-1985 DATA
SCATTER PLOT of 2-DAY SOLAR WIND LAG vs SEE1
SEE1 COUNT RATE
16
14
12
10
8
6
4
2
0
300
400
500
600
700
2-DAY OLD SOLAR WIND VELOCITY

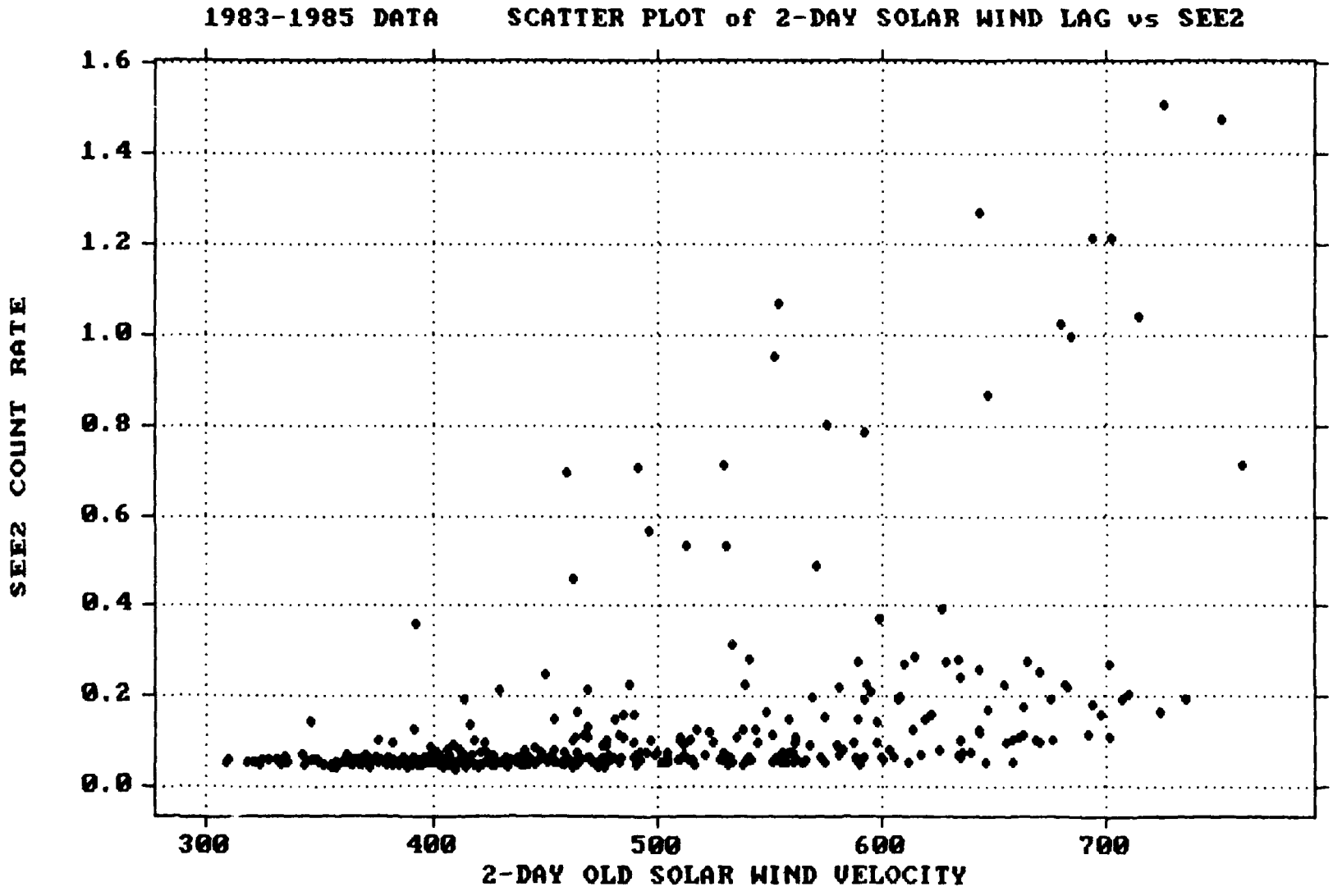
1983-1985 DATA SCATTER PLOT of 2-DAY SOLAR WIND LAG vs SEE2
SEE2 COUNT RATE
1.6
1.4
1.2
1.0
0.8
0.6
0.4
0.2
0.0
300
400
500
600
700
2-DAY OLD SOLAR WIND VELOCITY

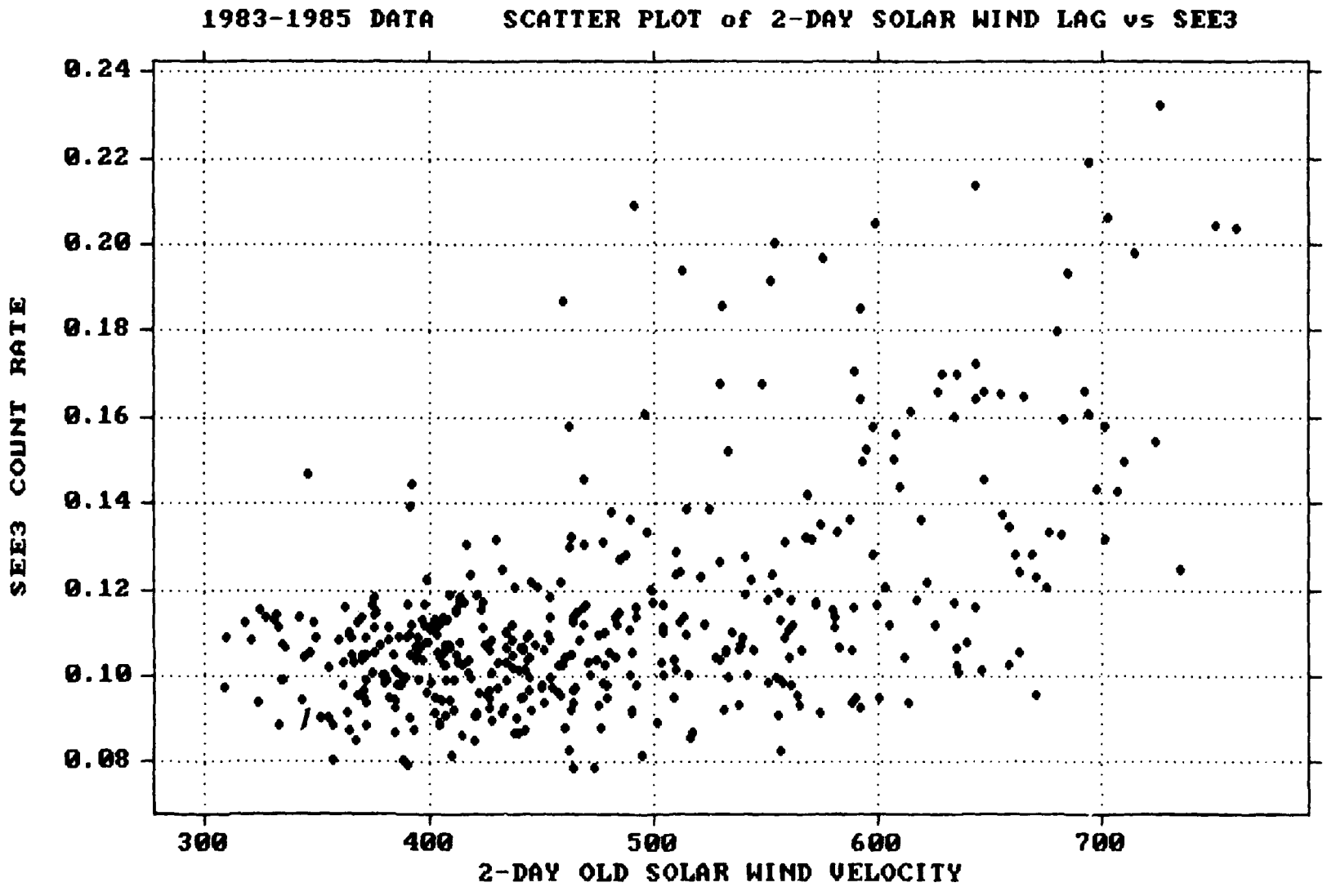
1983-1985 DATA SCATTER PLOT of 2-DAY SOLAR WIND LAG vs SEE3
SEE3 COUNT RATE
0.24
0.22
0.20
0.18
0.16
0.14
0.12
0.10
0.08
300
400
500
600
700
2-DAY OLD SOLAR WIND VELOCITY

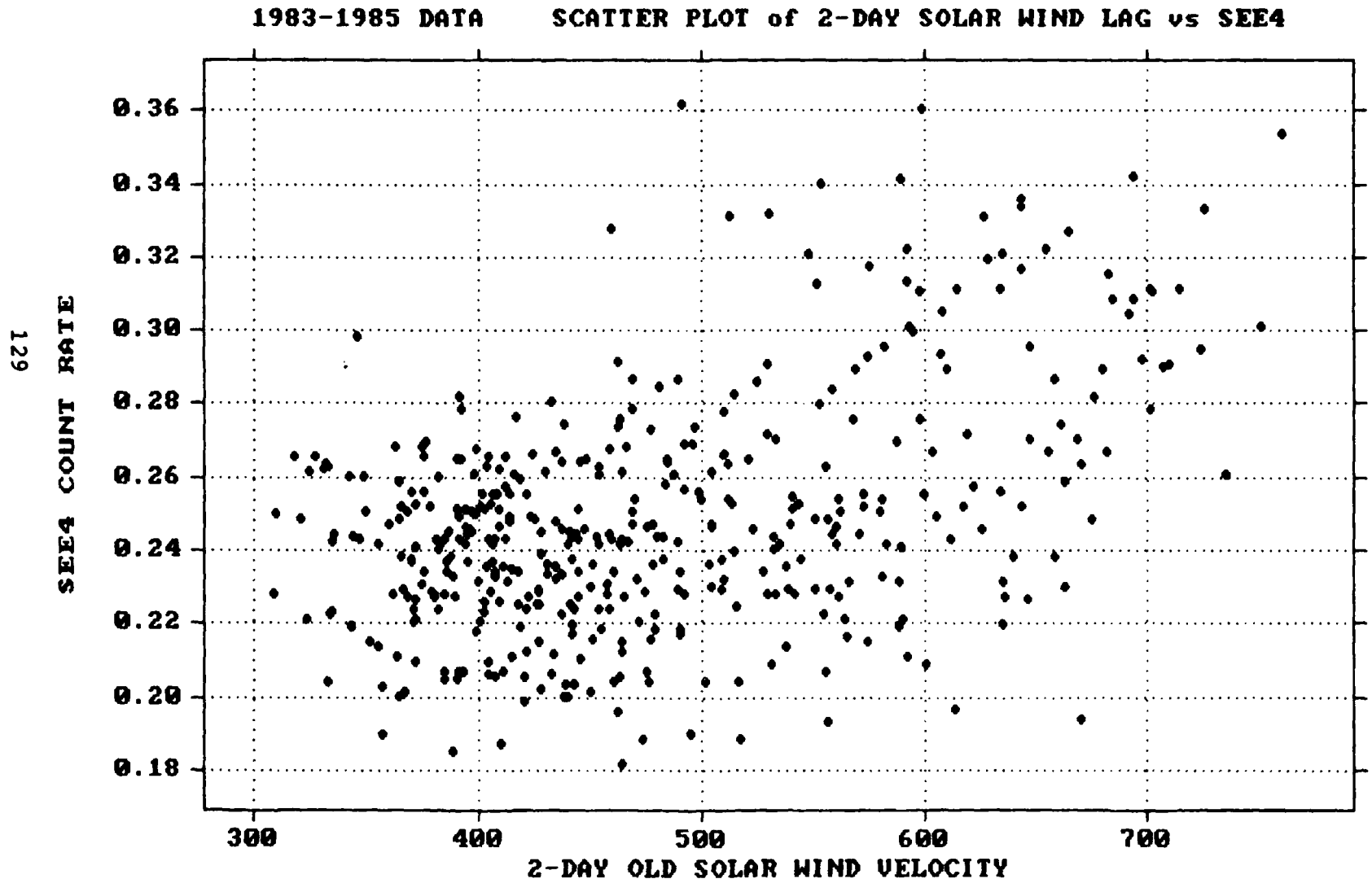
1983-1985 DATA SCATTER PLOT of 2-DAY SOLAR WIND LAG vs SEE4
SEE4 COUNT RATE
0.36
0.34
0.32
0.30
0.28
0.26
0.24
0.22
0.20
0.18
300
400
500
600
700
2-DAY OLD SOLAR WIND VELOCITY

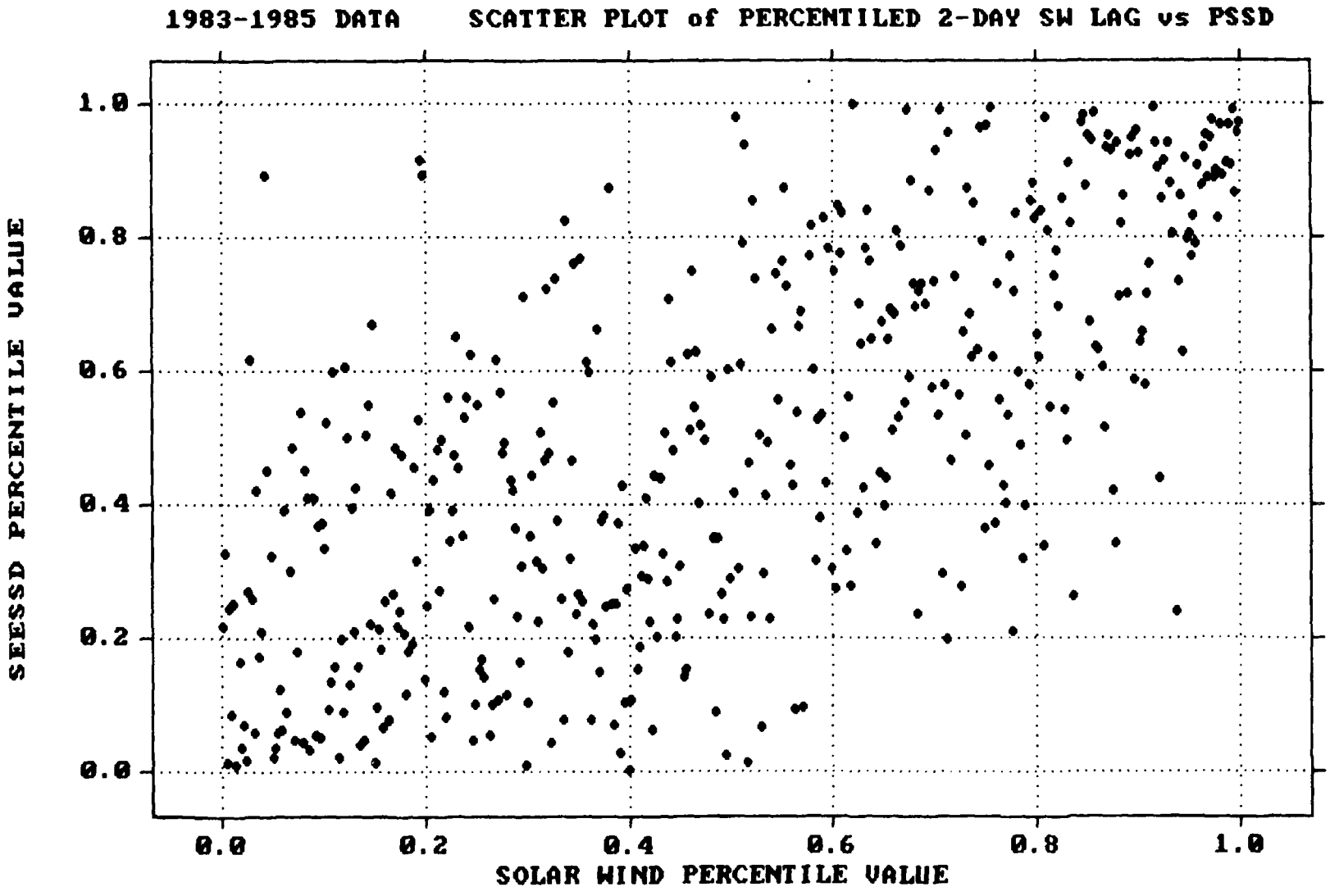
1983-1985 DATA SCATTER PLOT of PERCENTILED 2-DAY SW LAG vs PSSD
SEESSD PERCENTILE VALUE
1.0
0.8
0.6
0.4
0.2
0.0
0.0
0.2
0.4
0.6
0.8
1.0
SOLAR WIND PERCENTILE VALUE

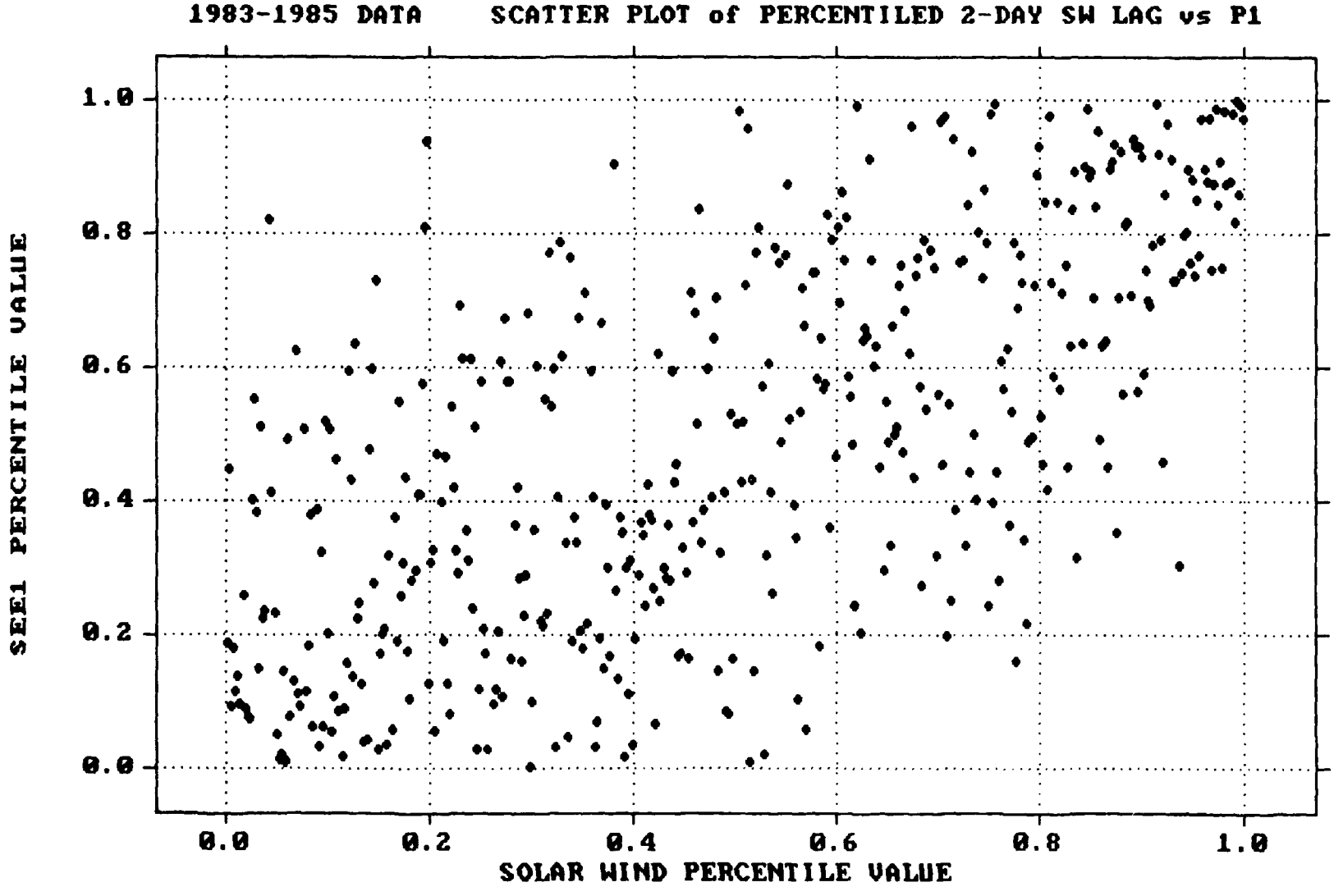
1983-1985 DATA SCATTER PLOT of PERCENTILED 2-DAY SW LAG vs P1
SEE1 PERCENTILE VALUE
1.0
0.8
0.6
0.4
0.2
0.0
0.0
0.2
0.4
0.6
0.8
1.0
SOLAR WIND PERCENTILE VALUE

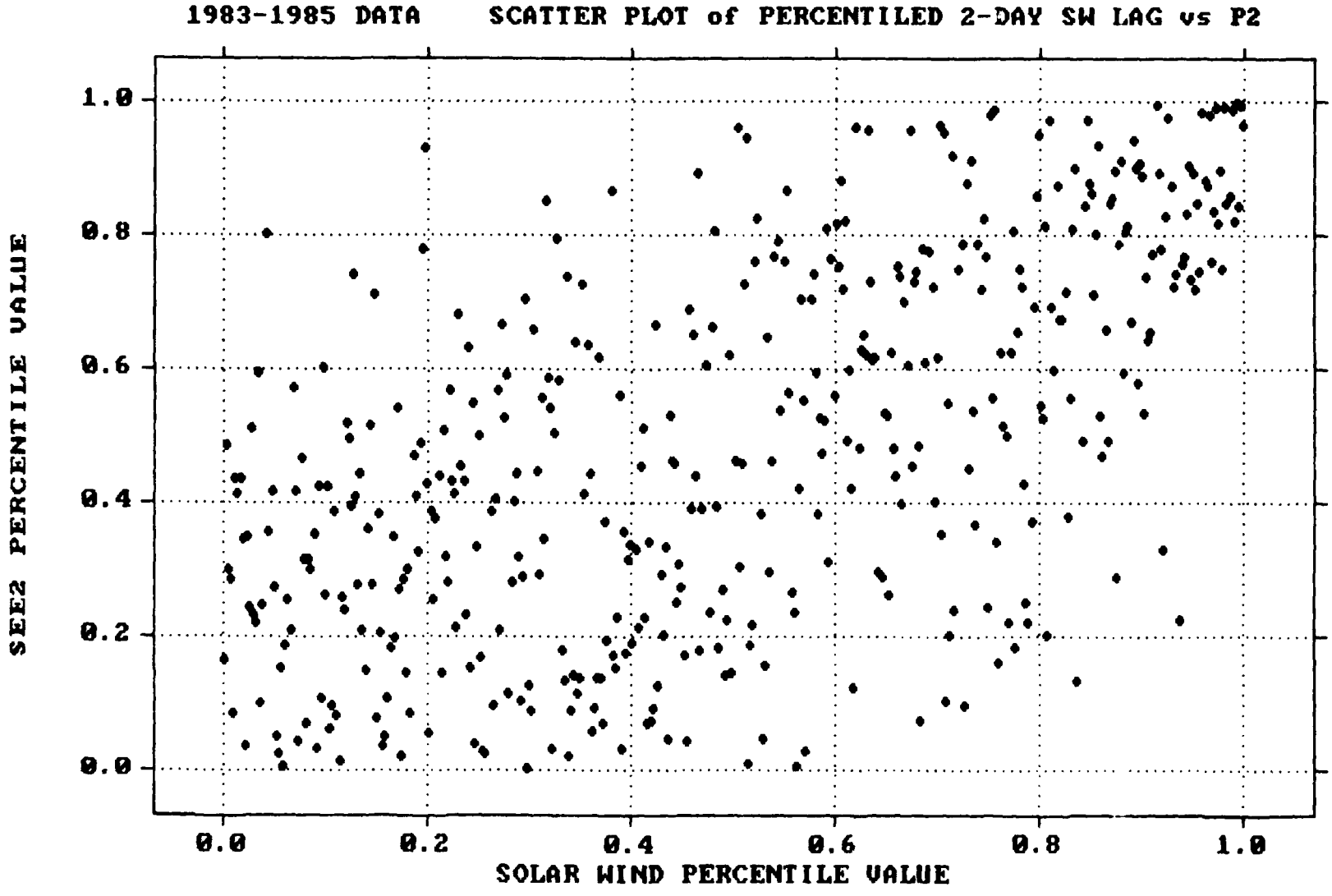
1983-1985 DATA SCATTER PLOT of PERCENTILED 2-DAY SW LAG vs P2
SEE2 PERCENTILE VALUE
1.0
0.8
0.6
0.4
0.2
0.0
0.0
0.2
0.4
0.6
0.8
1.0
SOLAR WIND PERCENTILE VALUE

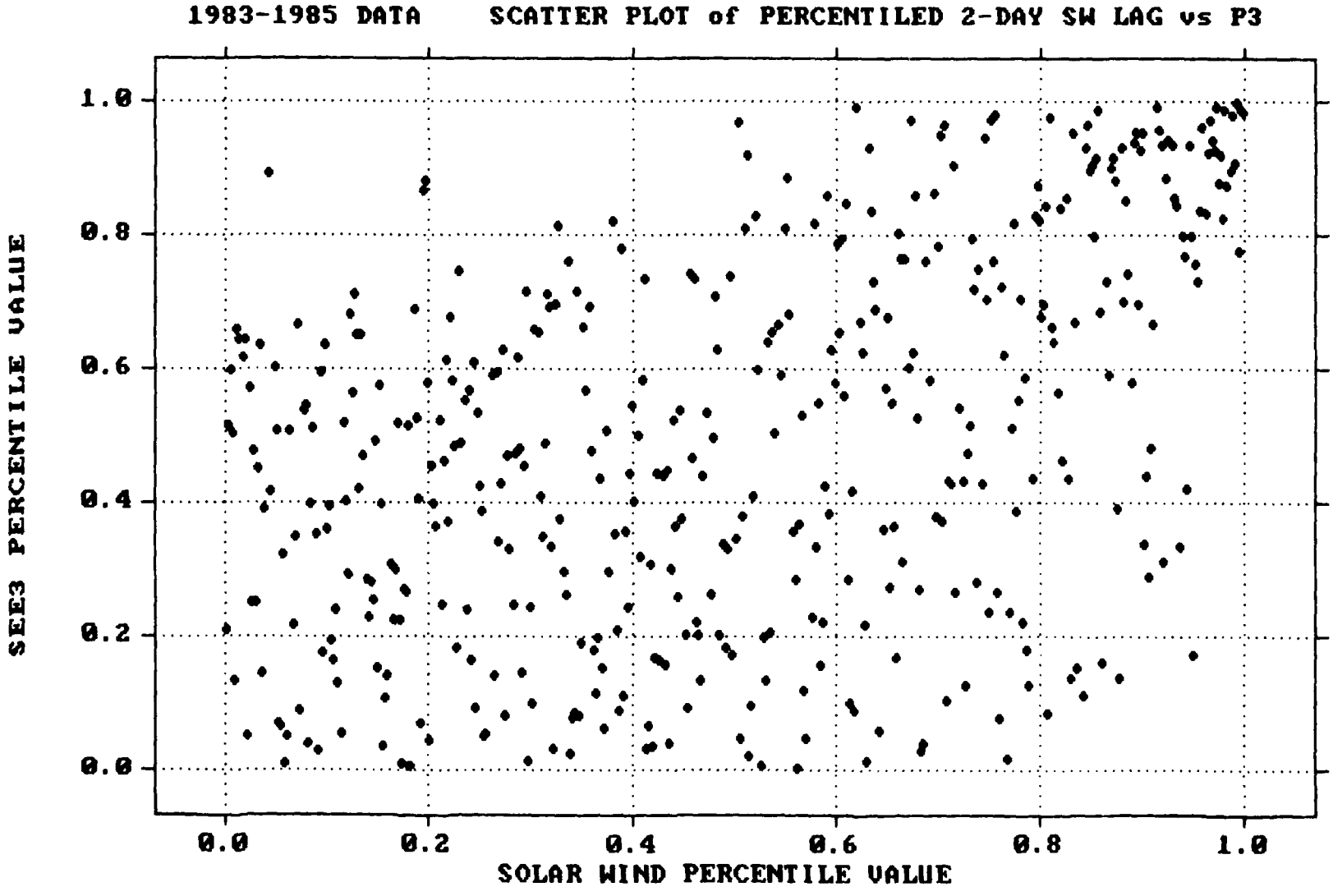
1983-1985 DATA SCATTER PLOT of PERCENTILED 2-DAY SW LAG vs P3
SEE3 PERCENTILE VALUE
1.0
0.8
0.6
0.4
0.2
0.0
0.0
0.2
0.4
0.6
0.8
1.0
SOLAR WIND PERCENTILE VALUE

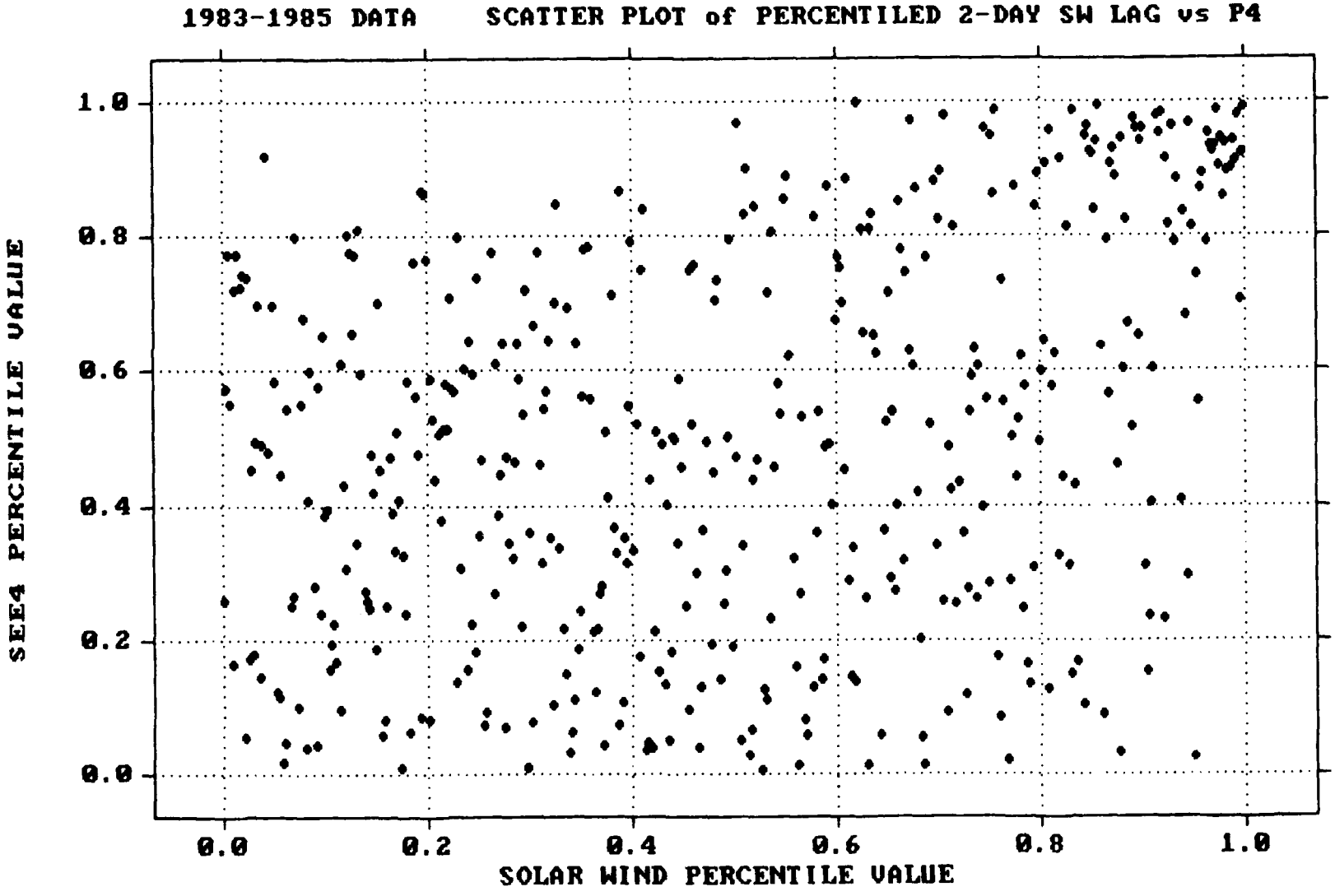
1983-1985 DATA SCATTER PLOT of PERCENTILED 2-DAY SW LAG vs P4
SEE4 PERCENTILE VALUE
1.0
0.8
0.6
0.4
0.2
0.0
0.0
0.2
0.4
0.6
0.8
1.0
SOLAR WIND PERCENTILE VALUE

Appendix E: Plots of R-Squared verses Solar Wind Lags

Page

1979-1981 Data 136

1983-1985 Data 141

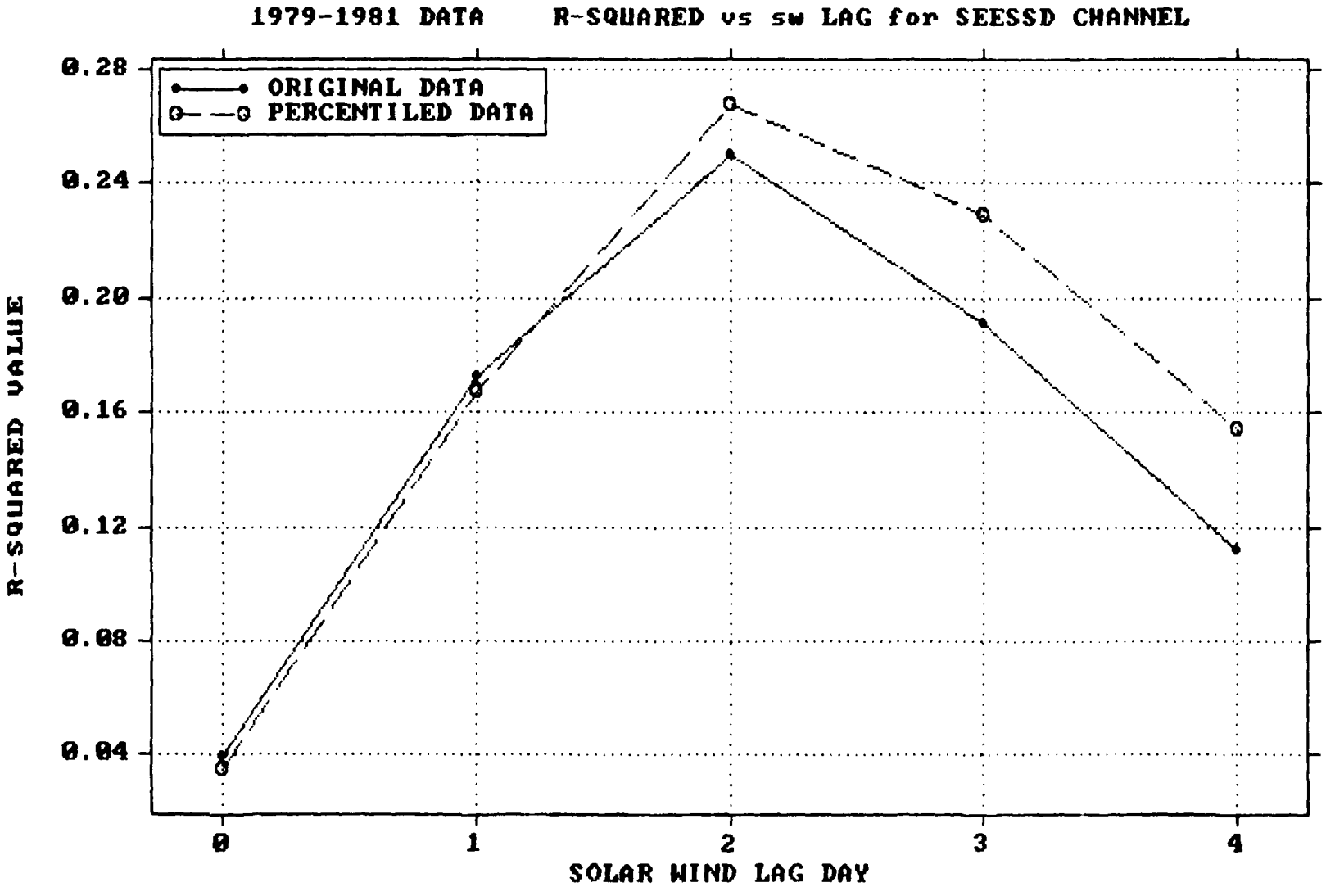
1979-1981 DATA R-SQUARED vs sw LAG for SEESSD CHANNEL
ORIGINAL DATA
PERCENTILED DATA
R-SQUARED VALUE
0.28
0.24
0.20
0.16
0.12
0.08
0.04
0
1
2
3
4
SOLAR WIND LAG DAY

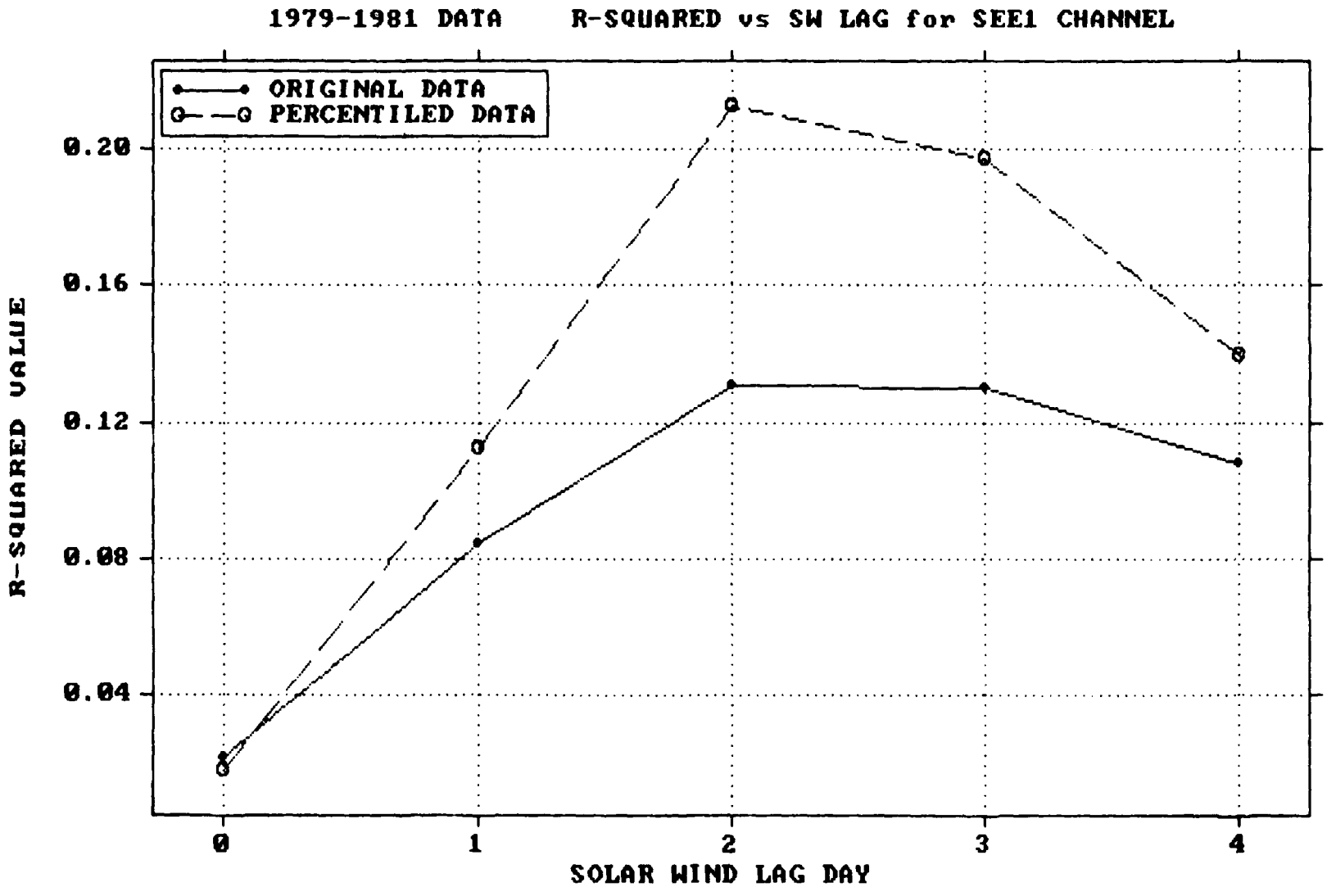
1979-1981 DATA R-SQUARED vs SW LAG for SEE1 CHANNEL
ORIGINAL DATA
PERCENTILED DATA
0.20
0.16
0.12
0.08
0.04
R-SQUARED VALUE
0
1
2
3
4
SOLAR WIND LAG DAY

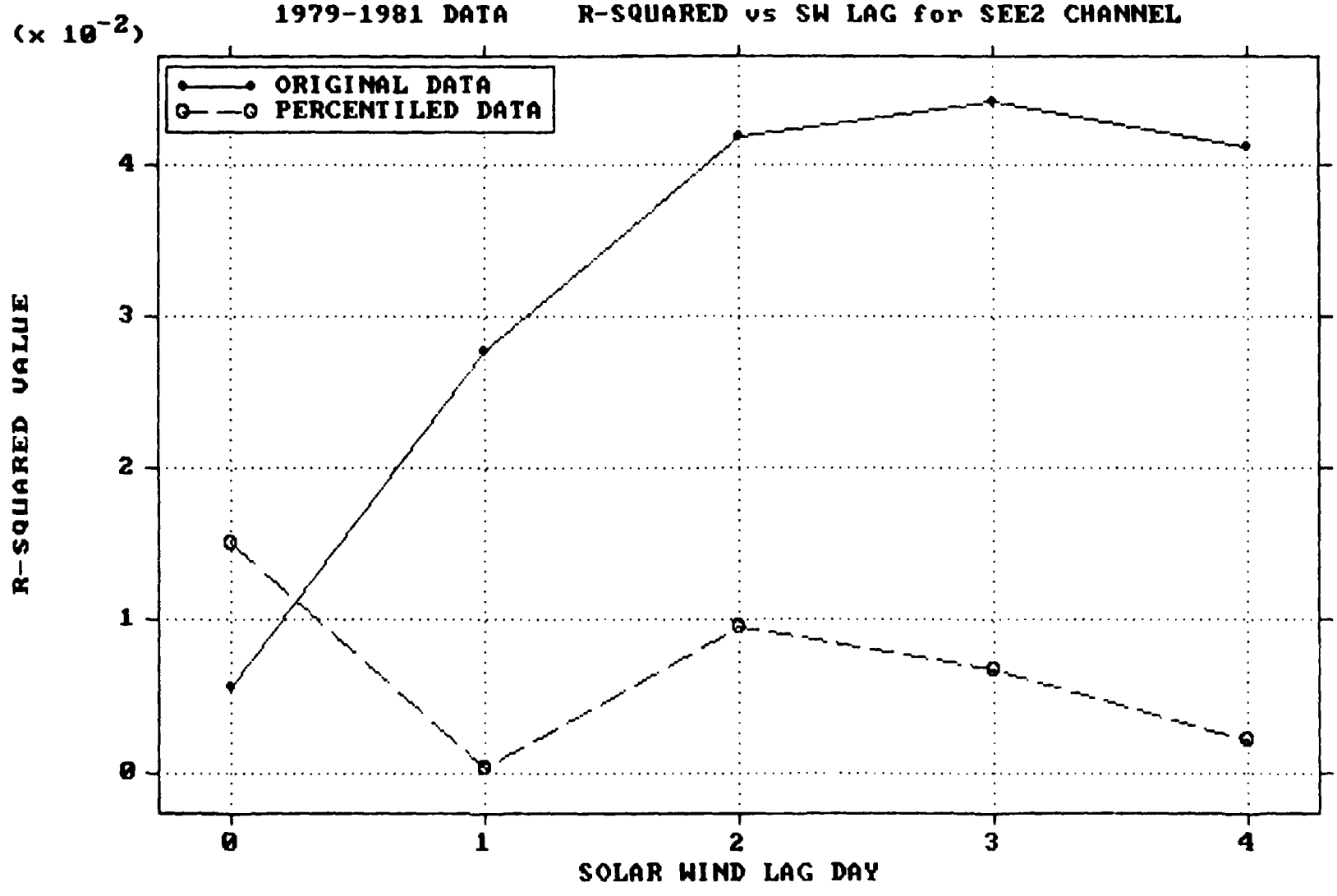
1979-1981 DATA R-SQUARED vs SW LAG for SEE2 CHANNEL
(x 10^-2)
ORIGINAL DATA
PERCENTILED DATA
R-SQUARED VALUE
0
1
2
3
4
SOLAR WIND LAG DAY

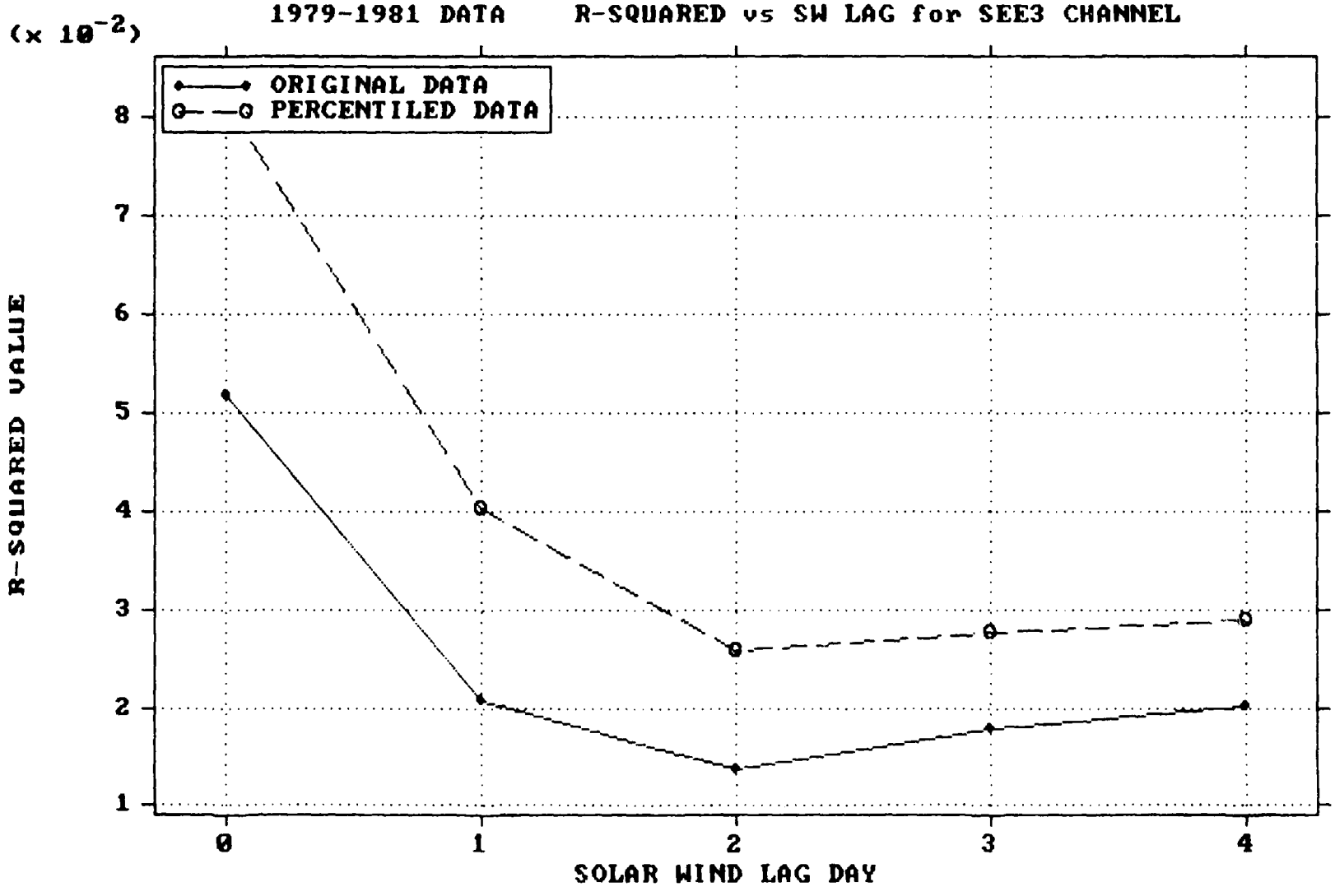
1979-1981 DATA R-SQUARED vs SW LAG for SEE3 CHANNEL
(x 10^-2)
ORIGINAL DATA
PERCENTILED DATA
R-SQUARED VALUE
8
7
6
5
4
3
2
1
0
1
2
3
4
SOLAR WIND LAG DAY

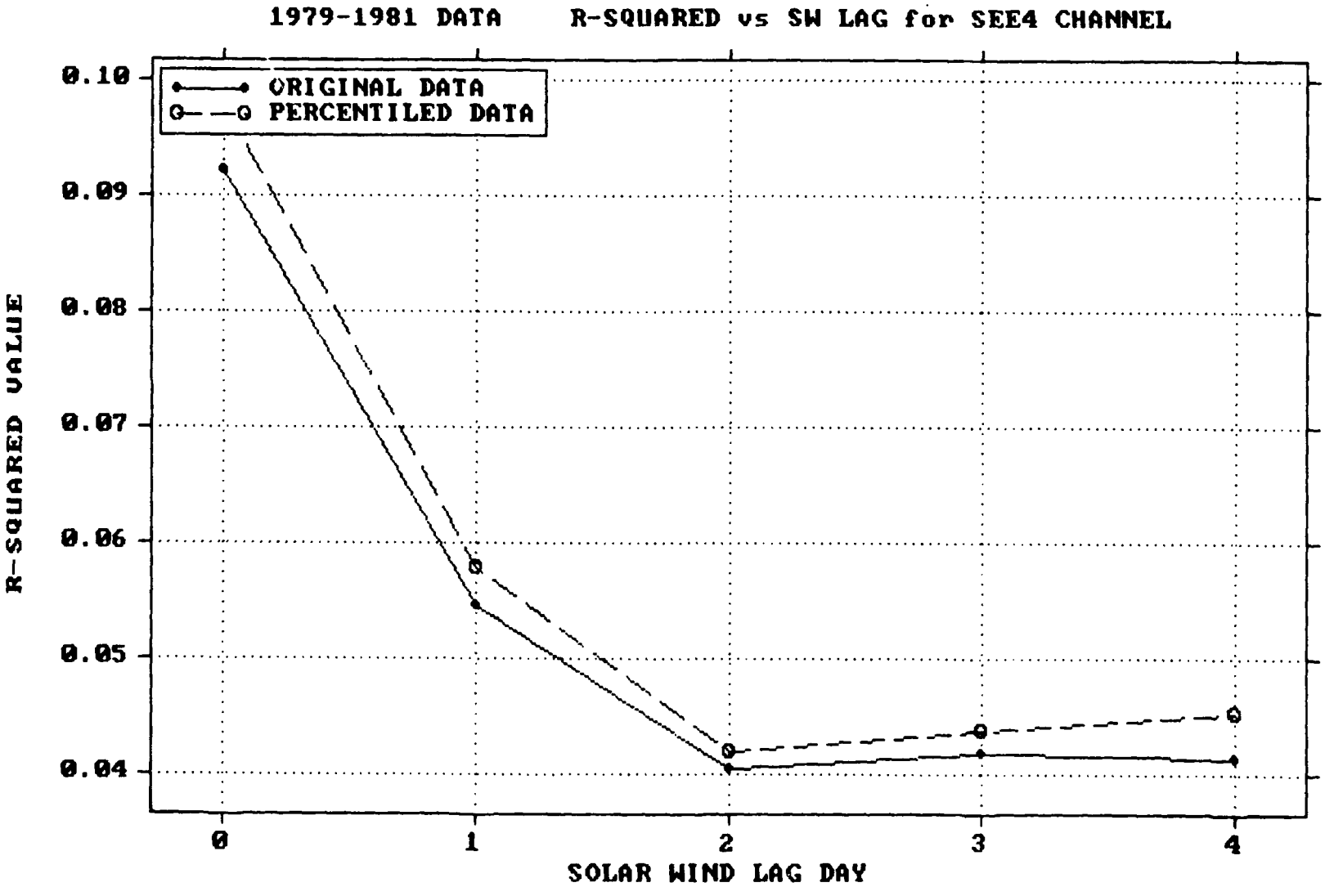
1979-1981 DATA R-SQUARED vs SW LAG for SEE4 CHANNEL
ORIGINAL DATA
PERCENTILED DATA
0.10
0.09
0.08
0.07
0.06
0.05
0.04
R-SQUARED VALUE
0
1
2
3
4
SOLAR WIND LAG DAY

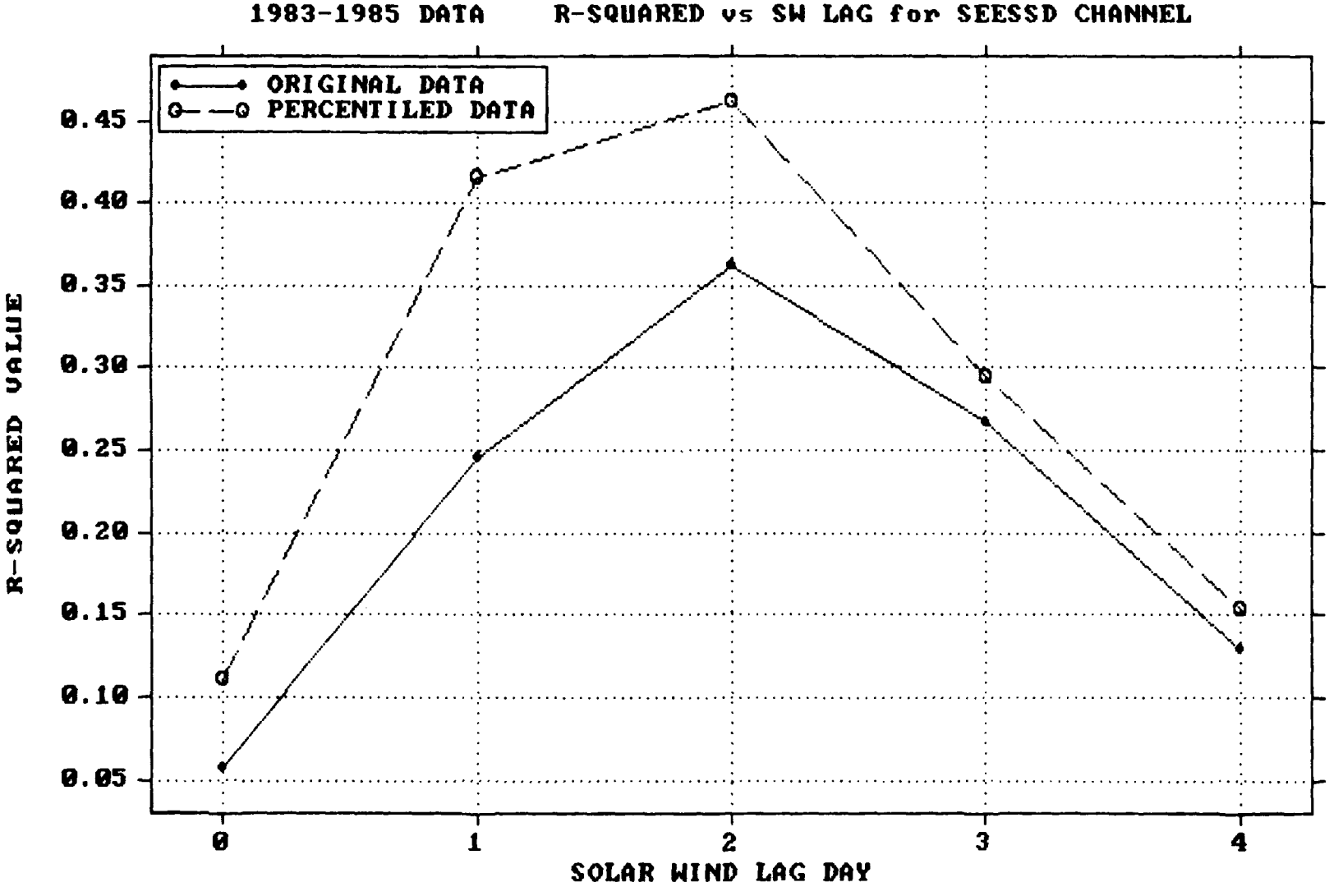
1983-1985 DATA R-SQUARED vs SW LAG for SEESSD CHANNEL
ORIGINAL DATA
PERCENTILED DATA
R-SQUARED VALUE
0.45
0.40
0.35
0.30
0.25
0.20
0.15
0.10
0.05
0
1
2
3
4
SOLAR WIND LAG DAY

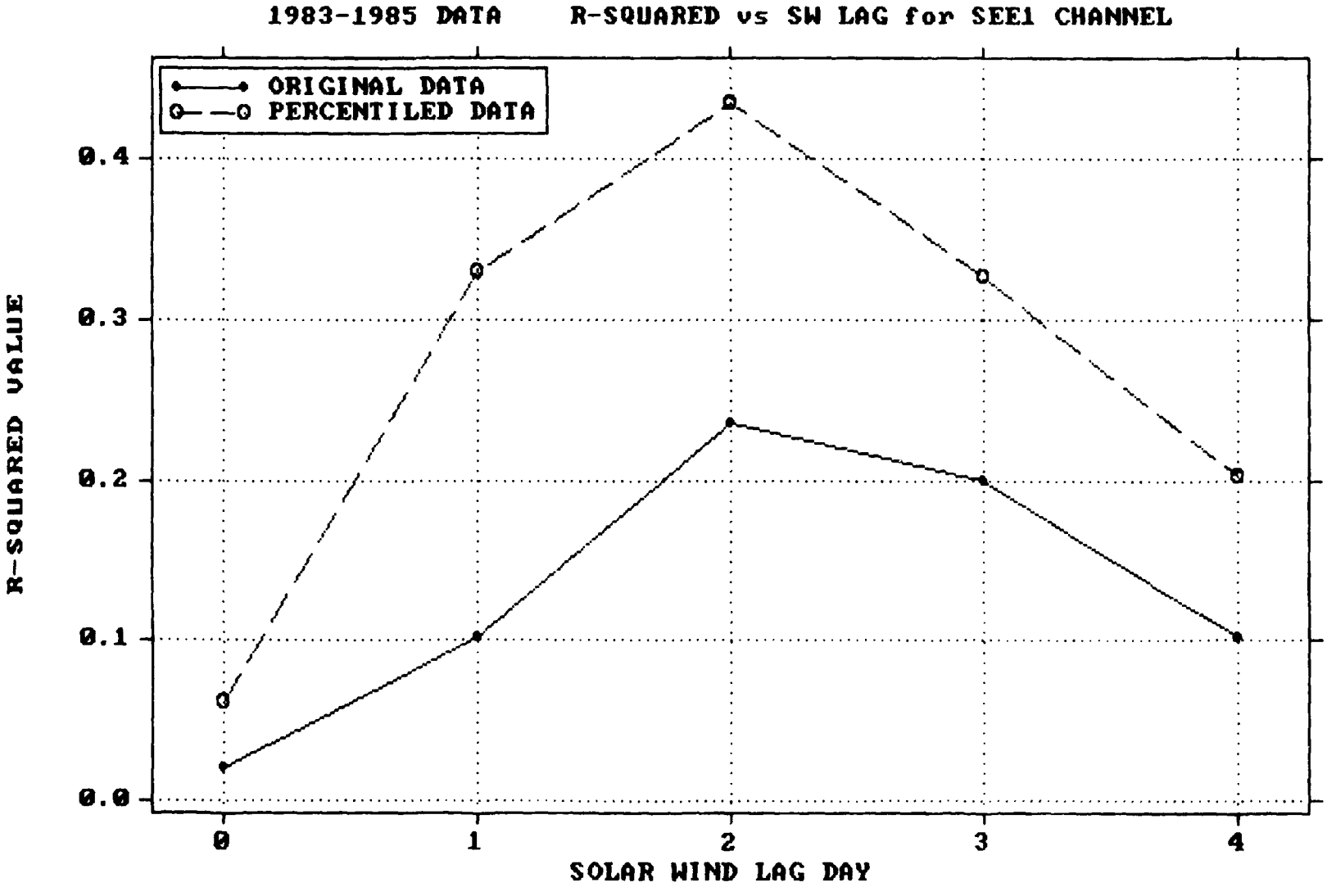
1983-1985 DATA R-SQUARED vs SW LAG for SEE1 CHANNEL
ORIGINAL DATA
PERCENTILED DATA
R-SQUARED VALUE
0.0
0.1
0.2
0.3
0.4
0
1
2
3
4
SOLAR WIND LAG DAY

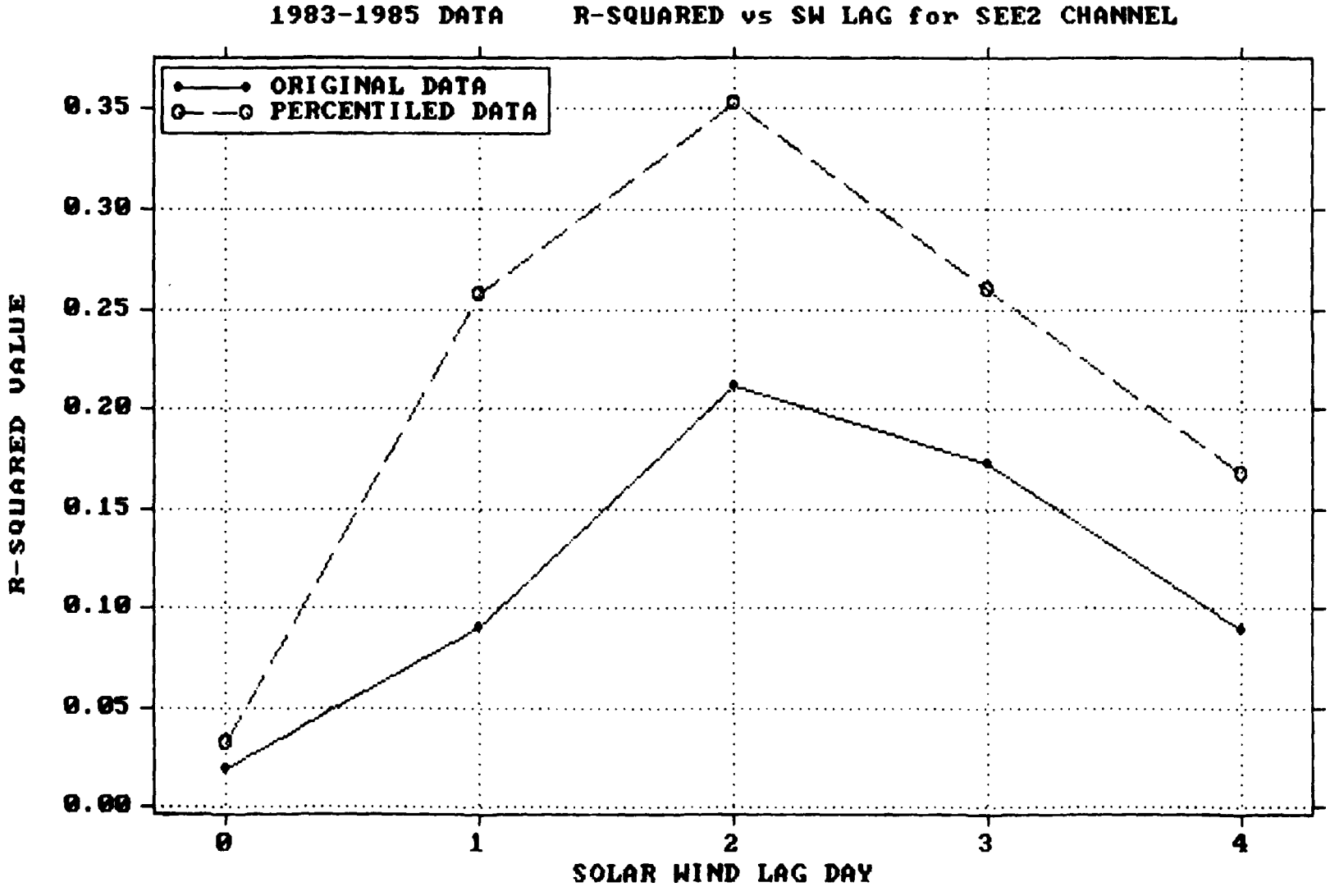
1983-1985 DATA R-SQUARED vs SW LAG for SEE2 CHANNEL
ORIGINAL DATA
PERCENTILED DATA
R-SQUARED VALUE
0.35
0.30
0.25
0.20
0.15
0.10
0.05
0.00
0
1
2
3
4
SOLAR WIND LAG DAY

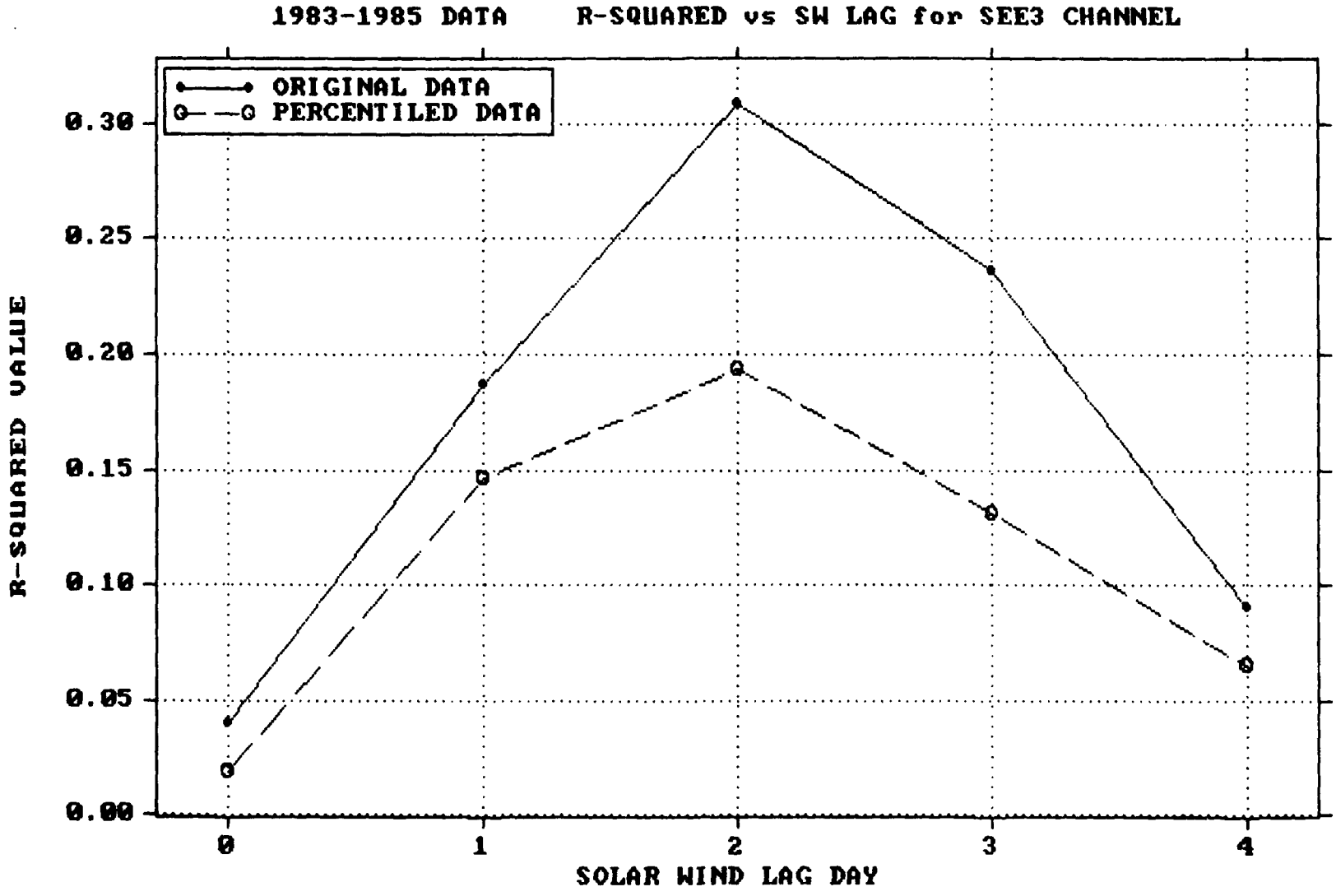
1983-1985 DATA R-SQUARED vs SW LAG for SEE3 CHANNEL
ORIGINAL DATA
PERCENTILED DATA
R-SQUARED VALUE
0.30
0.25
0.20
0.15
0.10
0.05
0.00
0
1
2
3
4
SOLAR WIND LAG DAY

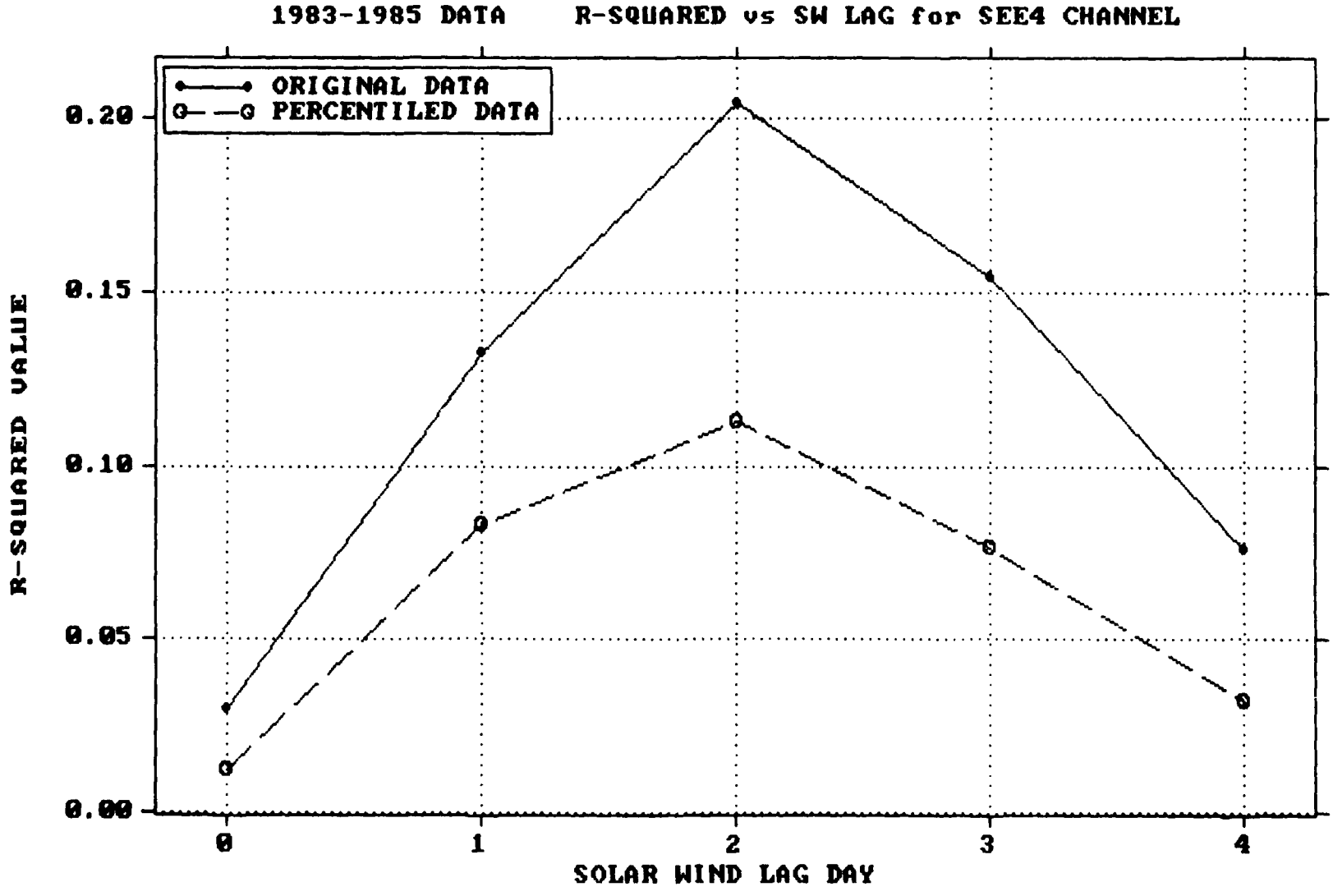
1983-1985 DATA R-SQUARED vs SW LAG for SEE4 CHANNEL
ORIGINAL DATA
PERCENTILED DATA
0.20
0.15
0.10
0.05
0.00
R-SQUARED VALUE
0
1
2
3
4
SOLAR WIND LAG DAY

Bibliography

1. Akasofu, Syun-Ichi. "Energy Coupling Between the Solar Wind and the Magnetosphere," Space Science Reviews, 21: 121-190 (1981).

2. Arnoldy, R. L. and K. W. Chan. "Particle Substorms Observed at Geostationary Orbit," Journal of Geophysical Research, 74: 5019-5027 (October 1969).

3. Baker, D.N. and others. "The Los Alamos Synchronous Orbit Data Set," The IMS Source Book, Guide to the International Magnetospheric Study Data Analysis, edited by C.T. Russel and D.J. Southwood. Washington: American Geophysical Union, 82-90, 1982.

4. Baker, D.N. and others, "Highly Relativistic Electrons in the Earth's Outer Magnetosphere: I, Lifetimes and Temporal History 1979-1984," Journal of Geophysical Research, 91: 4265-4276 (April 1986).

5. Coffey, Helen E. and John A. McKinnon. Solar-Geophysical Data Comprehensive Reports, 15. Boulder, CO.: National Geophysical Data Center, May 1988.

6. Department of the Air Force. MAC 01-83 Statement of Operational Need for Space Enviroment Monitoring. Scott Air Force Base, IL: HQ MAC, 17 March 1983.

7. Devore, Jay L. Probability and Statistics for Engineering and Sciences. Monterey CA: Brooks/Cole Publishing Company, 1987.

8. Eddy, John A. "Historical Evidence for the Existence of the Solar Cycle," The Solar Output and Its Variation, edited by O.R. White. Boulder, CO: Colorado University Press, 51-70. 1977.

9. Halpin, Michael P. A Time Series Analysis of Energetic Electron Fluxes (1.2 - 16 MeV) at Geosynchronous Altitude. MS thesis, AFIT/GSO/ENS-ENP/86D-1. School of Engineering, Air Force Institute of Technology (AU), Wright-Patterson AFB OH, December 1986 (Available through DTIC).

10. Higbie, P. R. "Short Term Magnetospheric Particle Variations," Solar Terrestrial Prediction Proceedings, 2. 433-440. Washington, D.C.: National Oceanic and Atmospheric Administration, 1980.

11. Hundhausen, Arthur. "Plasma Flow from the Sun," The Solar Output and Its Variation, edited by O.R. White. Boulder, CO: Colorado University Press, 36-39. 1977.

12. Jursa, Adolph S. (editor) Handbook of Geophysics and the Space Environment. Air Force Geophysics Laboratory, Springfield VA, 1985.

13. King, G.J. "Availability of IMP-7 and IMP-8 Data for the IMS Period," The IMS Source Book, Guide to the International Magnetospheric Study Data Analysis, edited by C.T. Russel and D.J. Southwood. Washington: American Geophysical Union, 10-20, 1982.

14. Lanzerotti, L.J. "Measures of Energetic Particles from the Sun," The Solar Output and Its Variation, edited by O.R. White. Boulder, CO: Colorado University Press, 383-404. 1977.

15. McCormick, Douglas I. Statistical Analysis of Energetic Electrons (1.2 - 16 MeV) at Geosynchronous Orbit. MS thesis, AFIT/GSO/ENP-ENS/84. School of Engineering, Air Force Institute of Technology (AU), Wright-Patterson AFB OH, December 1984 (AD-A159295).

16. Paulikas, G. A. and J.B. Blake. "Effects of the Solar Wind on Magnetospheric Dynamics: Energetic Electrons at the Synchronous Orbit." Aerospace Corporation Report No. ATR-79 (7642)-1, 27 November 1978.

17. Rosenvinge, T.T. "Data From ISEE-3 for the IMS Period," The IMS Source Book, Guide to the International Magnetospheric Study Data Analysis, edited by C.T. Russel and D.J. Southwood. Washington: American Geophysical Union, 1-9, 1982.

18. Smith, Warren L. Statistical Analysis of Energetic Electrons (3.4 - 16 MeV) at Geosynchronous Altitude and Their Relationship to Interplanetary Parameters. MS thesis, AFIT/GSO/PH/83. School of Engineering, Air Force Institute of Technology (AU), Wright-Patterson AFB OH, December 1983 (AD-A159217).

19. Su, S. Y. and A. Konradi. "Average Plasma Environment at Geosynchronous Orbit," Spacecraft Charging Technology. AFGL-TR-79-0082. Air Force Geophysical Lab, Hanscom AFB MA, 1979 (Available through DTIC).

VITA

Captain Gary P. Grover was born on [redacted] He graduated from Biddeford High School in June 1979 and subsequently entered the United States Air Force Academy. While at the Academy he was one of only eight students selected to participate in a six month exchange program with the French Air Force Academy. He graduated from the US Air Force Academy with a Bachelor of Science degree in June 1983. Captain Grover was assigned with Air Force Space Command from July 1983 to May 1987. During this period, he worked as an Orbital Analyst and as a Software Test Analyst. He was responsible for developing, testing and integrating new computer software for Cheyenne Mountain and several space systems. In May 1987, Captain Grover entered the School of Engineering, Air Force Institute of Technology at Wright-Patterson Air Force Base, Ohio.

[redacted]

REPORT DOCUMENTATION PAGE

1a. REPORT SECURITY CLASSIFICATION: UNCLASSIFIED	1b. RESTRICTIVE MARKINGS
2a. SECURITY CLASSIFICATION AUTHORITY	3. DISTRIBUTION/AVAILABILITY OF REPORT: Approved for public release; distribution unlimited.
2b. DECLASSIFICATION/DOWNGRADING SCHEDULE	
4. PERFORMING ORGANIZATION REPORT NUMBER(S): AFIT/GSO/ENP/88D-8	5. MONITORING ORGANIZATION REPORT NUMBER(S)
6a. NAME OF PERFORMING ORGANIZATION: School of Engineering; 6b. OFFICE SYMBOL (If applicable): AFIT/ENG	7a. NAME OF MONITORING ORGANIZATION
6c. ADDRESS (City, State and ZIP Code): Air Force Institute of Technology, Wright-Patterson AFB, Ohio 45433	7b. ADDRESS (City, State and ZIP Code)
8a. NAME OF FUNDING/SPONSORING ORGANIZATION; 8b. OFFICE SYMBOL (If applicable)	9. PROCUREMENT INSTRUMENT IDENTIFICATION NUMBER
8c. ADDRESS (City, State and ZIP Code)	10. SOURCE OF FUNDING NOS.

PROGRAM ELEMENT NO.	PROJECT NO.	TASK NO.	WORK UNIT NO.

11. TITLE (Include Security Classification): See Box 19	
12. PERSONAL AUTHOR(S): Gary P. Grover, B.S., Capt, USAF	
13a. TYPE OF REPORT: Thesis; 13b. TIME COVERED: FROM _____ TO _____	14. DATE OF REPORT (Yr., Mo., Day): 1988 December; 15. PAGE COUNT: 158
16. SUPPLEMENTARY NOTATION	

17. COSATI CODES			18. SUBJECT TERMS (Continue on reverse if necessary and identify by block number)
FIELD	GROUP	SUB. GR.	Magnetosphere, Van Allen Radiation Belt, Solar Wind, Electron Flux, Synchronous Satellites
04	01		
12	01		

19. ABSTRACT (Continue on reverse if necessary and identify by block number)

Title: GEOSYNCHRONOUS HIGH ENERGY ELECTRON (1.2-16 MeV) - SOLAR WIND CORRELATION ANALYSIS

Thesis Chairman: James Lange, Major, USAF

Approved for release in accordance with AFR 190-1
12 Jan 1989

20. DISTRIBUTION/AVAILABILITY OF ABSTRACT: UNCLASSIFIED/UNLIMITED ☐X SAME AS RPT. ☐ DTIC USERS ☐	21. ABSTRACT SECURITY CLASSIFICATION: UNCLASSIFIED	
22a. NAME OF RESPONSIBLE INDIVIDUAL: James Lange, Major, USAF	22b. TELEPHONE NUMBER (Include Area Code): 513-255-6141	22c. OFFICE SYMBOL: AFWAL/AARI

DD FORM 1473, 83 APR — EDITION OF 1 JAN 73 IS OBSOLETE.

19. ABSTRACT (continued)

This thesis investigated the relationship between high energy electron (1.2-16 MeV) count rates and solar wind velocity. The analysis used daily averages for all variables. Two data sets were examined: the first, from 13 June 1979 to 18 May 1981 occurred slightly after solar maximum; the second, from 8 May 1983 to 12 April 1985 occurred slightly before solar minimum. The electron count rate data came from DOD satellite 1979-053 in geosynchronous orbit while the solar wind data was collected by other satellites directly in the unobstructed solar wind. Methods used to analyze the data were daily average plots, frequency plots, probability plots, descriptive statistics, linear correlation analysis of both original and percentiled data, and event analysis.

The results of this study showed that solar wind velocity correlates differently with high energy electron count rates depending on where in the solar cycle the solar wind events occur. It was shown through event analysis that two to three days prior to a significant rise in high energy (1.2-16 MeV) electron count rates, a significant rise in solar wind velocity also occurred. However, due to the low linear correlation results achieved (all R-Squared values were less than 0.50), it is likely that solar wind velocity is only one of several variables determining the occurrences of high energy electron events at earth geosynchronous altitude.